CENTRIFUGE MODELLING RELATIVE TO SETTLING OF CLAY SUSPENSIONS

Alsayed M. Alammawi

A Thesis submitted to the Faculty of Graduate Studies and Research in partial fulfillment of the requirements for the degree of Master of Engineering

Department of Civil Engineering and Applied Mechanics
McGill University
Montreal, Quebec
Canada

TO

My Parents
My Brothers and Sisters
to J.

ABSTRACT

The initial settling behaviour of kaolinite suspensions under the influence of centrifugal and gravitational forces is examined. The object is to determine whether the results of centrifugally induced settling of solid particles can be used to predict the behaviour of kaolinite during batch settling. If the predictions were reliable, the experimentation time used in the tests would be greatly shortened.

The goals of the experimental investigation are:

a. Evaluation of the effect of kaolinite concentration on the settling behaviour of the suspensions.

b. Determination of the settleability coefficient for kaolinite suspensions.

c. Study of the effect of the imposed force on the settling behaviour of the kaolinite suspensions and the influence on the grain size distribution.

The experimental results show that the centrifugal force enhances the segregation of the solid particles, and hence, centrifugal tests cannot be used to predict the settling velocity of kaolinite suspensions under the influence of gravity.

RESUME

Le comportement initial du processus de décantation de suspensions de kaolinite, sous l'influence de forces centrifuges et gravitationelles, a été étudié. L'objet de cette étude est de voir s'il est possible de prédire d'avance le comportement des suspensions de kaolinite, durant la décantation discontinue, et ce, par des essais de décantation par centrifuge. Si les prédictions étaient fiables, il en résulterait une diminution importante du temps nécessaire à effectuer ces experiences.

Les buts de cette étude experimentale comportaient les points suivants:

a. Examen de l'influence de la concentration initiale de kaolinite, sur la décantation des suspensions
b. Détermination du coefficient de décantation des suspensions de kaolinite.
c. Etude de l'effet des forces imposées sur la décantation des suspensions de kaolinite, et sur leurs distribution granulométrique.

Les résultats des experiences démontrent que la force centrifuge accroît la ségrégation des particules solides. Il en suit que la méthode centrifuge ne peut être employée pour prédire la vitesse de décantation des suspensions de kaolinite, sous l'influence de la pesanteur.

ACKNOWLEDGEMENTS

The author wishes to express his sincere appreciation and gratitude to:

1. Dr. R.N. Yong, William Scott Professor of Civil Engineering and Applied Mechanics, and Director of the Geotechnical Research Centre at McGill University for his guidance and continued encouragement throughout this study.
2. Dr. A.J. Sethi, for invaluable suggestions and helpful advice and discussions.
3. Mr. F. Caporuscio and his laboratory staff for technical assistance.
4. Miss J. Armour for the typing of this thesis.

Finally, I would like to acknowledge the financial assistance of NSERC.

TABLE OF CONTENTS

CHAPTER 5: SUMMARY AND CONCLUSIONS

LIST OF FIGURES

LIST OF TABLES

CHAPTER 1

INTRODUCTION

1.1 STATEMENT OF THE PROBLEM

Mineral separation involves the separation of two phases, i.e. solid suspended in liquid. Separation processes may be classified according to the method involved (see Fig. 1.1). If the liquid is constrained and the particles can move freely within it (due to the acceleration), sedimentation and flotation occur. For sedimentation to occur, a density difference between the solids and the liquid is necessary. If particles are constrained by a medium and the liquid can flow due to hydraulic gradient, filtration and screening occurs, where a density difference is not necessary. Sedimentation is a process of solid-liquid separation whereby the solids separate under the effect of external forces (gravity or centrifugal force).

Continuous sedimentation, which involves settling of solid particles under the influence of gravity, occurs in settling tanks. A distinction is made between the different types of separation, depending on their purpose. If the clarity of the overflow is of primary importance, the process is called clarification and the feed slurry is usually dilute. If a thick underflow is the primary aim, the process is called thickening, and the feed slurry is usually more concentrated.

Gravity settling is still one of the most economical means of removing the solids produced during these processes. Because of variations in type, nature, and concentration of solids involved, as well as properties of the liquid and the settling tank design itself, no one theory or design approach can be used for all solid-liquid separation applications.

In discrete settling, the assumption is made that each particle moves through the liquid phase unaltered and unaffected by the surrounding conditions. The subsidence velocity of such particles can be estimated with reasonable accuracy, using the formulations of Newton and Stokes. With increasing particle concentration, the settling particles "hinder" the motion of adjacent particles. Because of this hindered settling of the suspension, and since fluid shear force may cause the partial breakup of flocs while subsiding, it is not possible to predict the performance of settling tanks from the theoretical relationships. Therefore, it is necessary to employ a settling test in order to predict the performance of the settling tank.

For the purpose of increasing the gravitational force and hence the rate of particle settling, a centrifuge is used; its effect is to accelerate the settling of solid particles, hence shortening the settling time. Centrifugation increases the force on the solid particles and the technique can be used to determine whether or not gravity

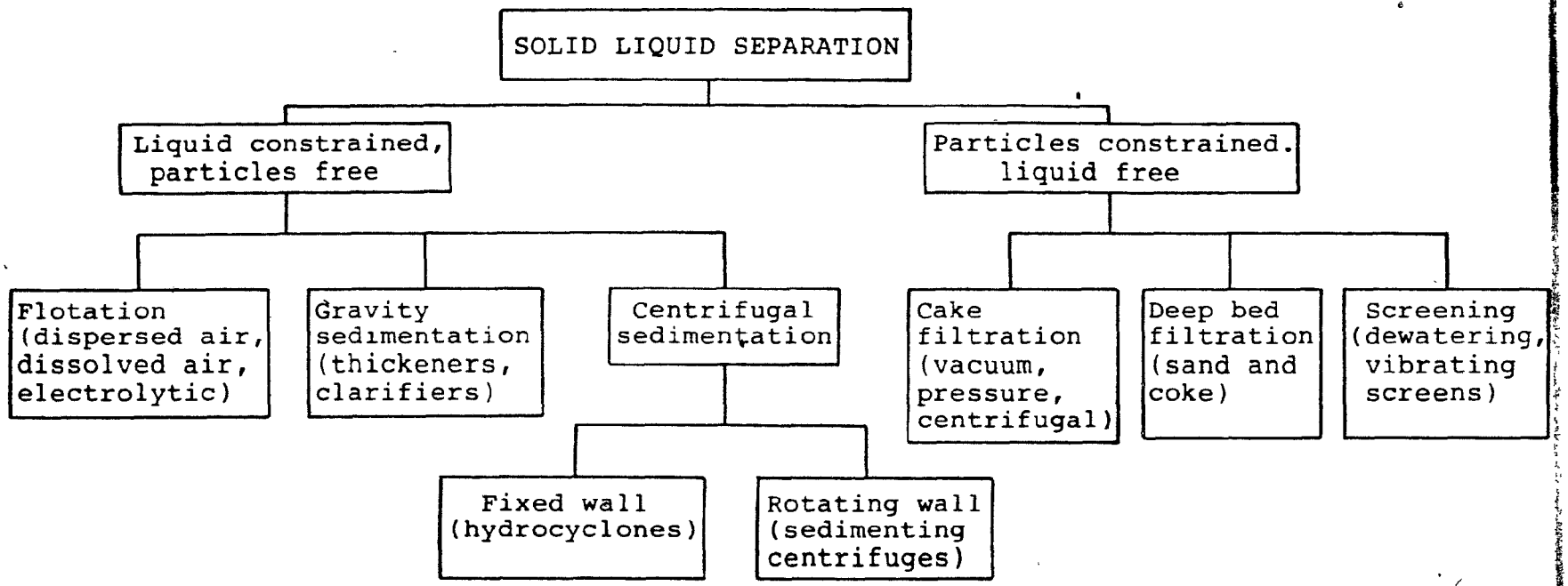

Fig. 1.1 Classification of Solid-Liquid Separation Processes

thickening is feasible, and whether or not it can subsequently be used to provide guidelines for the design of settling tanks.

1.2 PURPOSE AND SCOPE OF THESIS

The purpose of the study reported herein is to determine if centrifugally induced settling of solid particles can be used to predict the settling behaviour of solid particles during batch settling (i.e. the settling of solid particles under the influence of gravity). Basically, this study involves observation of the settling behaviour of two materials: a Hydrite Flat D Kaolinite and a Hydrite Ultra Fine Kaolinite. The experimental part of this study is divided into two phases as follows:

PHASE 1: Experimental evaluation of interface subsidence characteristics of a Hydrite Flat D Kaolinite and a Hydrite Ultra Fine Kaolinite, over a wide range of initial concentrations.

This was carried out by two methods: the first was a gravity test, and the second involved using a centrifuge at a constant rotational speed of 100 r.p.m. (6.25 times gravity).

The experimental evaluation is divided into:

a. Determination of the relationship between initial settling velocity and initial concentration in the centrifuge test (i.e. the settling of solid particles under the influence of centrifugal forces) for

concentrations 8% to 30% by weight for a Hydrite Flat D Kaolinite, and 8% to 20% by weight for a Hydrite Ultra Fine Kaolinite.

b. Determination of the relationship between initial settling velocity and initial concentration in the gravity test (i.e. the solid particles settle under the influence of gravity force) for concentrations similar to those used in the centrifuge test.

PHASE 2: In this phase, the Hydrite Flat D is investigated in more detail by concentrating on six compositions (16%, 20%, 24%, 27%, 30% and 33% by weight) and using five rotational speeds for each concentration.

The purpose of these choices is to obtain a basic understanding of the settling behaviour of the clay suspension. For any concentration, the velocity of the sharp interface increases with increasing rotational speed. However, some questions remain:

1. Does the particle size distribution remain the same in the column or does it change with depth on increasing the rotational speed (i.e. external force)?
2. If segregation occurs, how is it affected by the changing rotational speed?
3. For different concentrations but at the same rotational speed, does the concentration affect the particle size distribution, and if so, how to relate the distribution to the settling velocity of the interface?

Further evaluation of the experimental test results on settling include:

1. Establishment of the validity of the settleability coefficient used in reference to the centrifuge test.
2. Determination of the particle size distribution of the tested material, under the influence of centrifuging field, for two conditions:
   a. at a fixed concentration of 16% by weight, at different rotational speeds.
   b. at a fixed rotational speed but changing the range of concentration.
3. Determination of the particle size distribution of the tested material under the influence of the gravitational field.
4. Establishment of the relationship between the theoretical diameter, determined from the viscosity of the suspensions, and the actual diameter measured from the sedigraph 5000 D.

1.3 ORGANIZATION OF THE THESIS

This thesis consists of five chapters and two appendices. The contents of the five chapters are as follows:

Chapter 1: of which this section is a part, is an introductory chapter which presents the problem and the purpose of the present study.

Chapter 2: Consists of a literature review of some aspects of the settling of suspensions.

Chapter 3: Provides a complete description of the experimental methods, and the characteristics of the materials.

Chapter 4: Contains typical experimental results obtained from both centrifuge tests and gravity tests, as well as a discussion of the results.

Chapter 5: Contains the summary and conclusions and suggestions for future studies.

The contents of the appendices are as follows:

Appendix A: Contains samples of calculations

Appendix B: Contains all of the test results, from which representative samples were used in Chapter 4.

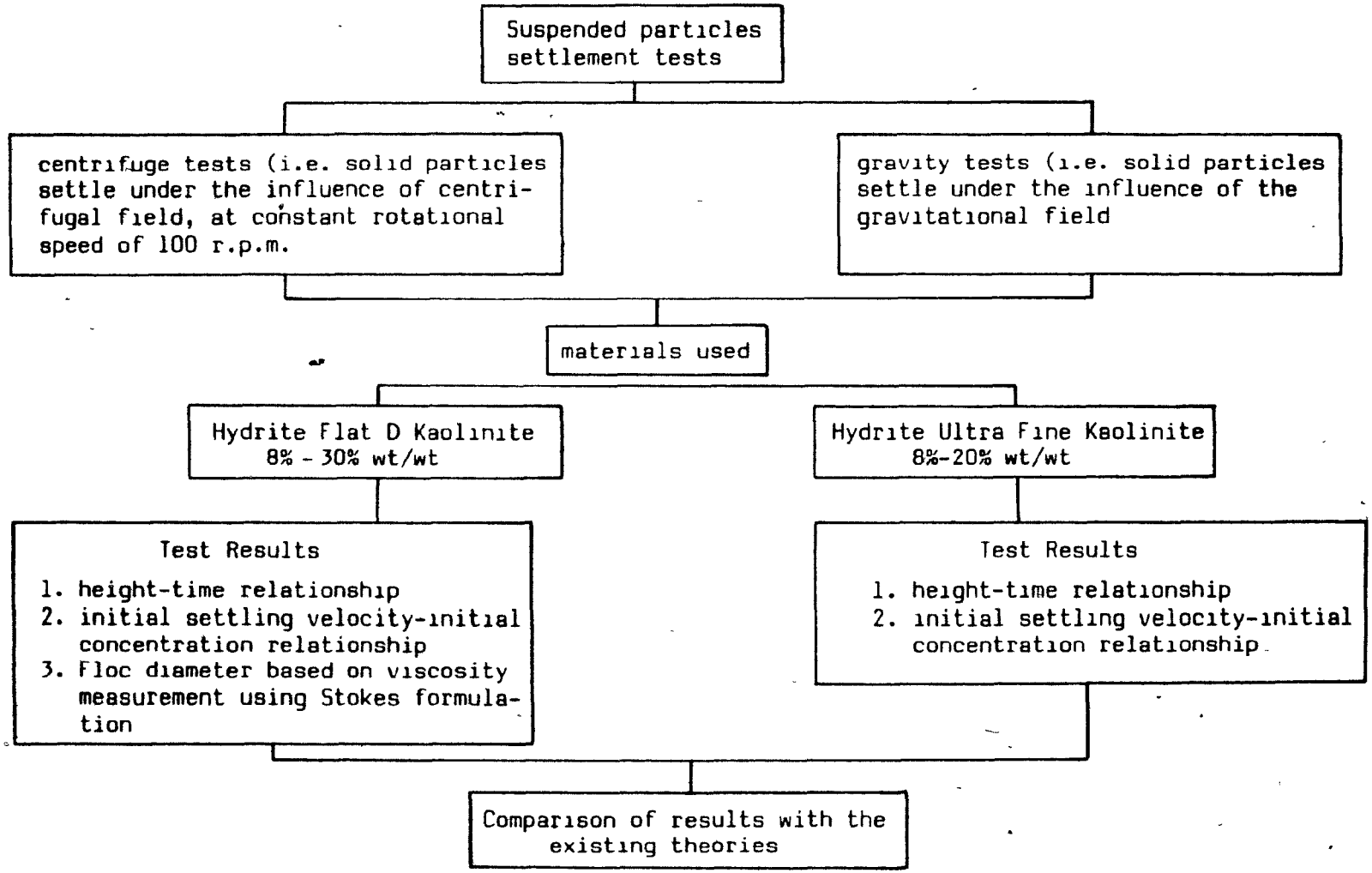

Fig. 1.2 Flow Chart Outlining the Scope of Study Phase 1

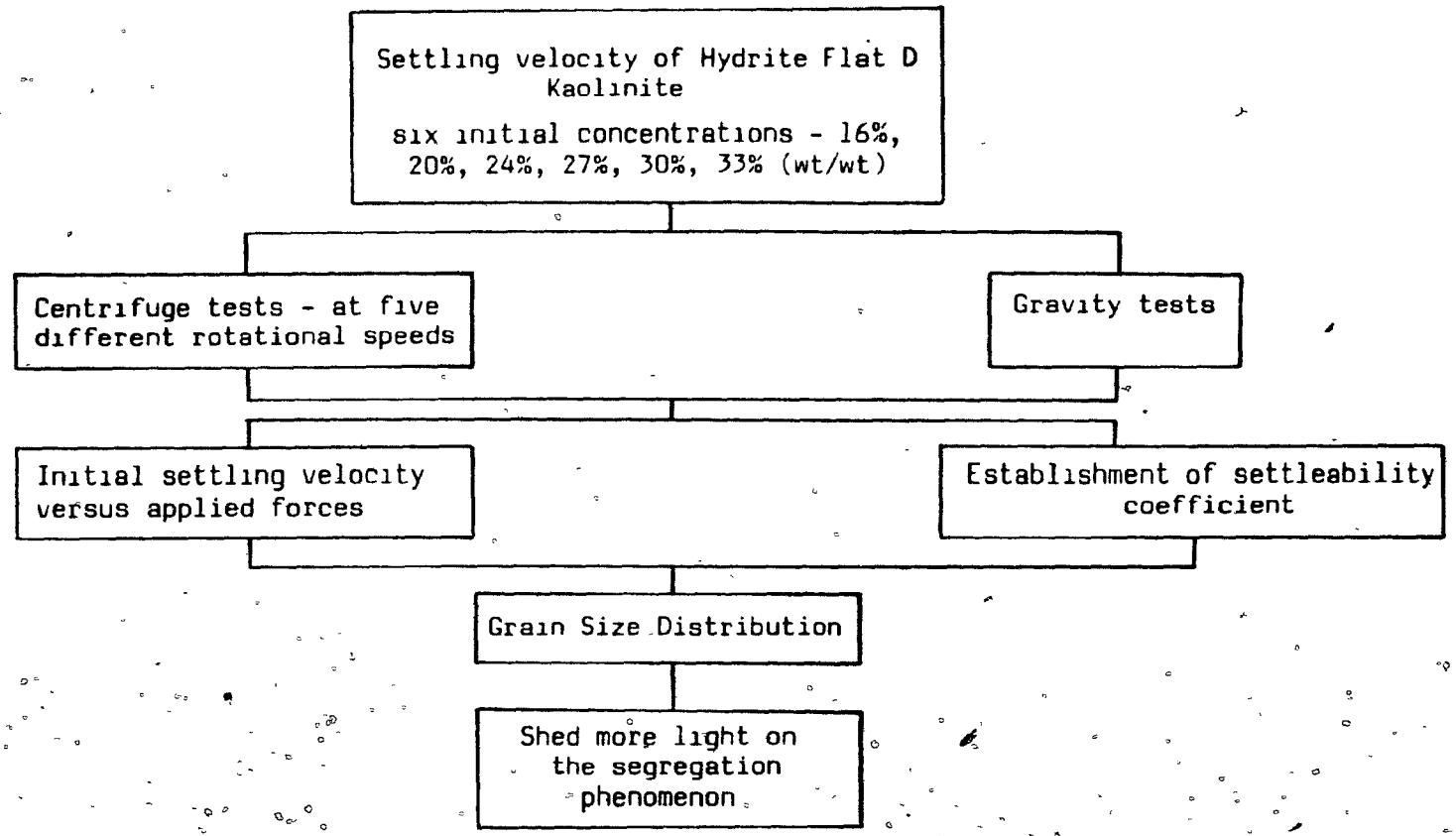

Fig. 1.3 Flow Chart Outlining Scope of Study Phase 2

CHAPTER 2

LITERATURE REVIEW

2.1 INTRODUCTION

According to Fitch (1958) suspended particles settle in any of four markedly different ways, depending upon concentration and relative tendency of the particles to agglomerate. Figure 2.1 describes the four classes as follows:

Class 1: discrete non-flocculating particles which settle at a characteristic constant rate. These rates depend on:

1. individual particle characteristics
2. properties of the fluid through which it settles.

Class 2: the settling rates of particles depend also on the size, shape and density of the settling particles, as well as the properties of the fluid.

Because of the ability of class 2 particles to adhere to one another, the size, shape, effective density, and accordingly, the settling velocities change throughout the process.

With increasing particle concentration, a corresponding reduction in settling velocity is observed. This reduction may be attributed to the following:

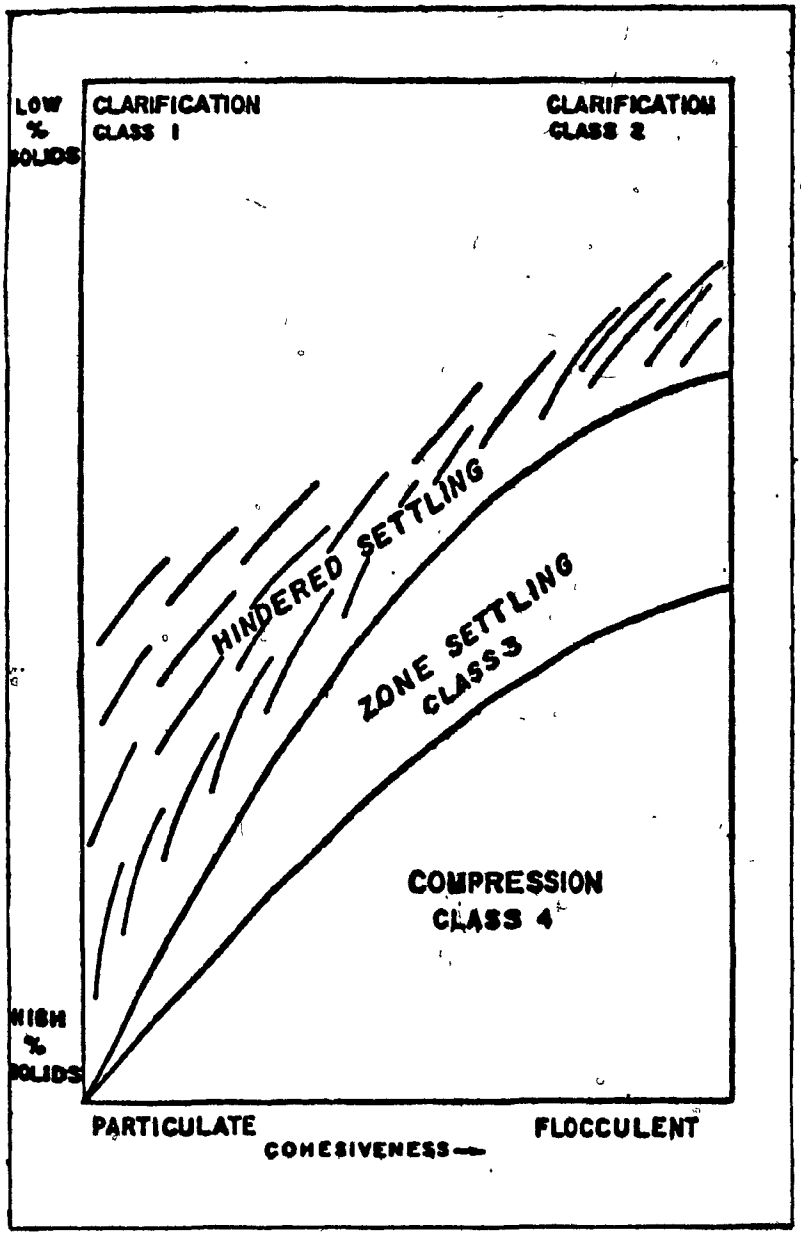

FIGURE 2-1 PARAGENESIS DIAGRAM

1. upward velocity of displaced fluid through restricted spaces between particles.
2. interference of velocity fields
3. interference of velocity field by the presence of solid objects such as the container wall.

The retarding effect of these phenomena on the settling velocity is called "hindered settling". Under these conditions, the particles cohere into a structure, such that all particles in a given neighbourhood subside at the same rate, but the structure does not lend mechanical support. Under these conditions, the hindrance of liquid flow between particles is so great that a clear slurry/clear supernatant interface is formed, indicating the collective sedimentation of all particles, irrespective of size.

Class 3: An extreme case of hindered settling occurs when the solid concentration is sufficiently high to cause all the particles in the suspension to settle at the same velocity. In this situation, the solids settle as a blanket, the velocity of subsidence being an inverse function of concentration. This type of settling (class 3) is known as zone settling.

Class 4: Settling, or compression, occurs when the particles are in physical contact and are supported to some degree by particles directly below. The main reasons for the modification of settling behaviour in hindered settling have been well summarized by Coulson and Richardson (1955), as follows:

1. Large grains are settling relative to a suspension of fine grains, and this suspension has a higher viscosity and density than the pure fluid, thus tending to reduce the settling velocity.
2. The fluid displaced by settling grains flows upward between the grains, so that the settling velocity is less than the true relative velocity between the grain and the fluid. If there is a large range in grain sizes, finer grains may actually be swept upward by the fluid rising up through the spaces between the larger settling grains.
3. Velocity gradients close to the grains are increased as a result of close pressure of other grains.
4. For cohesive grains, close proximity and resulting random collisions between grains may trigger flocculation.

It would seem that the whole problem hinges upon the proper calculation of the velocity of a suspended particle acted upon by a force. The laws controlling the movement of particles through a continuous fluid phase have been defined

by Newton, Stokes and Svedberg: When a force is applied to a particle, the particle is accelerated, F = ma, until it reaches a velocity at which the resistance to its motion equals the applied force. In a settling tube, the applied force is the force of gravity, while in a centrifuge it is the centrifugal field w^2r. The two forces differ only in direction and order of magnitude. The gravitational field is along a radius of the earth (i.e. vertically down), while the centrifugal field is along a radius normal to the axis of rotation.

2.2 EFFECT OF SUSPENSION CHARACTERISTICS ON THE SETTLING BEHAVIOUR

A typical settling curve for a relatively concentrated flocculated suspension (class 3) is shown in Fig. 2.2 (Behn, 1957; Bond, 1960). Section 1 is termed the pre-flocculation period, in which the particles are interacting and growing in size; subsequently very little settling takes place. Section 2 is a period where the slurry interface travels downward at constant rate. This is commonly referred to as the initial rate period; the slope of the curve in this period, for a given material, is inversely proportional to concentration. Section 2 is a period of decreasing slope of the interface/time curve, and is commonly referred to as the changing rate period. The effect of increased concentration is to reduce the rate of settling along all portions of the settling curve.

A study of concentrated suspensions began with the work of Coe and Clevenger (1916). They studied the settling behaviour of slimes and described two types of settling.

Type 1: in which the slurry interface settles at a constant rate, down to a point which they identify as the critical point.

Type 2: in which the slurry interface settles at a constantly decreasing rate to the critical point, as shown in Fig. 2.3.

Coe and Clevenger define their critical point as the top of zone "D" just when zone "C" disappears, and state that, at this point, the flocs at the surface just rest upon each other, but compression has not yet started in the surface. Eckenfelder and Melbinger (1957) and Anderson and Sparkman (1959) stated that the mass rate of settling of solids is generally a minimum at Coe and Clevenger's "critical point" and the area requirement for thickening is determined by the concentration and settling velocity at that point.

Work and Kohler (1940) studied the effect of initial concentration on the settling properties of calcium carbonate and basic aluminum sulphate with barium sulfate. A log-log plot of slurry height versus time showed two straight line portions for each settling curve. The first portion began immediately after the constant settling rate period, where the subsidence rate begins to decrease. The second portion occurred when the settling was fairly advanced, and this

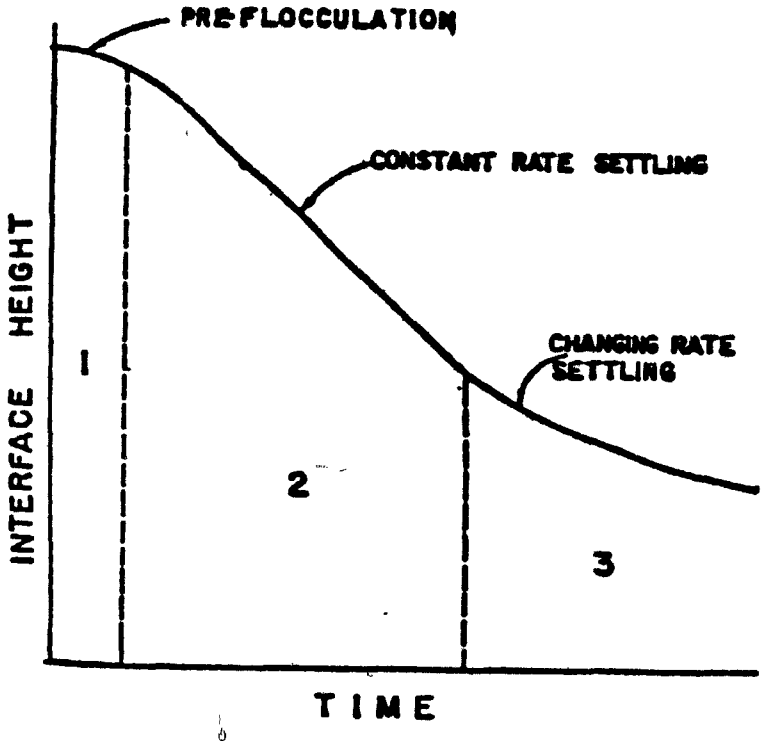

Figure 2-2: TYPICAL SETTLING CURVE FOR A FLOCCULENT SUSPENSION

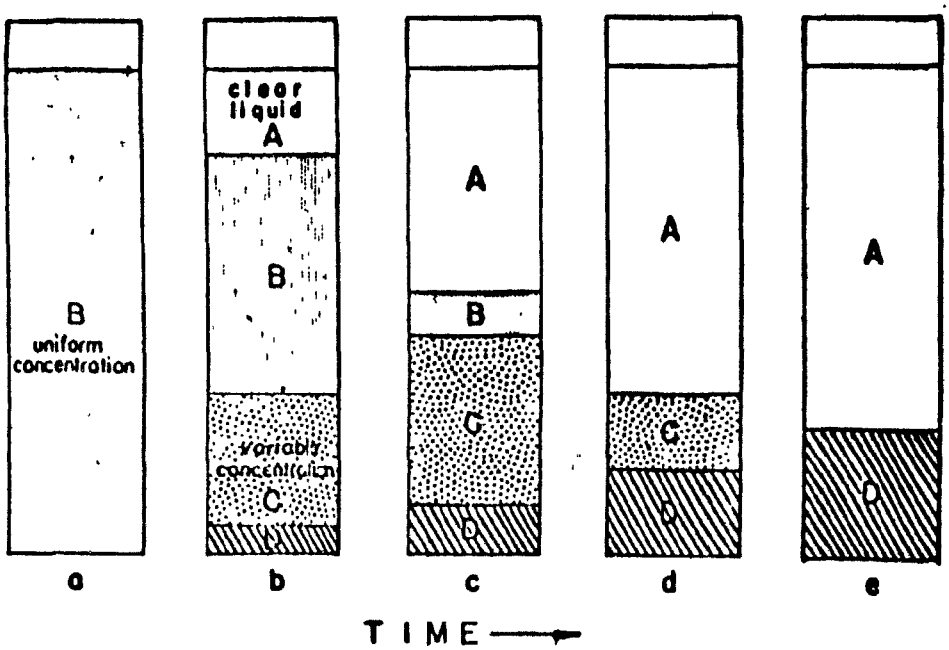

Figure 2-3: CHANGES IN CONCENTRATION LAYERS WITH TIME IN BATCH SEDIMENTATION

behaviour was likened to consolidation of soil. The slopes of both straight line portions were unaffected by initial concentration.

Several workers have proposed empirical or semi-empirical formulae relating concentration to settling velocity; most of these deal with the initial or straight line portion of the settling curve. Robinson (1926) proposed the use of a modified Stokes equation, in which the density of the solid particles and the viscosity of the fluid are replaced by the density and viscosity of the suspension.

Steinour (1944) made a fairly comprehensive settling study of various types of materials, expressing concentration in terms of voidage E. In a series of three papers, he reported on investigations of non-flocculant uniform size spheres, angular particles of uniform size, and flocculated powder suspensions. His equation for the spheres related settling velocity of individual particles to the voidage. This basic equation was modified for the more complicated cases by a factor w_1, which accounted for water carried down with the suspensions as part of the settling particles. As flocculation effects increased, the amount of entrained or trapped water, and accordingly, the values of w_1, increased. Dollimore and McBride (1976) investigated Steinour's equation by testing samples of metal carbonates; the plot of log v versus initial concentration yields a straight line with a slope (-b). Extrapolation of this graph to zero concentration

gives the rate of fall of a single particle in an infinite fluid. Substitution of this velocity into the Stokes equation yields a very simple method for the determination of the mean particle diameter of the solid undergoing sedimentation.

Hawksley (1951), gave an expression for the rate of settling of concentrated suspensions, based on the assumption that during the settling process, an "equilibrium arrangement" of particles was established. Lateral forces were assumed to produce a more or less uniform spacing in a horizontal plane, and the particles were presumed to arrange themselves in such a way that they offered the minimum resistance to the flow of the displaced fluid. The rate of settling of a suspension, relative to the fluid, was assumed to be equal to the Stokes velocity of a single particle falling in a fluid of viscosity μ_s, and density P_s, where μ_s, P_s, are the apparent viscosity and density of suspensions.

Robinson, Steinour, Hawksley all assumed that the effective buoyancy force acting on the particle depends on the density of the suspension. This cannot be true for a suspension of uniform particles all settling at the same rate, because each particle displaces its own volume of liquid as it settles. On the other hand, if a large particle is settling in a suspension of particles which are sufficiently small to behave as part of the liquid, the particle displaces an equal volume of suspension.

Richardson and Zaki (1954) examined experimentally the effect of concentration of suspended particles on their rate of settlement in view of finding a satisfactory method of correlating the results. The experimental work was confined to uniformly sized spherical particles, greater than 100 microns in diameter (glass Ballotini). For conditions of viscous flow, a relation was obtained, connecting the terminal falling velocity of a single spherical particle in an infinite medium (V_o), with the velocity of fall V, of a suspension of uniform spherical particles, contained in a vessel whose diameter was large compared with that of the particles. The relation was:

$$V = V_o \, E^n \tag{2.1}$$

where E is the voidage of the suspension, and

n is a constant equal to 4.65

Davies et al. (1976) have shown that n may be represented by

$$n = \frac{E_1}{1 - E_1} \tag{2.2}$$

where E_1 is the initial porosity, corresponding to maximum solid flux, for any system obeying the Richardson and Zaki equation (initial porosity for maximum sedimentation mass transfer).

Table 2.1 summarizes several of the proposed formulations relating slurry concentration to settling-velocity. The nomenclature for Table 2.1 may be found in Appendix A.

TABLE 2.1 Equations Relating Settling Velocity to Concentration*

Author(s)	Equation
Robinson	$V_g = \frac{K_2 d^2 (P_s - P_f)\ g}{\mu_s}$
Hawksley	$V_g = \frac{d^2 (P_s - P_f)\ g}{18\ \mu_s}$
Steinour	$V_g = \frac{V_o\ E^3}{1 - E} \cdot \Phi(E)$
Steinour	$V_g = 0.123\ V_o \frac{E^2}{1-E}$
Steinour	$V_g = K\ V_o \frac{(E - w_i)^3}{1 - E}$
Rouse	$V_g = \frac{V_t}{b} \left[1 - (\frac{C}{a})^{2/3} \right]$
Kalinske	$V_g = V_t - K_1 q$ where $q = FC^P$
Loeffler and Ruth	$V_g = V_o \left[\frac{1}{E} + \frac{2K_2(1-E)}{E^3} \right]^{-1}$
Bond	$V_g = V_t \left[1 - fC^{2/3} \right] = V_t E_c$
Richardson and others	$V_g = V_t\ E^n$
Richardson and Meikle	$V_g = 0.14\ g\ V_o \frac{E^3}{(1-E)}$
Oliver	$V_g = V_o\ (1 - K_3 C)(1 - K_3 C^{1/3})$

* The variables appearing in these equations are explained in Appendix A.

Figure 2.4 shows a typical family of settling curves for flocculant suspensions (Escritt, 1953). As the initial concentration increases, the following occurs:

a. length of pre-flocculation phase increases.
b. slope of constant rate period decreases.
c. changing rate section is shifted upward and to the right.

Figure 2.5 illustrates a typical family of settling curves for a non-flocculant suspension. The most significant differences between the two types of curves are the absence (or near absence) of pre-flocculation in the non-flocculant suspension settling curve, and the length of the changing rate settling section. The non-flocculant suspension curves appear to have a more clearly distinguished changing rate section and approach a definable final settled height; the changing rate section of the flocculant suspension curves is longer and does not approach a well-defined final settled height, but settles at a slowly decreasing rate, approaching the final settled height.

2.3 EFFECT OF ELECTROVISCOSITY ON SEDIMENTATION ANALYSIS

In clay suspensions, Eugene (1917) has pointed out that the only considerable force opposing the applied force is osmotic pressure, which is a property common to colloidal particles. A second property of colloids is the presence

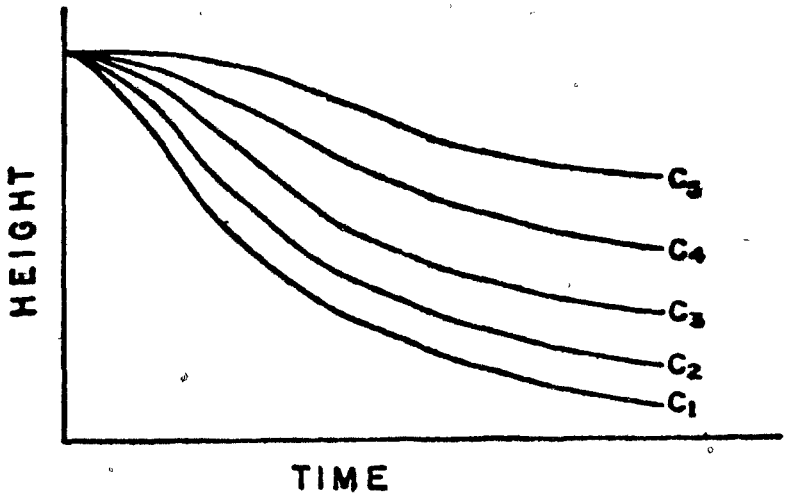

Figure 2.4: TYPICAL FAMILY OF SETTLING CURVES FOR A FLOCCULENT SUSPENSION.*

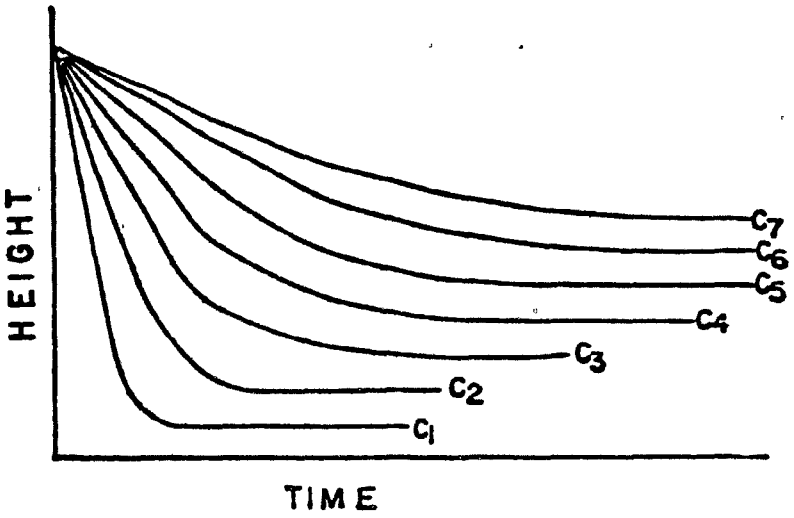

Figure 2-5: TYPICAL FAMILY OF SETTLING CURVES FOR A NON-FLOCCULENT SUSPENSION **

* Bond, A.W., (May 1960)

** Shannon, Dehaas, Stroupe and Tory (1964)

of an electric charge at the surface of the particles. The charge can be either positive or negative, and is due to the adsorption of ions or the ionic dissociation at the surface of the particles. Naturally, the presence of similar electric charges on the particles would lead to an electro-repulsion force between particles.

Pavlik and Sansone (1973) pointed out that charged particles in weak electrolytes have associated with them an electrical double-layer. When these particles settle under the force of gravity, the double layer is distorted with the result that an electric field, opposed to the force of gravity, is set up. The force exerted by this field (electroviscous force) may represent an appreciable fraction of the total resistance to motion for small particles. A charged particle suspended in an electrolyte solution attracts to its surface a layer of oppositely charged ions. When the charged particles are settling in a liquid, a potential gradient or "sedimentation potential" develops in the fluid. The electric field exerts a force opposed to the downward motion of the sedimenting particles and this force has been termed the electroviscous force.

The magnitude of electroviscous force depends on the thickness of the double-layer surrounding the particles. Elton and Hirchler (1954) have proposed the following expression to describe the sedimentation of monodispersed spheres, taking into account the possible electroviscous effect:

$$V = \frac{(P_p - P_f)\, g\, d^2}{18\mu} - \frac{d \cdot E \cdot \sigma}{3\mu} \qquad (2.3)$$

where E is the sedimentation potential gradient (volt/cm)
$= \pi\, d^2\, \sigma\, V\, N/K$

N is the number of particles per unit volume of suspension cm^{-3}

K is the specific conductivity of the suspension ($ohm^{-1}\ cm^{-1}$)

σ is the electrokinetic charge per unit area of the particle ($e.s.u./cm^2$)
$= \left(\frac{P_p\, \mu K\, (V_o - V)}{2\, M\, v}\right)^{1/2}$

v is the terminal velocity in a given fluid

V_o is the terminal velocity determined in the absence of electroviscosity.

and M is the mass of particles per unit volume of suspension.

It can be seen that the reduction in the settling rate of a sphere due to the electroviscous effect is directly proportional to the magnitude of the sedimentation potential gradient and the electrical charge on the particle.

2.4 EFFECT OF CENTRIFUGAL FORCE ON SEPARATION OF MATERIALS OF DIFFERENT DENSITIES

According to P. Arrne Vesilind (1977) a batch settling test can be conducted at high centrifugal forces using a desk top centrifuge and strobe light; the test tubes

are filled with the suspension and spun on a horizontal plane, and the strobe light is synchronized with the centrifuge so that the height of the slurry-liquid interface can be observed with time at any centrifuge speed.

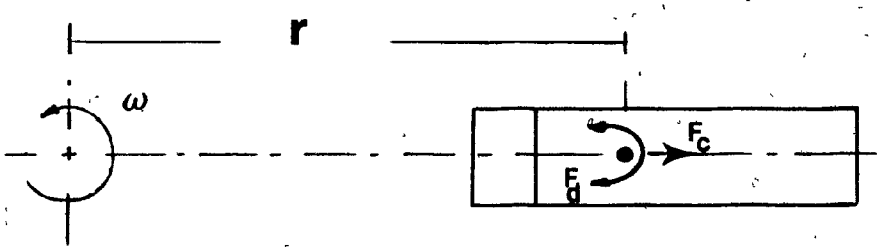

Fig. 2.6 A Particle Settling Under Centrifugal Force in a Test Tube

Centrifugal sedimentation is based on a density difference between solid and liquid. Consider a particle in a solution, held in a rapidly spinning centrifuge. This particle, as it is settling in the centrifugal field, has two forces acting on it, the centrifugal force and the drag force. If the rotor turns with an angular velocity w (radians per second), the particle experiences a centrifugal force. This force can be described as

$$F_c = w^2 r \, (P_s - P) \, V \qquad (2.4)$$

where r = radius from the centre of rotation to the particle (cm)

P_s = density of the particle (gm/cm^3)

P = density of the fluid (gm/cm^3)

V = volume of the particle (cm^3)

The force is balanced by the drag force F_d, which can be written as

$$F_d = C_D \frac{A\ v^2\ P}{2} \qquad (2.5)$$

where A = projected area of the particle (cm^3)

C_D = drag coefficient

v = particle velocity (cm/sec)

Assuming laminar flow (C_D = 24/Reynolds number) and spherical particle shape

$$F_c = F_d \qquad (2.6)$$

the above equation can be rearranged to read (Appendix A-21)

$$\frac{v}{w^2 r} = \frac{(P_s - P)\ d^2}{18\ \mu} \qquad (2.7)$$

The term on the right hand side is Stokes' law, with the gravity term missing, and contains variables which are solely properties of the slurry, while the term on the left hand side of the equation represents an operational variable of the centrifuge.

The term v/w^2r has been used in biology to characterize the stability of single cells in ultra-centrifuge and is termed the "settling coefficient" S. In gravitational thickening, if it is assumed that the slurry interface velocity is a function of the solid concentration only, then the same assumption can be made for settling in a test tube centrifuge. However, the radius changes as the solids

move rapidly outward and thus, the centrifugal force imposed on the slurry increases and the interface velocity could well be influenced by the increasing radius during settling. This difficulty can be eliminated by recognizing that

$$v = \frac{dr}{dt} \tag{2.8}$$

$$\frac{dr}{dt} = w^2 r\ S \tag{2.9}$$

Integrating,

$$\text{Ln}\ \frac{r_2}{r_1} = w^2\ S\ (t_2 - t_1) \tag{2.10}$$

where r_1 and r_2 are the positions of the interface at times t_1 and t_2 respectively.

A graph of Ln (r_2/r_1) versus (t_2-t_1) yields the slope w^2s and hence S, since the rotational speed is known. If the settling coefficient is truly a variable which describes the settleability of a slurry in a centrifugal field, v/w^2r should be independent of w^2r.

In other words, as either w or r increase, the settling velocity should increases so as to hold the value of v/w^2r unchanged.

The "settling coefficient" is suggested as a measure of settleability of a slurry in a centrifuge and is thus representative of the slurry characteristics. According to White and Lockyear (1978), when a suspension is subjected to a centrifugal force two important effects are apparent. First, the rate of settlement of individual particles increases;

furthermore, in the case where the concentration of particles is such that hindered or zone settling occurs, the rate of settlement of the interface (between the suspension and the supernatant liquor) increases also. The increase in settling rate is given by:

$$V_c = a\ V_g \qquad (2.11)$$

where V_c is the settling rate under an applied centrifugal force of ag

and V_g is the settling rate under gravity force with acceleration g

Secondly, as the suspension thickens and becomes more concentrated, water is expelled and must rise through the blanket. If the water has to pass through a long column of the suspension, the rate of thickening will be lower than for a short column. This effect can be further elucidated from the following argument. Consider a layer of slurry of concentration C and of thickness ΔX in a gravity column. The time required for the liquid, rising with velocity V, to pass through the layer is given by

$$T = \Delta X / V_g \qquad (2.12)$$

It is assumed that the same concentration of slurry occupies a layer in the centrifuge tube of thickness Δx, and that the liquid rises through the slurry with a velocity

$$V_c = B\ V_g \qquad (2.13)$$

where B is constant and reflects the different geometries of the two systems.

The time, t, taken for the liquid to pass through the layer will then be

$$t = \Delta x/B\ V_g \qquad (2.14)$$

It is also assumed that the ratio of thickness of the slurry layers, $\Delta X/\Delta x$, is equal to the ratio of the initial suspension heights, H/h; then,

$$T = B\ t\ (H/h) \qquad (2.15)$$

The depth of slurry in centrifuge tube is small compared with a gravity thickener, and so the rate of thickening is very rapid.

According to Brugger (1976), the size determination by centrifugal sedimentation is limited for small particles by their Brownian motion. The terminal speed $\dot{r}$, of a particle at a radial position r in the centrifuge, and Δt, the time required to move radially between r_1 and r_2, is given by the familiar centrifugal equations

$$\dot{r} = 1/18 \cdot \Delta P/\mu \cdot D^2\ w^2 r \qquad (2.16)$$

and

$$\Delta t = 18 \cdot \mu/\Delta P \cdot 1/D^2\ w^2 \cdot \mathrm{Ln}\ r_2/r_1 \qquad (2.17)$$

where D represents the Stokes diameter of particle

ΔP is the density difference between particle and fluid

μ is the viscosity of the fluid

w is the angular velocity of the centrifuge

On the other hand, the mean square displacement in a radial direction due to Brownian motion, in the time

interval Δt, is given by

$$\Delta \bar{r}^2 = \left(\frac{2KT}{\mu}\right) \Delta t \qquad (2.18)$$

where μ is the coefficient of the Stokes drag term = $3\pi\mu D$

K is Boltzmann constant = 1.38×10^{-16} erg/K^{o}

T is absolute temperature (^{o}K)

For a size determination to be meaningful, the displacement of the particles due to Brownian motion must be smaller than their displacement under the centrifugal force, hence the condition

$$D^3 >> 12/\pi \cdot KT/\Delta P \; w^2 \cdot \mathrm{Ln}\,(r_2/r_1)/(r_2-r_1) \qquad (2.19)$$

Ambler (1952) has specified the situations in which the centrifuge could be used; these are:

1. Separation of immiscible liquids
2. Removal and recovery of solids from a dispersion
3. Removal of excess liquid from solids.

He also modified Stokes law to take account of the centrifugal force. The mathematical relationship governing the velocity of migration of the dispersed phase was developed by Stokes. The centrifugal force causes the particles of the dispersed phase to migrate with a velocity (v_c) in a direction opposite to that of the continuous phase. The effective force operating on a particle in a centrifugal field is

$$F = (m - \bar{m})\, w^2 r \qquad (2.20)$$

where m is the mass of dispersed particles

$\bar{m}$ is the mass of equivalent volume of continuous phase that it displaces

w is angular velocity (r.p.m.)

r is distance from the centre of rotation.

If it is assumed that the particle is a sphere of diameter D then the equation becomes

$$F = \pi \Delta P \frac{D^3}{8} w^2 r \qquad (2.21)$$

where $\Delta P = P - P_1$

P_1 = density of continuous phase

P = density of dispersed phase

The movement of the dispersed phase particle is hindered by the resistance of the continuous phase to motion through it. This resistance force is proportional to the velocity of the moving particle and, for the particular case of a spherical particle, is defined by Stokes law as

$$F_1 = 3 \pi \eta D v \qquad (2.22)$$

where η = viscosity of the continuous phase

From 2.21 and 2.22

$$V_c = \frac{\Delta P D^2 w^2 r}{18 \mu} \qquad (2.23)$$

In a gravitational field, $V_g = \frac{\Delta P D^2 g}{18 \mu}$

Thus, the centrifugal field differs from the gravitational field in that it may be hundreds or thousands of times greater. Also it varies in proportion to the distance from the centre of rotation (r), so that the sedimentation

velocity of a particle increases as it moves outward from the axis of rotation, while in the gravity field, its equilibrium velocity is independent of position.

2.5 CURRENT APPROACHES TO SETTLING TANK DESIGN

The first attempt to consider the effect of solids concentration on settling velocity and to develop a rational basis for continuous thickener design, was made by Coe and Clevenger (1916). Working with metallurgical slimes, they developed procedures for determining the relationship between settling velocity and concentration from the results of batch settling studies. This procedure requires several separate settling tests, which involve the experimental determination of the initial settling velocity at several concentrations between the influent and desired underflow concentrations.

Their method is based on the premise that, in a continuous thickener, the solids must be able to pass through all concentration levels between the inflow and underflow concentrations, as rapidly as they are fed into the unit. If, at any particular level, the area is insufficient to accommodate the mass of solids passing, this concentration layer will build up in the basin and all solids in excess of the basin capacity - under these conditions of feed and underflow - will overflow. The most limiting concentration value between the influent and desired underflow concentrations

has been termed the critical concentration. Considering water release and solids balance in a continuous thickener under dynamic equilibrium conditions, Coe and Clevenger derived the following formula

$$U.A. = 1.33 \frac{(F - d)}{V_g G} \qquad (2.24)$$

where U.A. = required unit area of basin (ft^2/ton solids/day)

F = feed dilution (mass ratio liquids to solids)

d = underflow dilution (mass ratio liquids to solids)

V_g = settling rate (ft/hr)

G = specific gravity of liquid

The experimentally determined values of F and R, for a desired underflow concentration, are inserted in the above equation and the maximum value of unit area (U.A.) is used as the area requirement. The solid concentration associated with the maximum area is the critical concentration. The major disadvantage of the Coe and Clevenger approach is the necessity of conducting several settling tests. Most of the recent approaches to basin design involve attempts to determine the capacity-limiting concentration from the results of a single batch settling test. The most promising of these approaches is based on Kynch's (1952) mathematical analysis of the batch settling process.

Kynch, assuming that the velocity of fall of particles in a dispersion is a function of the local concentration only, proved mathematically that the concentration layers

travel upwards at a constant rate and develop the shape of the subsidence curve for the liquid-solid interface. Kynch's conclusions do not depend on any assumptions as to the mechanism of the settling process.

Talmadge and Fitch (1955) were the first to utilize the Kynch analysis for basin design purposes. Using the results of a single settling test, they determined the relationship between settling velocity and concentration as follows:

Considering a batch test with uniform initial concentration sufficiently high to result in zone settling, a plot of interface height versus time might be illustrated as shown in Fig. 2.7. The interface will be observed to move downward at a constant velocity, until a time t_A', after which the rate begins to decrease. Solids in the height time O-A'-H_o are all at the initial concentration and are settling at the rate associated with that concentration. As the solids settle toward the bottom of the container, concentration layers build up from the bottom. Line OA' represents the path of upward propagation of a solid concentration layer C_A, which is just slightly higher than the initial concentration. When C_A intersects the slurry-liquid interface, at time t_A, the subsidence velocity of the interface changes to that associated with the concentration C_A. The settling velocity is an inverse function of concentration, and since C_A is greater than the initial concentration C_o, the result is a reduction of the slope,

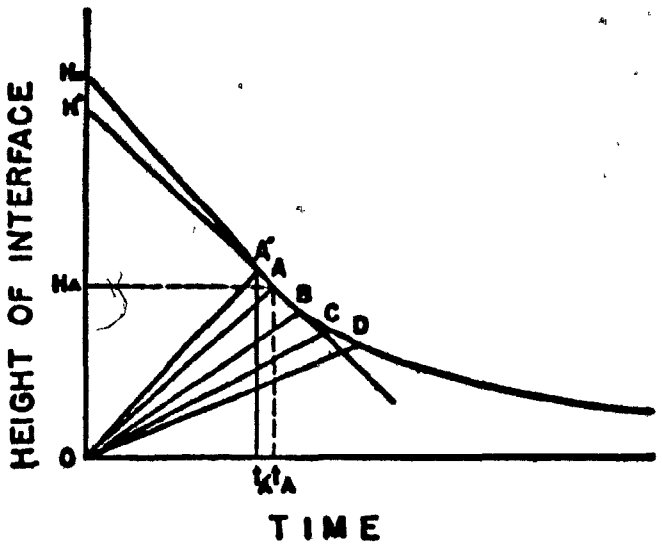

Figure 2-7: DETERMINATION OF VELOCITY CONCENTRATION RELATIONSHIP (TALMADGE AND FITCH APPROACH).

or settling velocity of the interface. Similarly, lines OB, OC, and OD are lines of progressively greater concentration, travelling upwards at different but constant rates, and changing the rate of interface subsidence to that rate associated with the concentration at the interface.

If concentration layers travel upwards in straight lines, from the origin to the interface, and upon intersection with the interface, determine the slope (settling velocity) of the curve, it is then possible to determine the relationship between concentration and settling velocity, by use of a material balance equation. Using the concentration layer C_A of Fig. 2.6 as an example, the value of C_A may be determined as follows:

Layer C_A starts from the origin (bottom of cylinder at time zero), travels upwards at a constant rate, U_A, and intersects the liquid-solid interface at time t_A. While layer C_A travels along this path, O-A, all solids present in the basin ($C_O H_O A$) must have passed through this layer, because it starts at the bottom and ends at the slurry-liquid interface. Assuming the settling velocity to be a function of concentration only, the rate of passage of solids relative to the layer C_A would be the sum of the rise velocity, U_A, of the layer, and the settling velocity, V_A, of the solids relative to the wall (slope of the interface at A, the point of intersection). The solids balance would be as follows:

$$C_o H_o A = C_A (V_A + U_A) A t_A \quad (2.25)$$

where V_A is numerically equal to $H'-H_A/t_A$

and U_A may be expressed as H_A/t_A

Inserting these terms and simplifying

$$C_o H_o = C_A H' \quad (2.26)$$

or

$$C_A = \frac{C_o H_o}{H'} \quad (2.27)$$

where C_o = initial concentration

H_o = initial height

A = area of settling vessel

C_A = interface concentration at point A

V_A = slope of settling curve (settling velocity) at point A

U_A = rise velocity of concentration layer C_A

t_A = time to point A on settling curve

H' = intercept on vertical axis of tangent to settling curve at point A

Since C_o, H_o and H' are known or easily obtained, C_A, the concentration associated with settling velocity V_A can readily be calculated. Concentrations at other points such as B, C, D, can be calculated in a similar fashion and graphs relating the settling velocity to the concentration can be prepared.

The values of concentration and velocity can then be inserted into Coe and Clevenger's equation, and the unit area requirement determined.

In many cases, it is more convenient to use a modified form of their equation. A common form is as follows:

$$U.A. = \frac{1/C_x - 1/C_u}{V_x} \qquad (2.28)$$

where U.A. = unit area requirement (1000 cm^2/gm of solids/min)

C_x = concentration at any point x (gms solids/liter slurry)

C_u = desired underflow concentration (gms solids/liter slurry)

V_x = settling velocity at concentraiton C_x (cm/min)

The term $1/C_x - 1/C_u$ is comparable to the term $(F-D)/S$ of the Coe and Clevenger equation, in that both are numerically representative of the unit volume of water released from the feed, as it is concentrated to the underflow concentration. This volume, divided by the rise velocity of the released water, is equal to the basin area requirement.

Since this rise in velocity is greater than the settling velocity of solids, the solids will then overflow the basin. The maximum area calculated by equation (2.28) is thus the minimum that could be used to prevent solids overflow.

CHAPTER 3

EXPERIMENTAL MATERIALS, EQUIPMENT AND TECHNIQUES

3.1 MATERIALS FOR SETTLING TEST

Hydrite Flat D and Hydrite Ultra Fine Kaolinite, products of the Georgia Kaolin Company, were the test materials used in this study. Hydrite Flat D and Hydrite Ultra Fine Kaolinite clays were chosen because of their settling properties which cause them to undergo hindered settling (class 3 and 4) over a wide range of concentrations. The range of concentration evaluated was:

80 to 300 grams per liter for Kaolin Flat D

and 80 to 200 grams per liter for Kaolin Ultra Fine

The X-ray diffraction patterns, the grain size analysis and the index properties for the two clays used are shown in Figs. 3.1, 3.2 and Table 3.1 respectively.

3.2 SAMPLE PREPARATION

To ensure dispersibility of particles in the fluid, the kaolinite clay was dispersed in 15 meq/l sodium bicarbonate ($NaHCO_3$) solution. This choice of solution concentration was based on the need to establish proper dispersion of the clay particles, as discussed in previous studies by Yong et al. (1978) and Douglas and Yong (1981) on the effects of ion concentration on the dispersion stability of kaolinite particles in suspension.

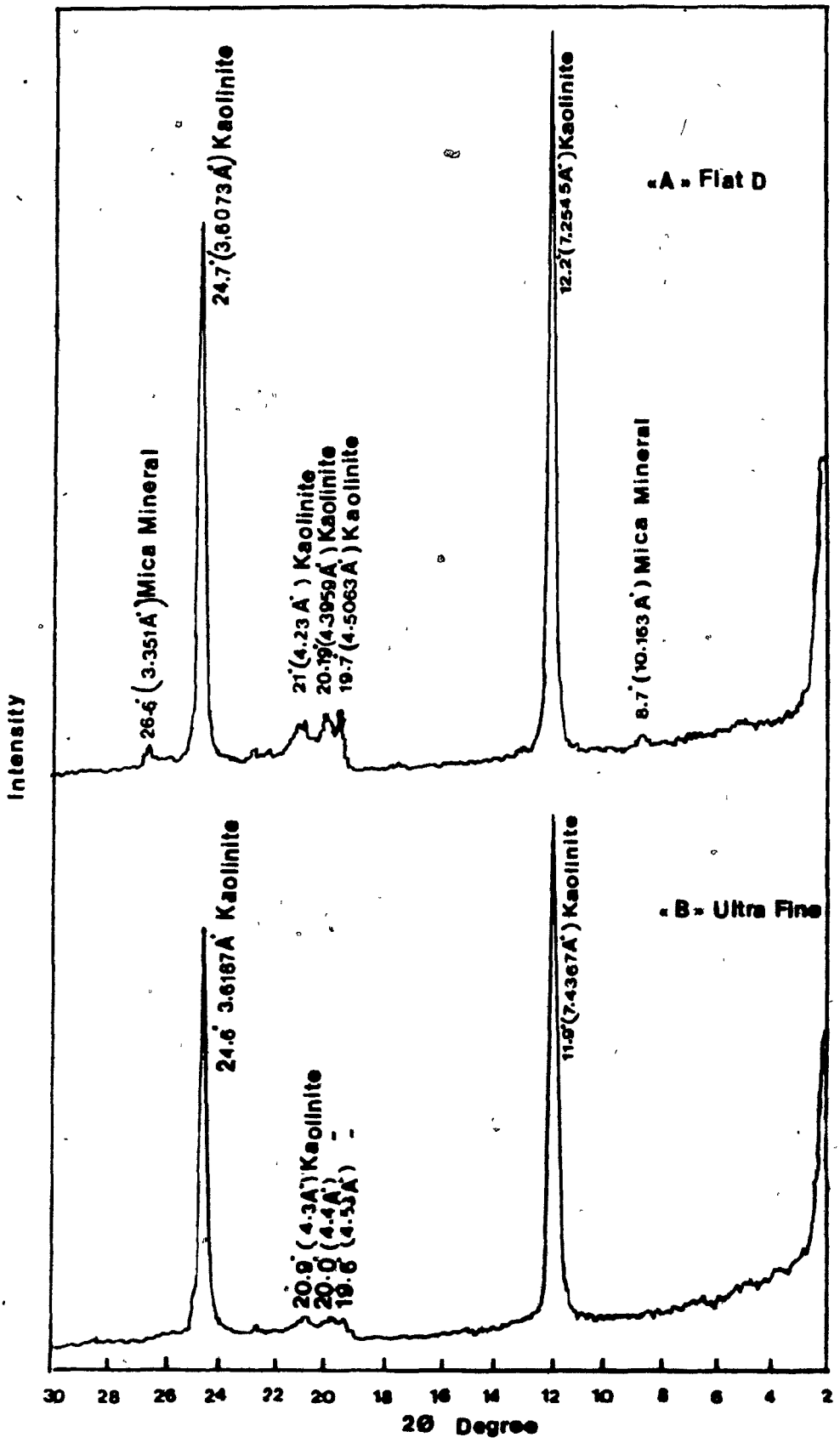

FIGURE 3-1 X-RAY DIFFRACTION PATTERN OF :
A-HYDRITE FLAT D KAOLINITE
B-HYDRITE ULTRA FINE KAOLINITE

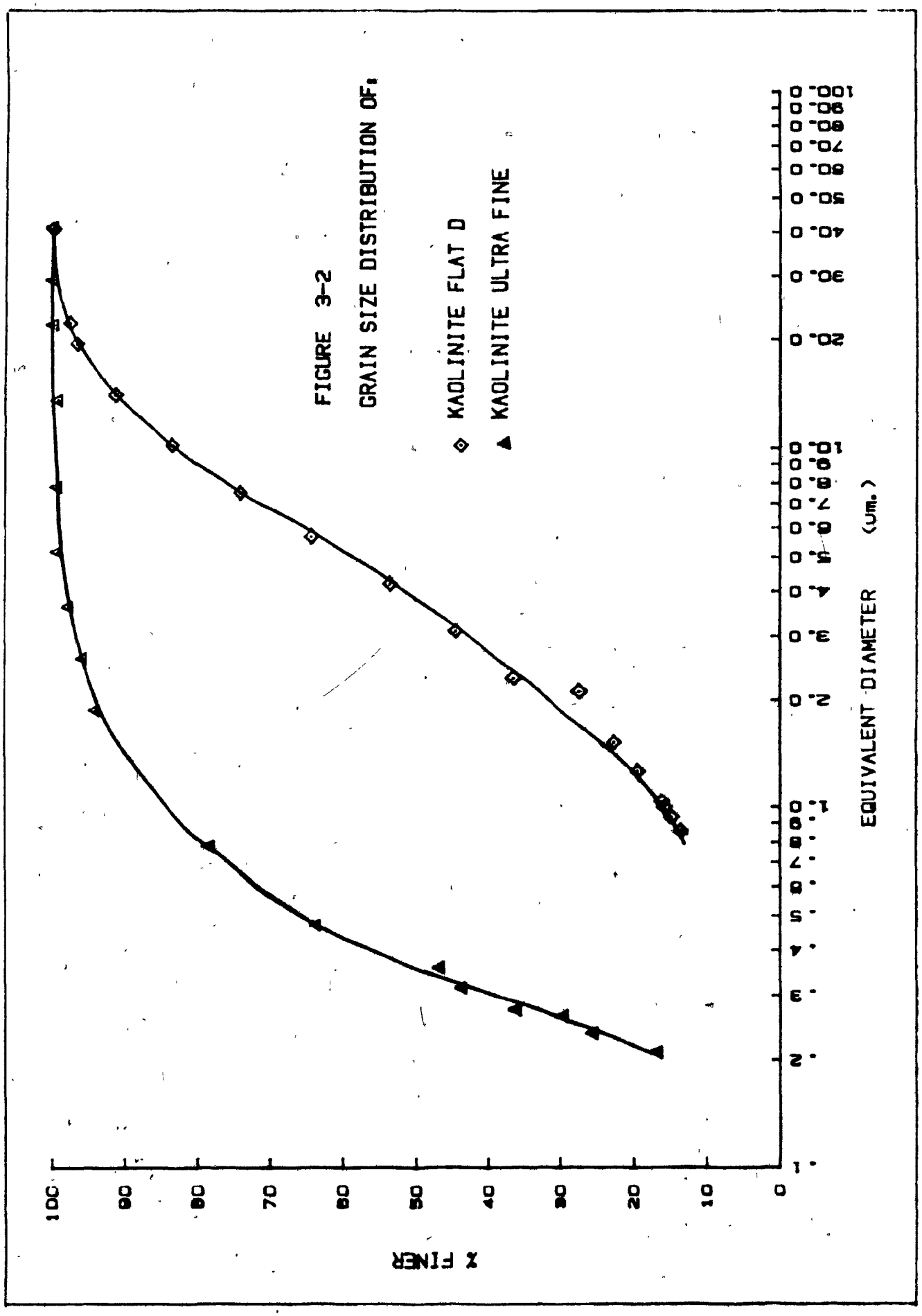
FIGURE 3-2
GRAIN SIZE DISTRIBUTION OF:
KAOLINITE FLAT D
KAOLINITE ULTRA FINE
% FINER
EQUIVALENT DIAMETER (um.)

TABLE 3.1 Index Properties

Properties	Hydrite Flat D	Hydrite Ultra Fine
Liquid Limit (L.L.)	46%	65%
Plastic Limit (P.L.)	29.5%	45%
Plastic Index (P.I.)	16.5%	20%
Specific Gravity (G_s)	2.62	2.58
D_{10}	0.62	17
D_{50}	3.8	36
D_{60}	5.3	45
Cu*	8.55	2.65

*Coefficient of uniformity (Cu) = D_{60}/D_{10}

The kaolinite suspensions were left for a period of 24 hours to reach equilibrium. To start the test, the settling tubes were turned end over end by hand 8 to 10 times. The choice of inverting the tubes (i.e. turning end over end) is based on studies by Alan and Justine (1962) which indicated that this method allows the aggregates to approach a fairly uniform average equivalent diameter.

3.3 DESCRIPTION OF THE SETTLING TEST

The settling characteristics of Hydrite Flat D and Hydrite Ultra Fine kaolinite were obtained by observing the solid-liquid interface in transparent plexiglass cylinders at frequent intervals. Both centrifuge and gravity tests were conducted in plexiglass cylinders with 112.5 mm diameter. The initial height of all suspensions was 320 mm. Plots of interface height versus time were made for each test run and the slope of the straight line portion was obtained directly from the graph as illustrated in Fig. 3.3. The slope so determined, is termed "initial settling velocity" and is related to the initial solids concentration.

3.3.1 Centrifuge Test

In this investigation, a laboratory centrifuge, as shown in Fig. 3.4, was employed. The centrifuge itself consists of a vertical shaft on top of which is mounted a 20 mm thick aluminum disc of 600 mm diameter. The shaft (and hence the disc) is rotated via a hydraulic motor.

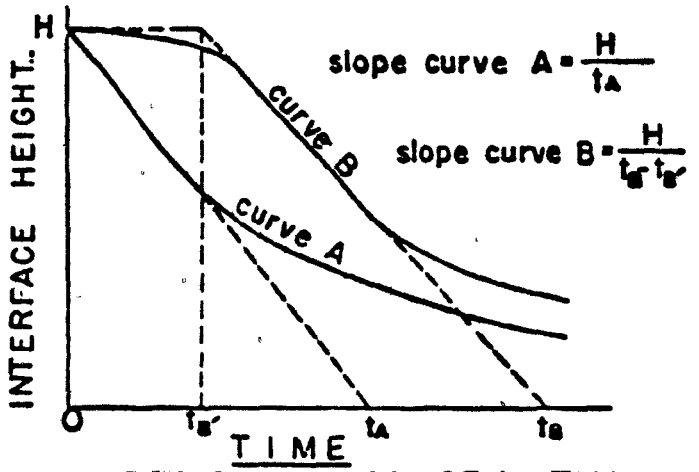

FIGURE 3-3 DETERMINATION OF INITIAL SETTLING VELOCITY.

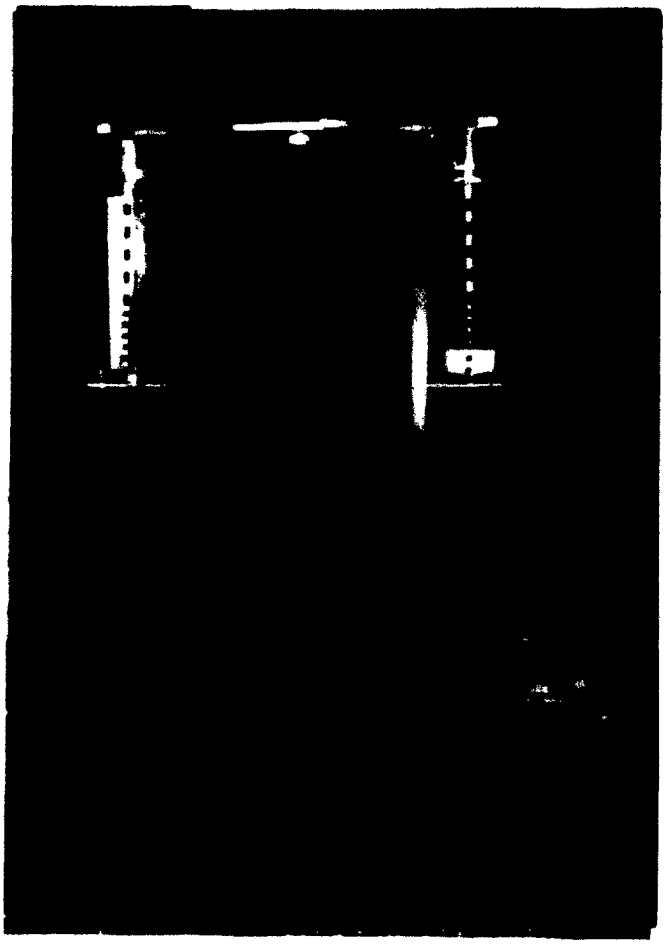

FIGURE 3-4 LABORATORY CENTRIFUGE APPARATUS

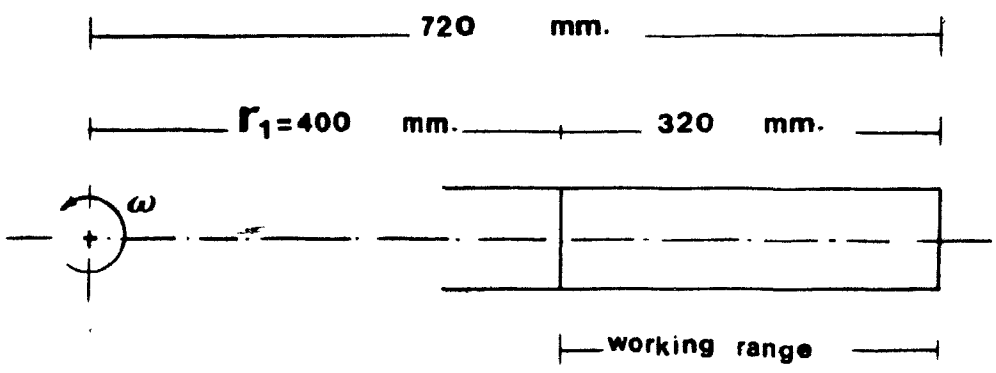

FIGURE 3-5 SCHEMATICALLY DIAGRAM OF CENTRIFUGE CYLINDER

COLOURED PICTURES
Images en couleur

Two tubes can be fixed to the disc, one filled with the supsension being tested and the other with tap water. In order to maintain the balance required during the rotation of the machine, the two tubes are fixed at 180° to each other with respect to the center of rotation. The disc is illuminated with a stroboscope so that the interface between the suspension and the supernatant can be observed. The relative centrifugal force (RCF) varies along the length of the tube. The change in RCF over the working range of the interface height (400-720 mm) is about 80%, see Fig. 3.5.

3.3.1.1 Limitations of Setting Centrifugal Speed

In determining settleability coefficients, it would have been desirable to use the same set of five speeds, for each of the seven concentrations tested, in order to facilitate the interpretation of results. Due to instrument limitations, associated with setting the centrifuge at pre-desired speeds, no five speeds for one concentration could be duplicated for any other concentration. Speeds were set via an excessively sensitive valve (equivalent to a fine adjustment knob only on a microscope) controlling the hydraulic pump. Due to the sensitivity of the valve, the duplication of any particular speed was difficult.

3.3.2 Gravity Test

The conditions for conducting the gravity tests were identical to those of the centrifuge tests, except for the

absence of any externally applied force (i.e. centrifugal force). The height of all suspensions, as in the centrifuge tests, was 320 mm and the tests were conducted in the same transparent plexiglass cylinders. Figure 3.6 depicts the cylinders employed for the gravity tests and the centrifuge tests. As in the centrifuge tests, the cylinders were turned end over end 8-10 times before the start of the gravity tests.

3.4 SEDIGRAPH PARTICLE SIZE ANALYZER

Figure 3.7 shows the sedigraph 5000 D particle size analyzer. It measures the sedimentation rates of particles in suspension and automatically presents the data as a cumulative mass percent distribution in terms of the Stokesian or equivalent spherical diameter in microns. The instrument determines, by means of a finely collimated beam of X-rays, the concentration of the particles remaining at decreasing sedimentation depths, as a function of time. The logarithm of the difference in transmitted X-ray intensity is electronically generated, scaled and presented linearly as "cumulative mass percent" on the Y-axis of an X-Y recorder. The instrument typically yields a particle diameter distribution over the range 50 to 0.18 μm. For details concerning the sedigraph 5000 D and its use, see Appendix A.

The construction of the sedigraph is illustrated schematically in Fig. 3.8. The radiation from an X-ray tube (1) with its associated power supply (2) is collimated by horizontal slits (3) and (4) to a beam .05 mm high and

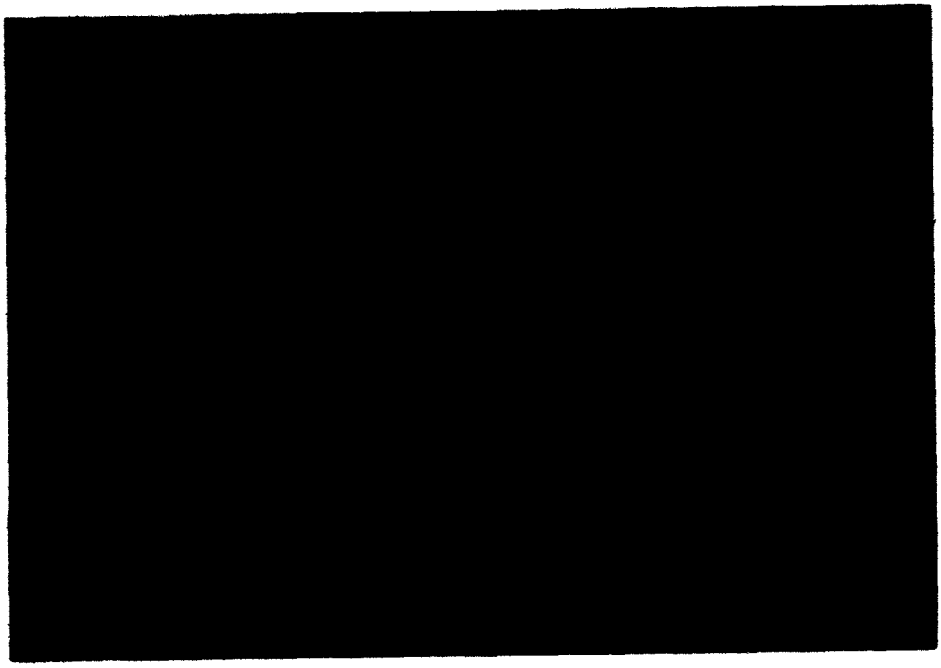

FIGURE 3-6 PLEXIGLASS CYLINDERS FOR GRAVITY AND CENTRIFUGE TESTS

COLOURED PICTURES
Images en couleur

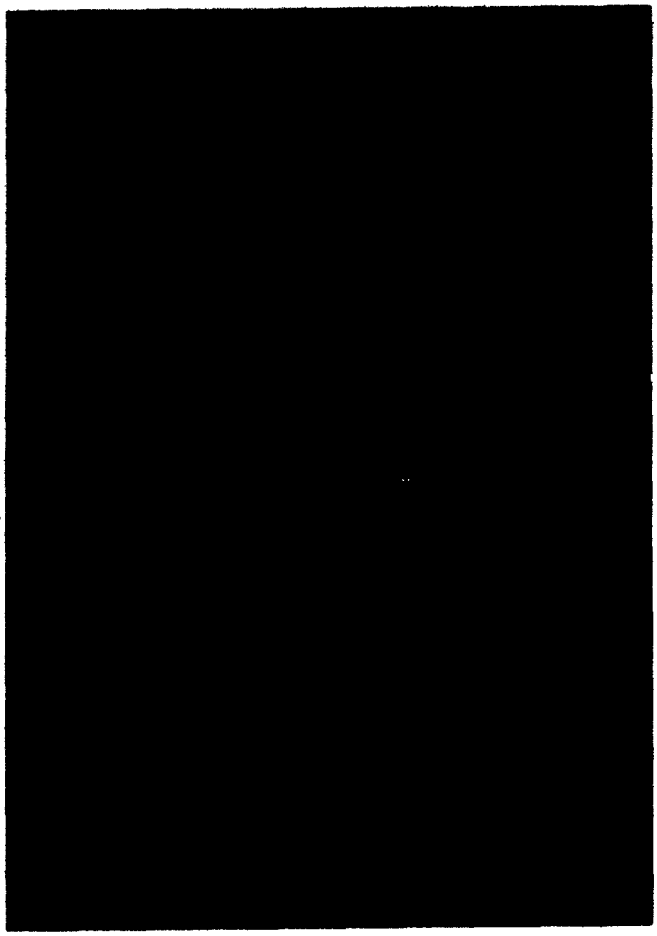

FIGURE 3-7 SEDIGRAPH 5000D

PARTICLE SIZE ANALYZER

COLOURED PICTURES
Images en couleur

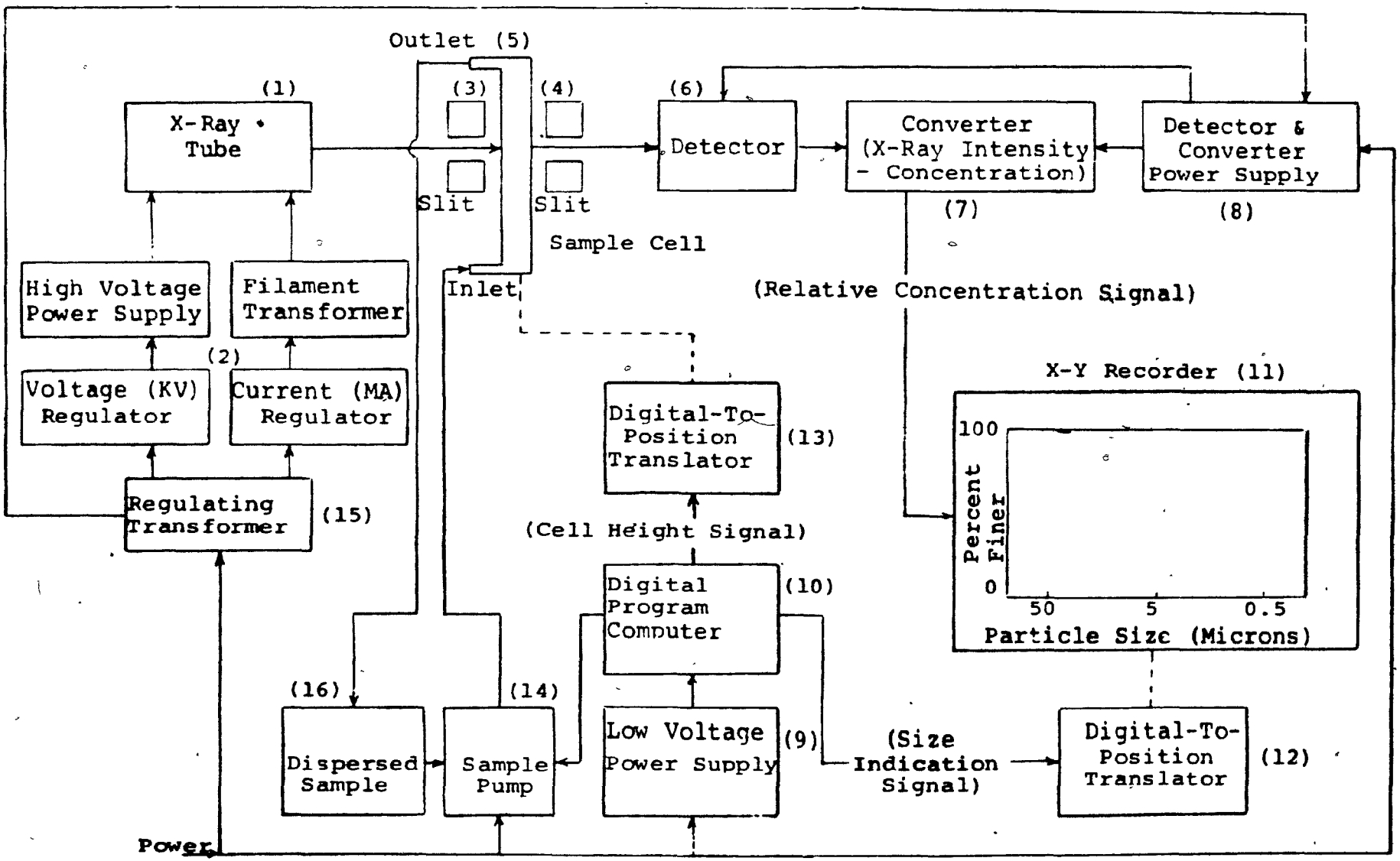

Figure 3-8 Functional Diagram of the Instrument

9.5 mm wide. The X-ray tube is a small, air cooled unit having a tungsten target inclined at about 30^{o} to a thin beryllium window. The tube is operated at a power level of about 13 watts. The X-ray beam passes through a sample cell (5), located midway between the collimating slits. The cell is of rectangular cross-section of internal diameter 12.7 mm , height 35 mm and thickness 3.5 mm. The cell is closed at the top and, in use, is completely filled with the dispersed sample.

3.5 RHEOLOGY

The Rheomat 15 T is used to determine the viscosity of the suspension, which is defined as the ratio of shearing stress to rate of shear, and can be visualized as a resistance to flow. Plotting the shear stress versus shear rate allows extrapolation of the value of gel strength, which is defined as the true shear stress at zero shear rate; its value is usually approximated, in Casson's model, by measuring the shear stress at a rate of shear of unity.

Figure 3.9 shows the Rheomat 15 T. The rotating part of the Rheomat 15 T is driven round in the clay suspension by a motor and the torque required to maintain a certain speed is measured. From the geometry of the measuring system, the rotational speed, the torque, the shear stress and shear

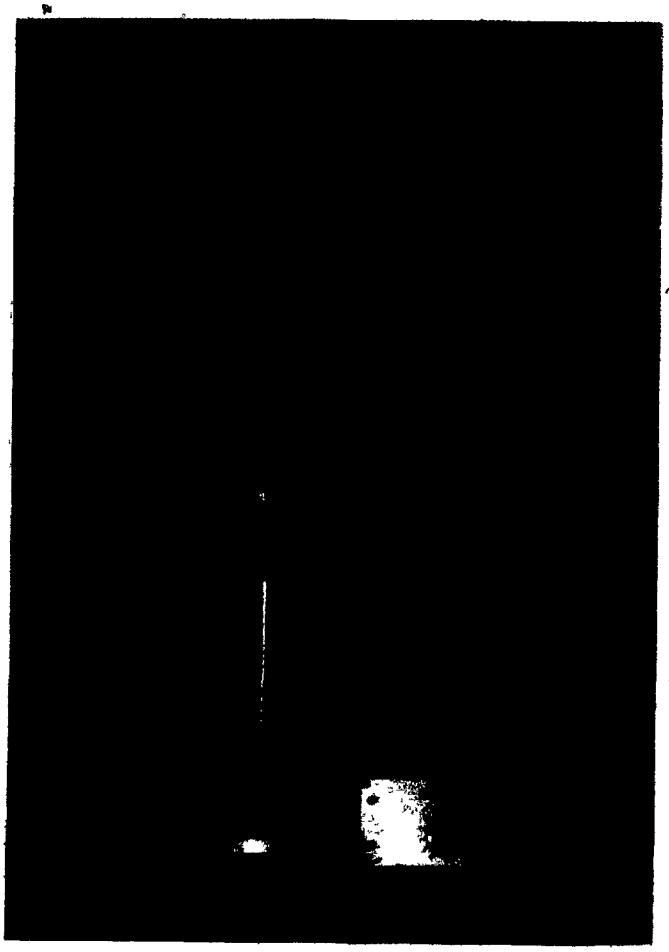

FIGURE 3-9 RHEOMAT 15T

FOR VISCOSITY MEASUREMENT

COLOURED PICTURES
Images en couleur

rate can be calculated and hence, the flow behaviour of the clay suspension can be deduced.

A number of suspensions (volume 200 cm^3) of Hydrite Flat D kaolinite in the concentration range of 8% to 50% by weight were prepared using the same technique discussed (Section 3.2). For each concentration, a suitable cup and cone was selected by trial and error; the readings of the torque indication scale were then taken for 15 speeds, starting from the lowest to the highest. These readings were then used in connection with the Casson model to determine the gel strength, the slope and the intercept. With these data, the viscosity at rate of shear of 50 sec^{-1} was determined.

CHAPTER 4

RESULTS AND DISCUSSION

4.1 RESULTS OF PHASE 1

Interface subsidence characteristics.

4.1.1 Relationship Between Initial Settling Velocity and Initial Concentration (Centrifuge Test, 100 r.p.m.)

4.1.1.1 Hydrite Flat D Kaolinite

The results of eleven settling tests are reported in this section. All tests were conducted in 112.5 mm diamenter cylinders, with an initial height of suspension of 320 mm. Solids concentration was the only variable and ranged from 8% to 30% (by weight). The method of preparing the samples is described in Section 3.2. The centrifuge speed was set (by trial and error) at a rotation speed of 100 r.p.m. and was kept constant throughout the tests. Initial settling velocities were determined by the technique shown in Fig. 3.3.

Figure 4.1 shows the settling curves for the eleven tests. From concentration 8% up to 16% (by weight) every curve shows a straight line portion beginning at the initial height of suspension, followed by a gradually decreasing settling rate; ultimately, in each curve, there is an abrupt change in the settling rate, indicating the virtual end of zone settling. An increasing tendency towards concavity in the curves can be observed with increasing concentration (beginning from 18% up to 30% (by weight)).

FIGURE 4-1 SETTLING CURVES AT DIFFERENT INITIAL CONCENTRATION (wt/wt)

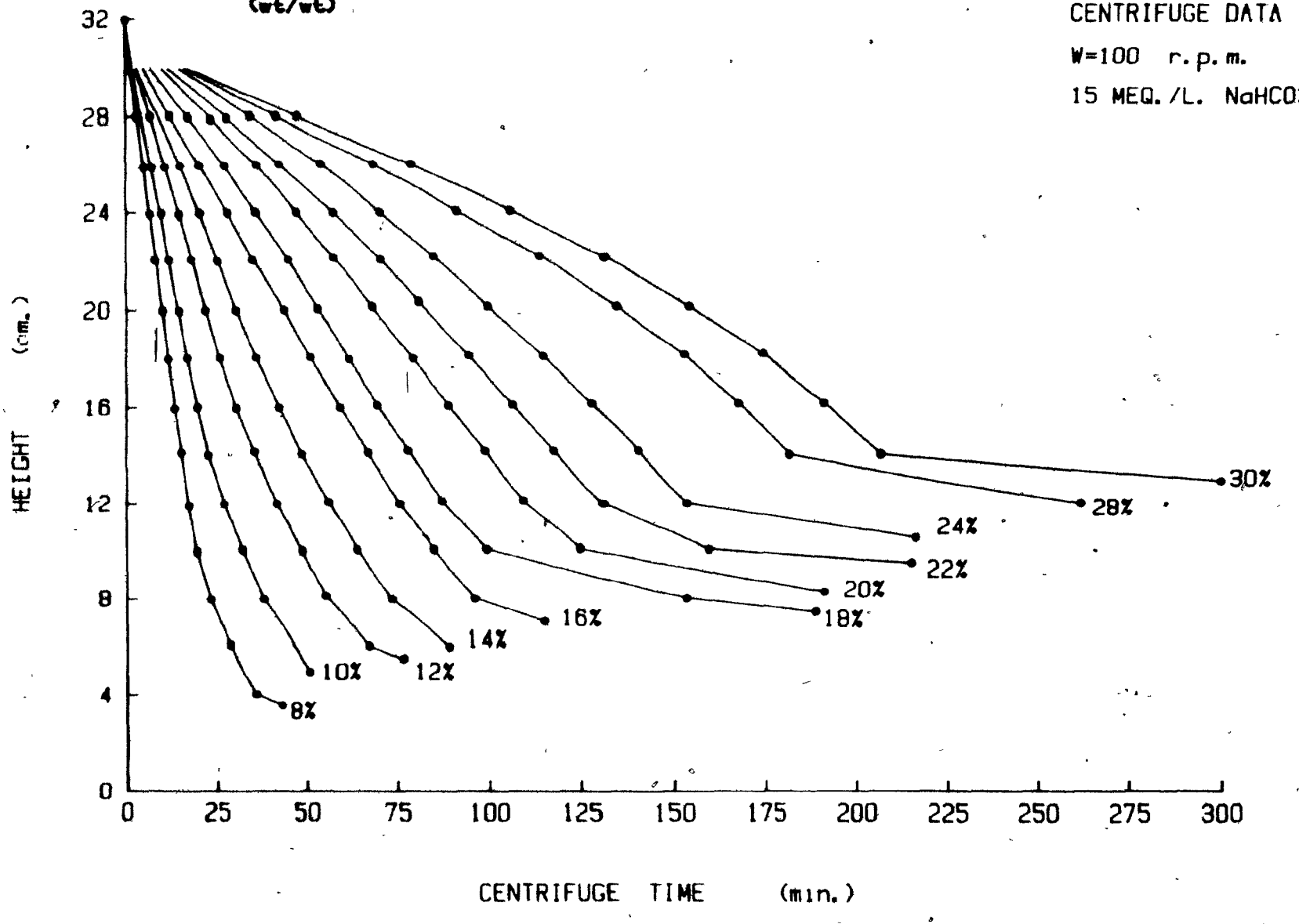

Figure 4.2 shows the relationship between initial settling velocity, see Section 3.3, and initial concentration, in the concentration range 8% - 30% (by weight). When the data points are plotted on a log-log scale (Fig. 4.5) a straight line is obtained, which may be approximated by the following equation:

$$V_c = 0.196 \times 10^{-3} \times C^{-1.858} \qquad (4.1)$$

$$R^2 = 0.998$$

where V_c = initial settling velocity under the influence of centrifugal acceleration in cm/sec

C = initial concentration in gm/cm^3

R^2 = correlation coefficient

4.1.1.2 Hydrite Ultra Fine Kaolinite

The results of seven settling tests using Hydrite Ultra Fine Kaolinite are shown in Fig. 4.3. The test conditions were similar to those of the Hydrite Flat D Kaolinite, with concentration being the only variable. The results indicate that the settling curves for concentration 8% and 10% (by weight) are characterized by a straight line portion describing most of the settling behaviour, followed by a gradual change in settling rate, indicating the end of zone settling. At concentrations of 12% through 20% (by weight) a tendency towards increasing concavity with increasing concentration can be observed in the greater part of the curve. This indicates an initially decreasing

FIGURE 4-2 INITIAL SETTLING VELOCITY-CONCENTRATION RELATIONSHIP

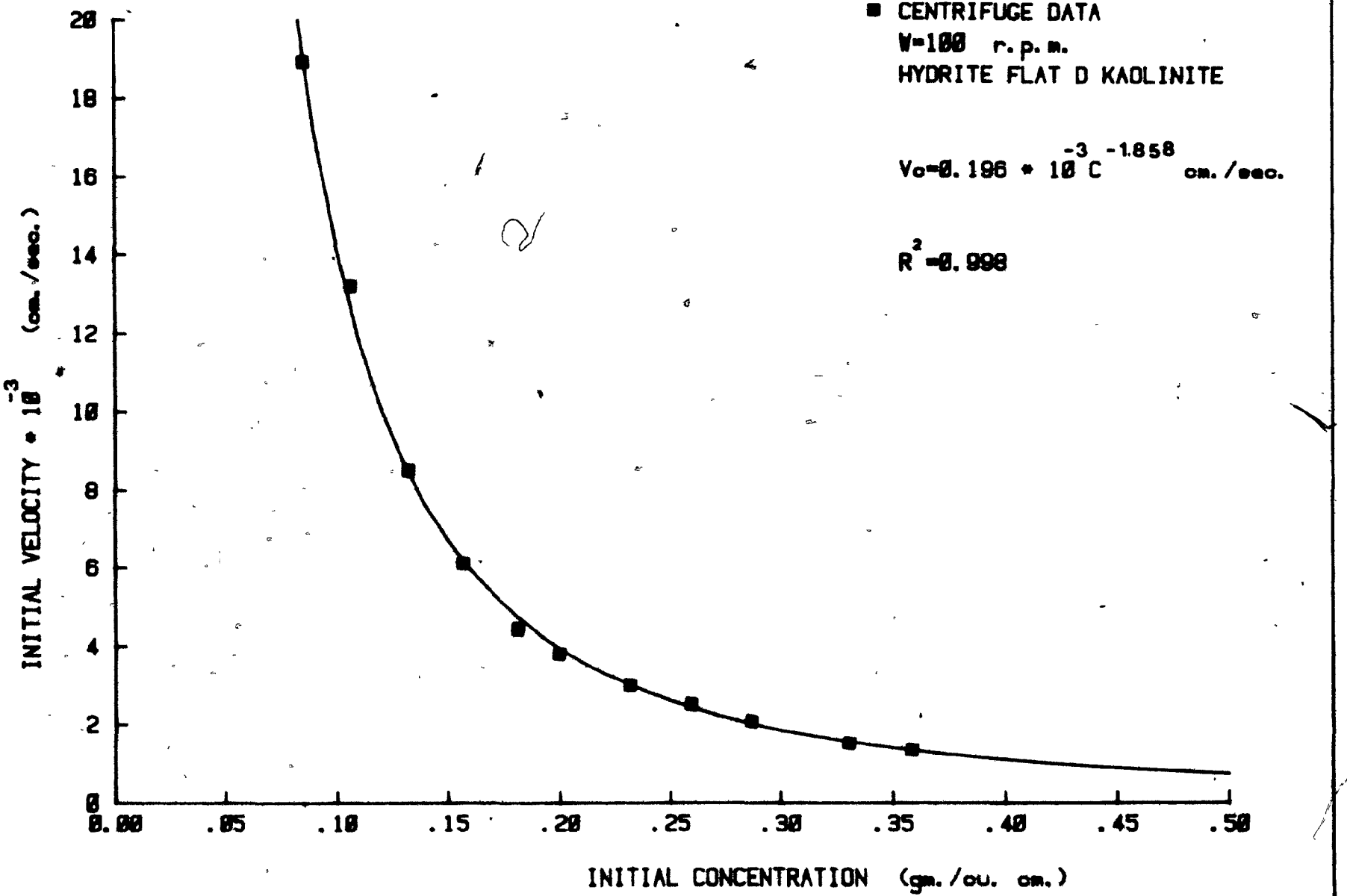

FIGURE 4-3 . SETTLING CURVES AT DIFFERENT INITIAL CONCENTRATION (wt/wt)

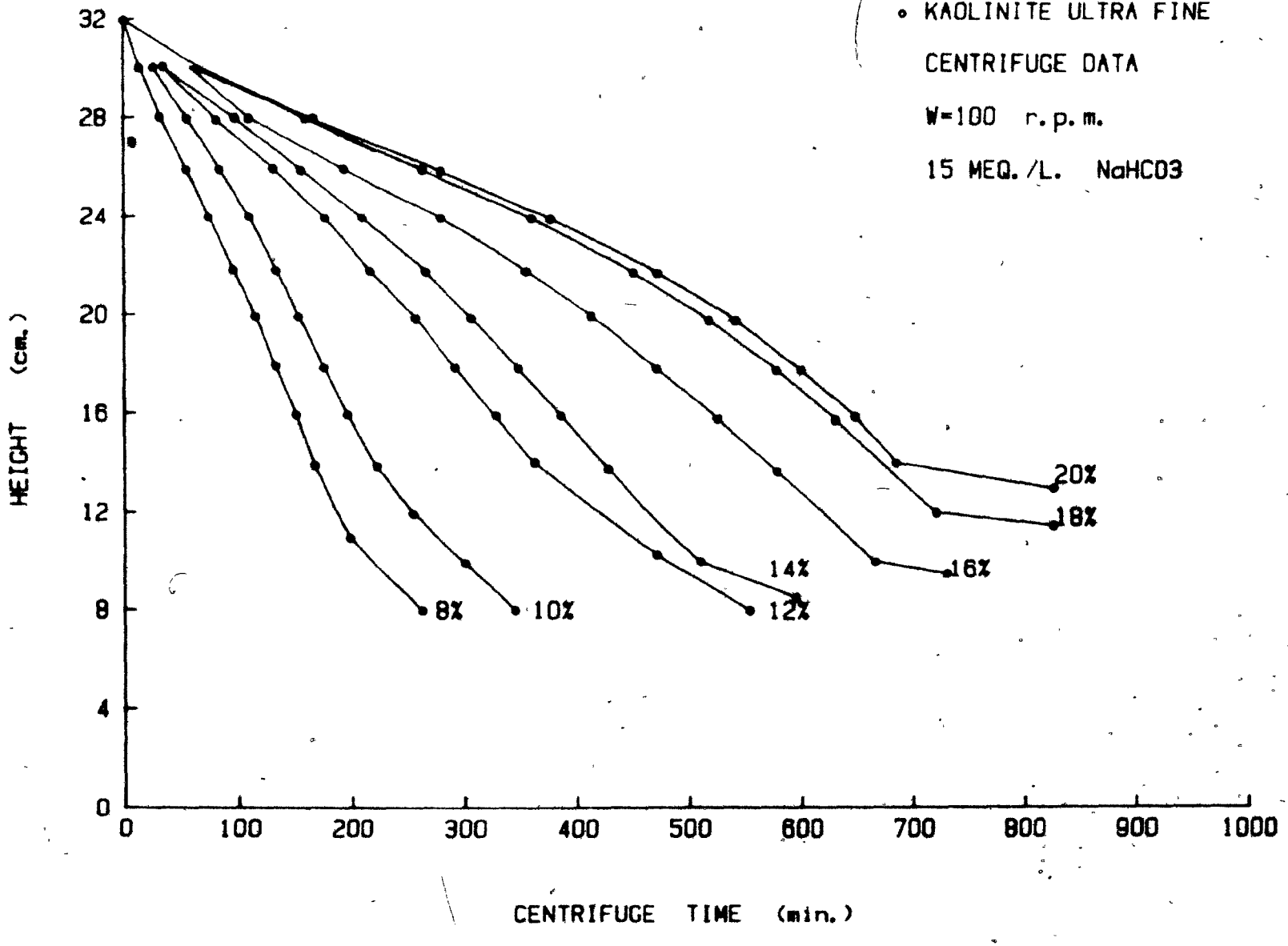

settling rate, followed by a gradually increasing settling rate. The concavity over most of the curve for these concentrations (i.e. 12% through 20%) is followed by an abrupt change in settling rates, indicating the end of zone settling.

Figure 4.4 shows the relationship between the initial settling velocity (see Section 3.3) and initial concentration, for the concentration range 8% - 20% (by weight). When the data points are plotted on a log-log scale (Fig. 4.5) a straight line is obtained, which may be approximated by the following equation:

$$V_c = 0.02 \times 10^{-3} \times C^{-1.819} \qquad (4.2)$$
$$R^2 = 0.974$$

where V_c = initial settling velocity under the influence of centrifugal acceleration in (cm/sec)

C = initial concentration in gm/cm^3

R^2 = correlation coefficient.

Figure 4.5 shows that the linear relationship describing the behaviour of the Hydrite Flat D kaolinite and Hydrite Ultra Fine kaolinite in log-log scales can be represented by parallel lines. The slopes of the two lines are approximately the same. This needs further explanation. The fact that the grain size distribution of Hydrite Ultra Fine kaolinite is finer than Hydrite Flat D kaolinite (see Fig. 3.1), indicates that the number of particles per gram solid of Hydrite Ultra Fine kaolinite

FIGURE 4-4 INITIAL SETTLING VELOCITY-CONCENTRATION RELATIONSHIP

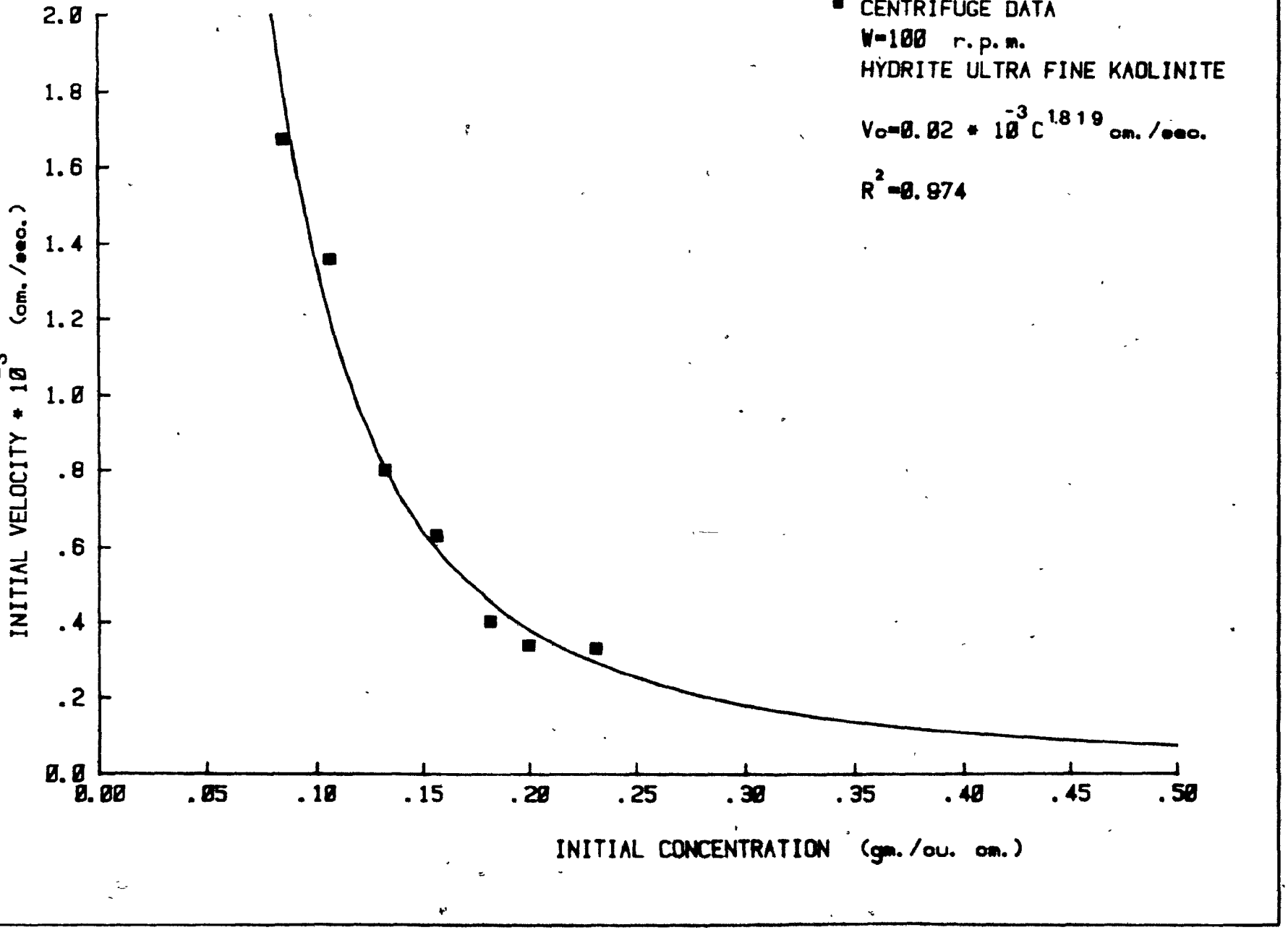

FIGURE 4-5 LOG (INITIAL SETTLING VELOCITY-INITIAL CONCENTRATION)RELATIONSHIP

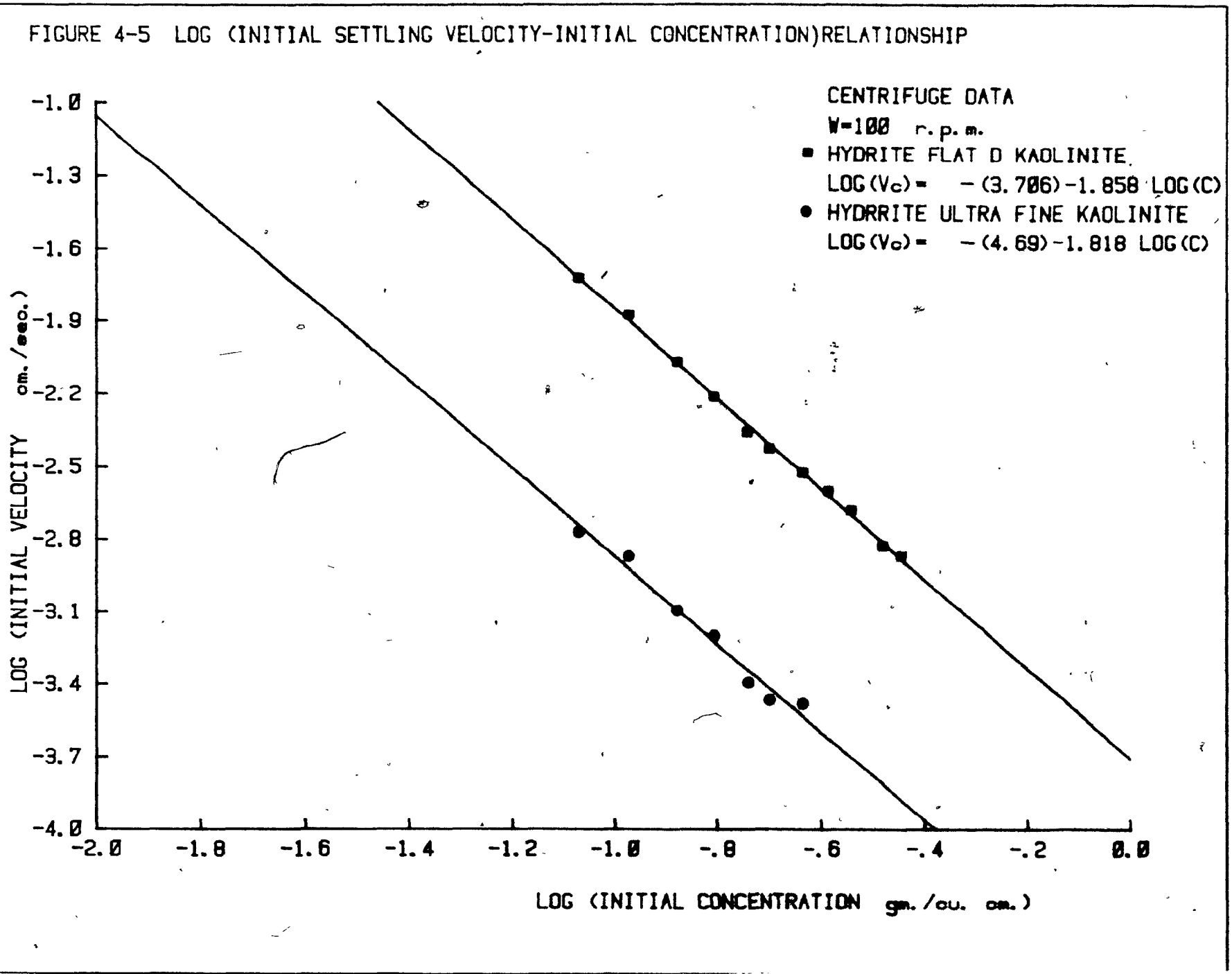

is larger that Hydrite Flat D kaolinite (Appendix A shows sample calculations of the number of particles per gram solid based on the grain size distribution (see Fig. 3.1)).

Figure 4.6 shows the relationship between log (initial settling velocity) and log (number of particles corresponding to the initial concentration) . The figure shows two straight lines with a small shift between them, which may be attributed to the approximate method used to calculate the number of particles per gram solid. It is expected that, had the determination of the number of particles been more accurate, the two segments would have joined into a single linear relationship. To examine the effect of viscosity, Fig. 4.7 shows the relationship between the product of velocity and viscosity versus initial concentration. The velocity is the initial settling velocity of Hydrite Flat D kaolinite. The viscosity is that at rate of shear 50 sec^{-1} (see Appendix B). The straight line parallel to the x-axis suggests that the settling velocity is inversely proportional to the viscosity of the suspension, so the product is independent of concentration.

FIGURE 4-6 LOG(INITIAL SETTLIING VELOCITY-NUMBER OF PARTICLES) RELATIONSHIP

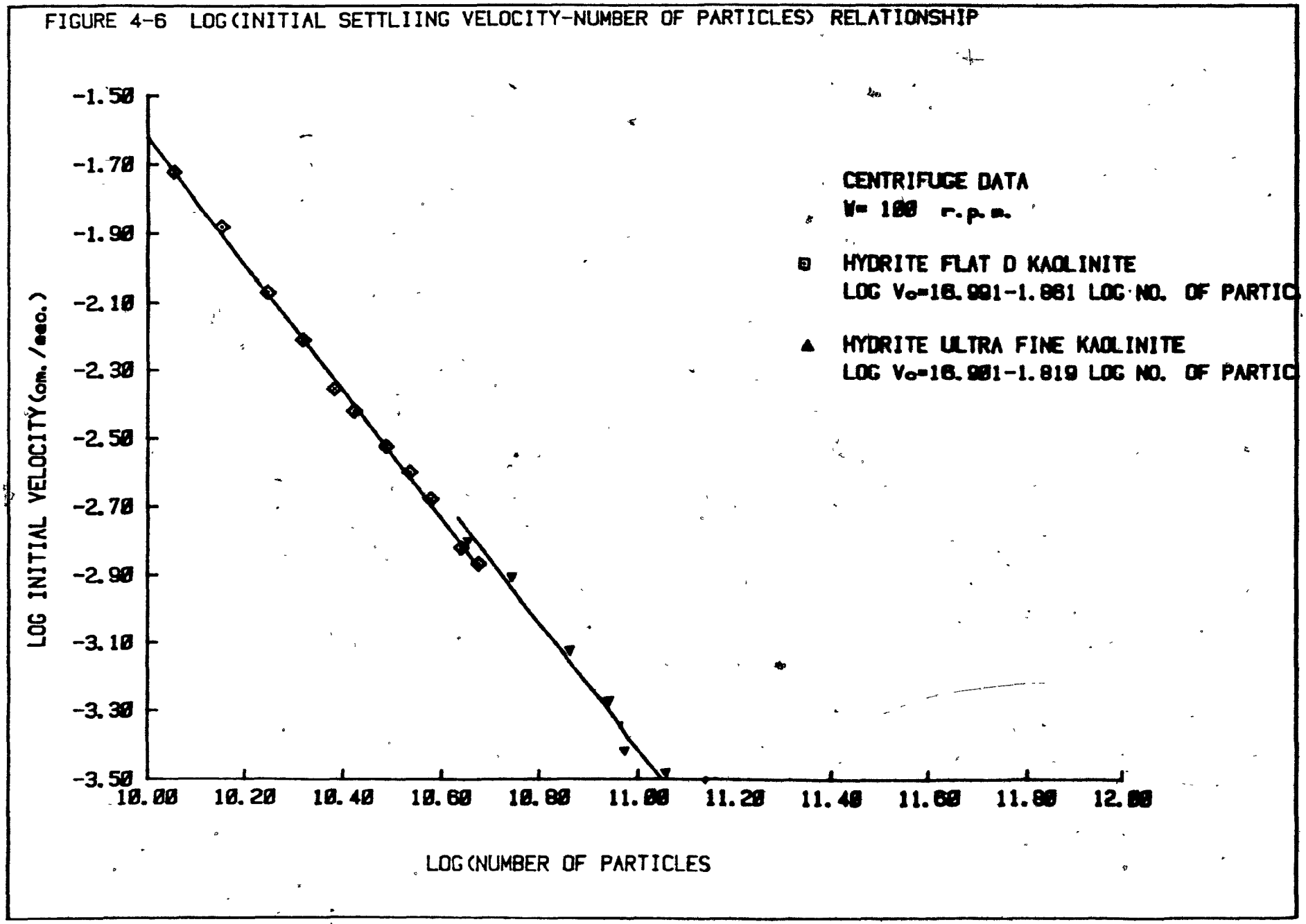

FIGURE 4-7 LOG-LOG GRABH OF V (INITIAL SETTLING VELOCITY*VESCOSITY) AGAINST INITIAL CONCENTRATION

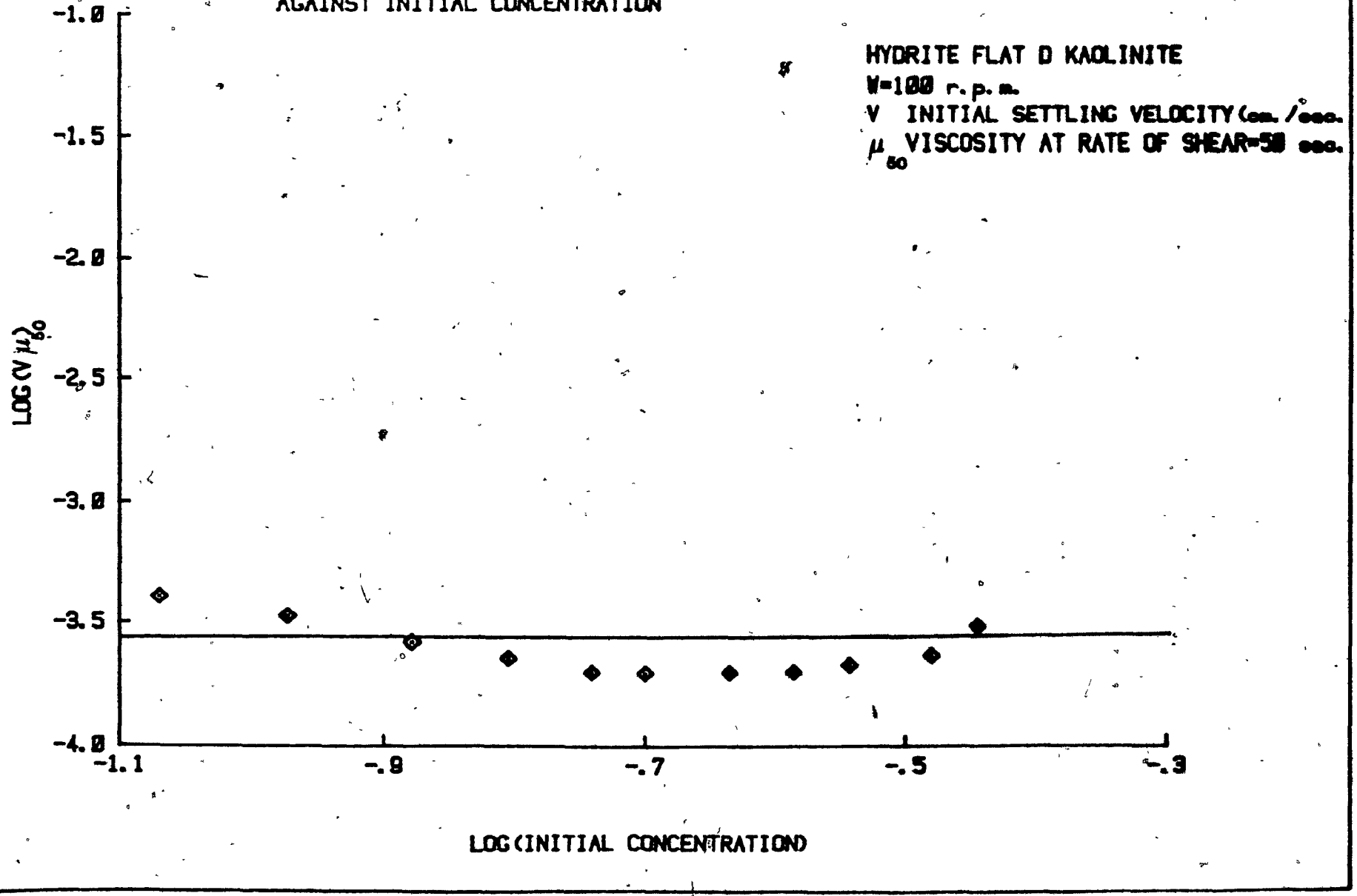

4.1.2 Relationship Between Initial Settling Velocity and Initial Concentration (Gravity Test)

4.1.2.1 Hydrite Flat D Kaolinite

The method of preparation of test samples and the conditions under which these tests were conducted were similar to those of centrifuge tests, with the exception of the force inducing the settling. In this case, the suspensions settled under the effect of gravity.

Figure 4.8 shows the curves obtained from eleven settling tests. It is seen that curves for concentrations less than or equal to 16% (by weight), are characterized by a straight line portion, describing the initial settling behaviour, followed by a rather abrupt change in settling rate, indicating the end of zone settling. The curves for concentrations greater than, or equal to 18%, are characterized by an apparent increasing concavity with increasing concentration, rather than by a straight line portion as in the former case; this is followed by an abrupt change in settling rate, indicating the end of zone settling. All tests show a very slow interface subsidence after the end of zone settling, indicating the possibility of either late sedimentation, compression, or consolidation in progress.

Figure 4.9 shows the relationship between the initial settling velocity of the interface (see Section 3.3) and the initial solids concentration. When the data points are

FIGURE 4-8 SETTLING CURVES AT DIFFERENT INITIAL CONCENTRATION (wt/wt)

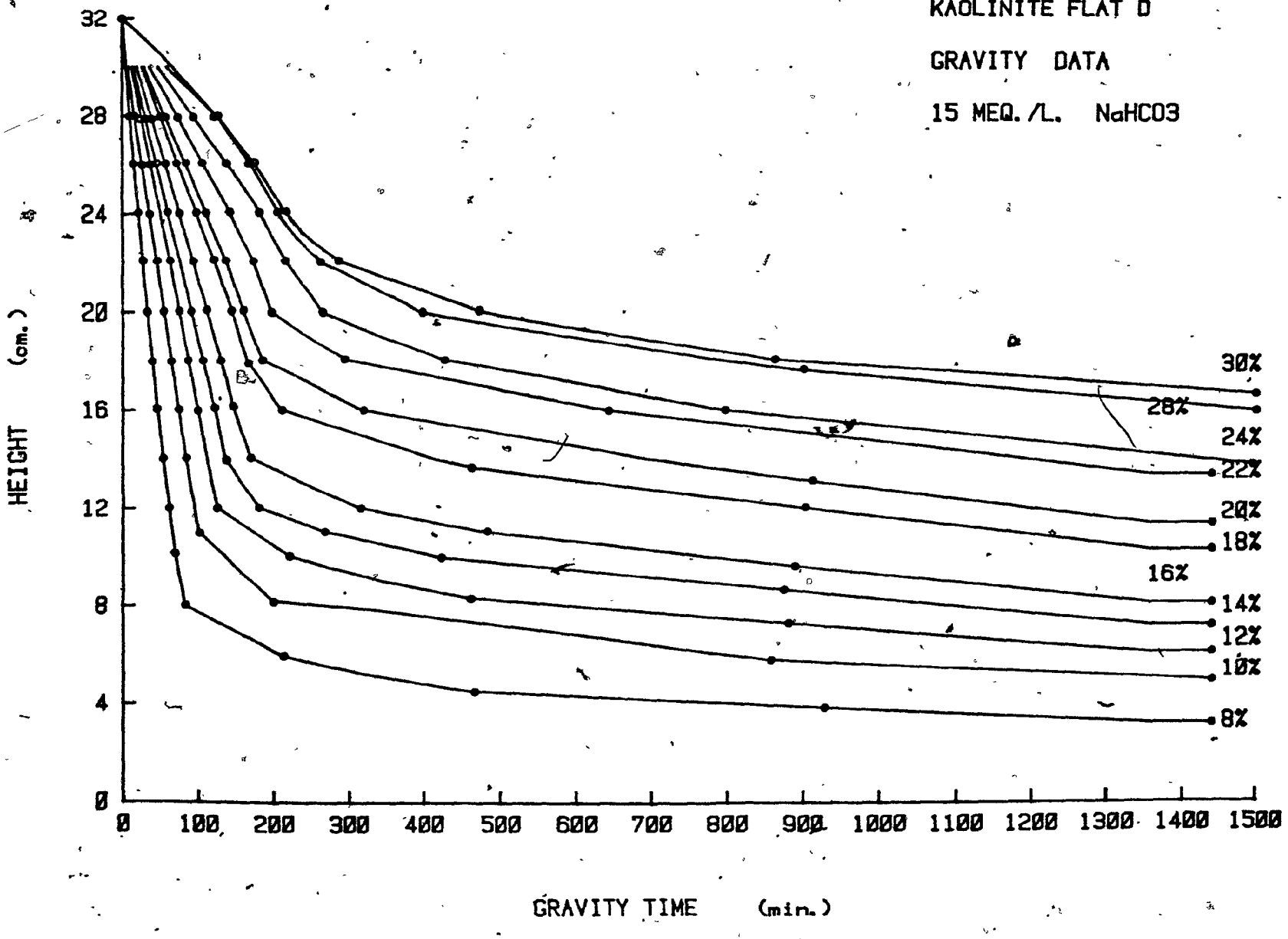

FIGURE 4-9 INITIAL SETTLING VELOCITY-INITIAL CONCENTRATION RELATIONSHIP

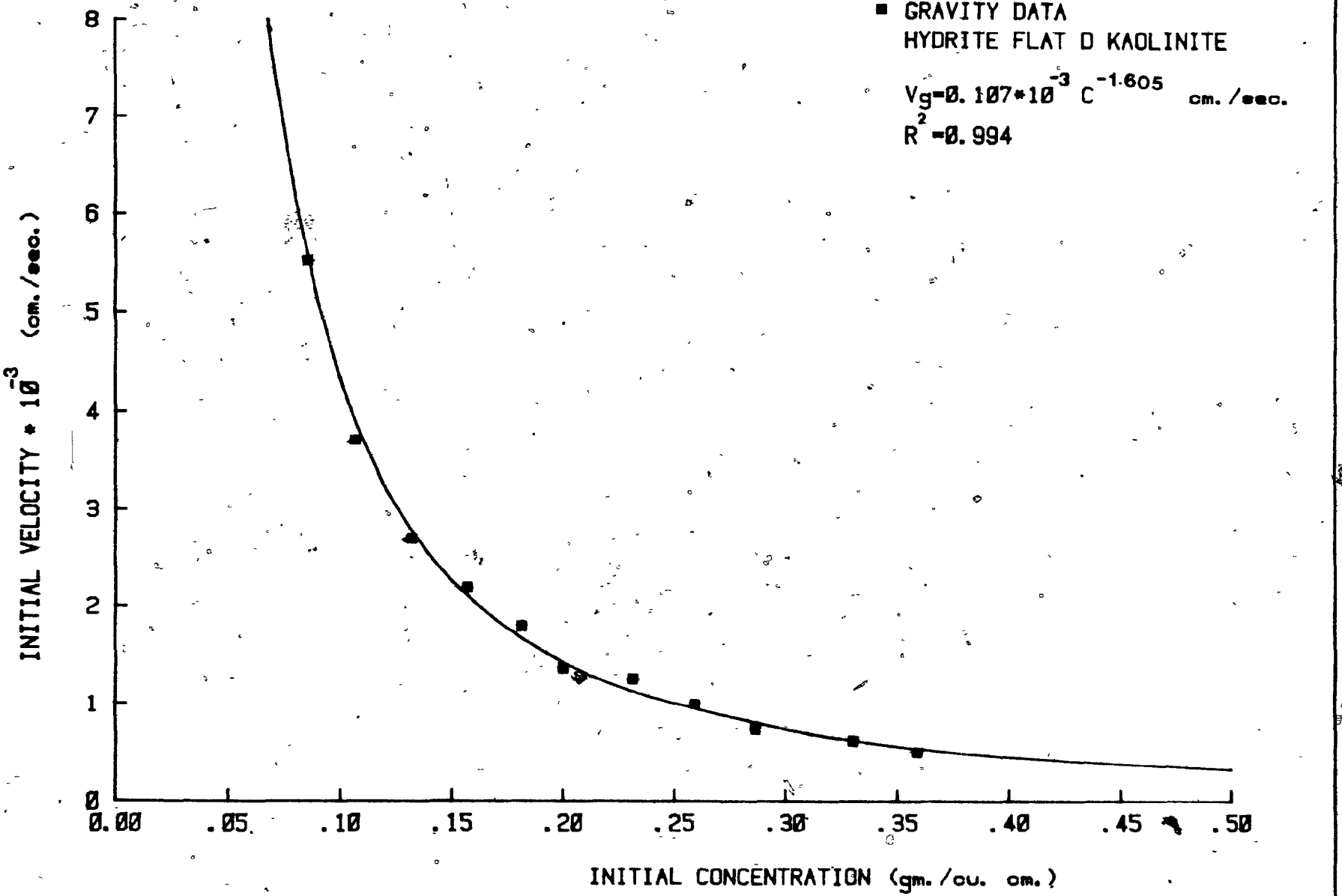

plotted on a log-log scale, a straight line is obtained as indicated in Fig. 4.12. The line may be approximated by the following equation:

$$V_g = 0.107 \times 10^{-3} C^{-1.605} \qquad (4.3)$$
$$R^2 = 0.994$$

where V_g = initial settling velocity of the interface under the influence of gravity force in cm/sec

C = initial solids concentration in gm/cm^3

R^2 = correlation coefficient.

4.1.2.2. Hydrite Ultra Fine Kaolinite

The method of preparation of test samples, and the conditions under which this test was conducted, were again similar to those of the centrifuge tests, except that the suspensions settled under the influence of gravity, rather than the centrifugal force.

Figure 4.10 shows the curves obtained from seven settling tests. The figure shows that in the concentration range 8% - 14%, every curve shows a straight line portion beginning at the initial height of suspension, followed by a gradually decreasing settling rate; ultimately, in each curve, there is an abrupt change in the settling rate, indicating the virtual end of zone settling. For concentrations 16%-20%, the curves are distinguished by the absence of gradually settling period; they exhibit a straight line portion, followed by an abrupt change in the settling rate, indicative of the virtual end of zone settling.

FIGURE 4-10 SETTLING CURVES AT DIFFERENT INITIAL CONCENTRATION (wt/wt)

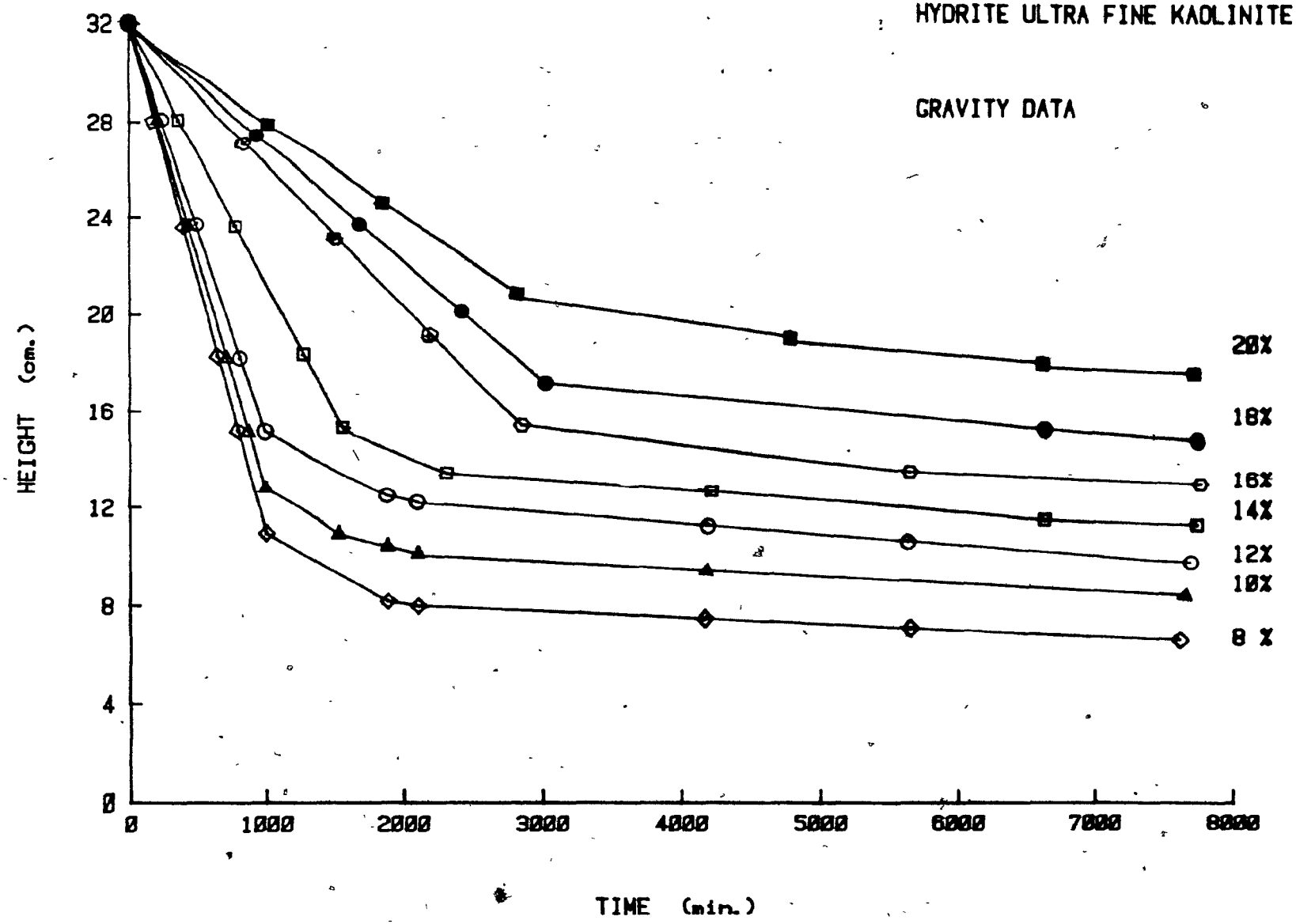

Figure 4.11 shows the relationship between initial settling velocity (see Section 3.3) and initial concentration in the concentration range 8%-20% (by weight). When the data points are plotted on a log-log scale, a straight line is obtained as indicated in Fig. 4.12. The line may be approximated by the following equation:

$$V_g = 0.03965 \times 10^{-4} \times C^{-1.94939} \qquad (4.4)$$

$$R^2 = 0.951$$

where V_g = initial settling velocity in cm/sec

C = initial solids concentration in gm/cm^3

R^2 = correlation coefficient

4.1.3 Calculation of Floc Diameter Based on Viscosity Measurement

The Stokes equation can be modified by using the viscosity of the suspension in two cases:

1. At gel strength (i.e. viscosity at rate of shear of unity)
2. At rate of shear of 50 sec^{-1}

Using the initial settling velocity (see Section 3.3) associated with the initial concentration, the equivalent particle diameter, as shown in Fig. 4.13, also in Appendix A, shows a sample calculation.

It is seen from the figure that, at viscosity at rate of shear of unity, the equivalent diameter obtained from gravity data are higher than those obtained from

FIGURE 4-11 INITIAL SETTLING VELOCITY-INITIAL CONCENTRATION RELATIONSHIP

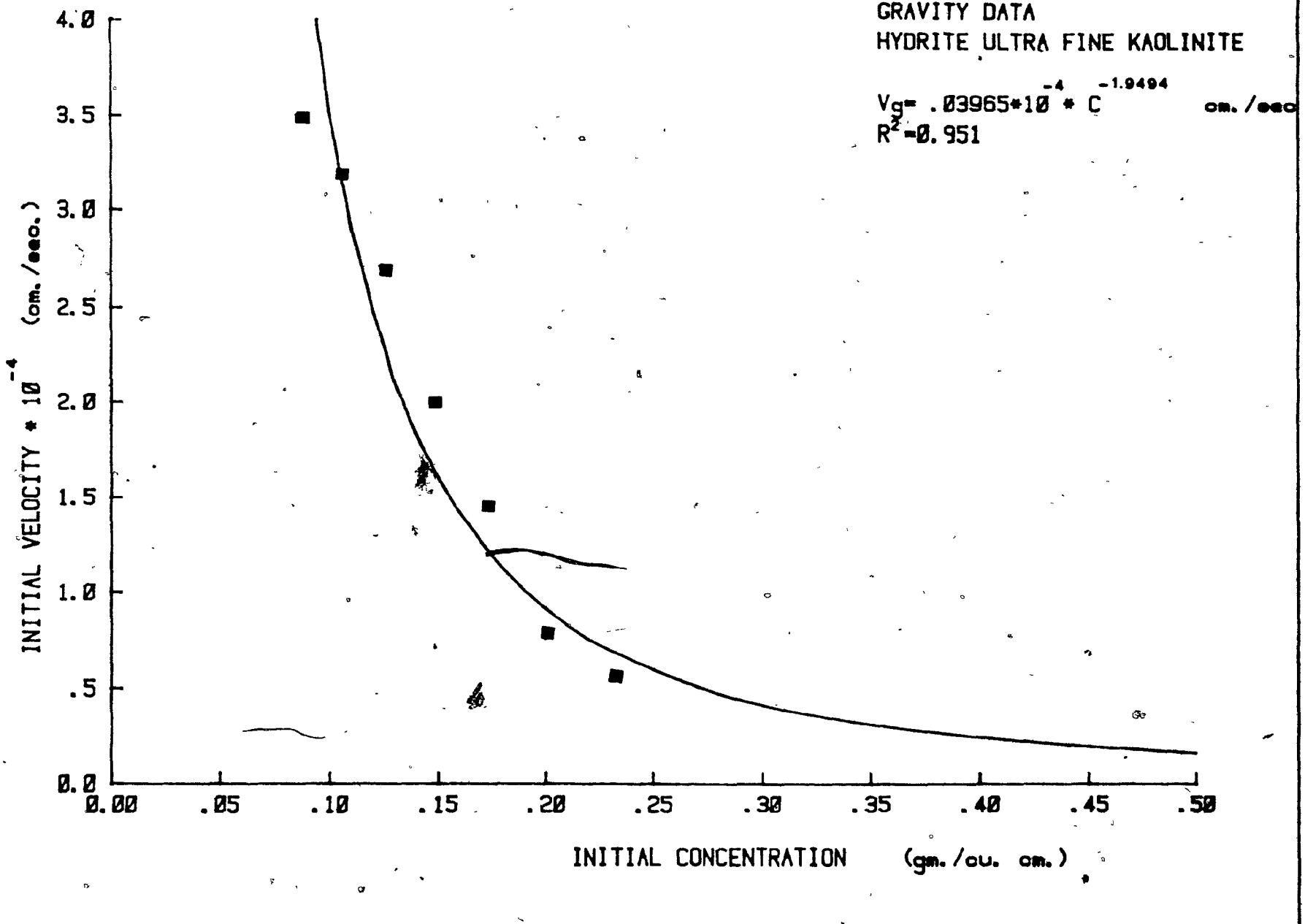

FIGURE 4-12 LOG(INITIAL SETTLING VELOCITY-INITIAL CONCENTRATION) RELATIONSHIP

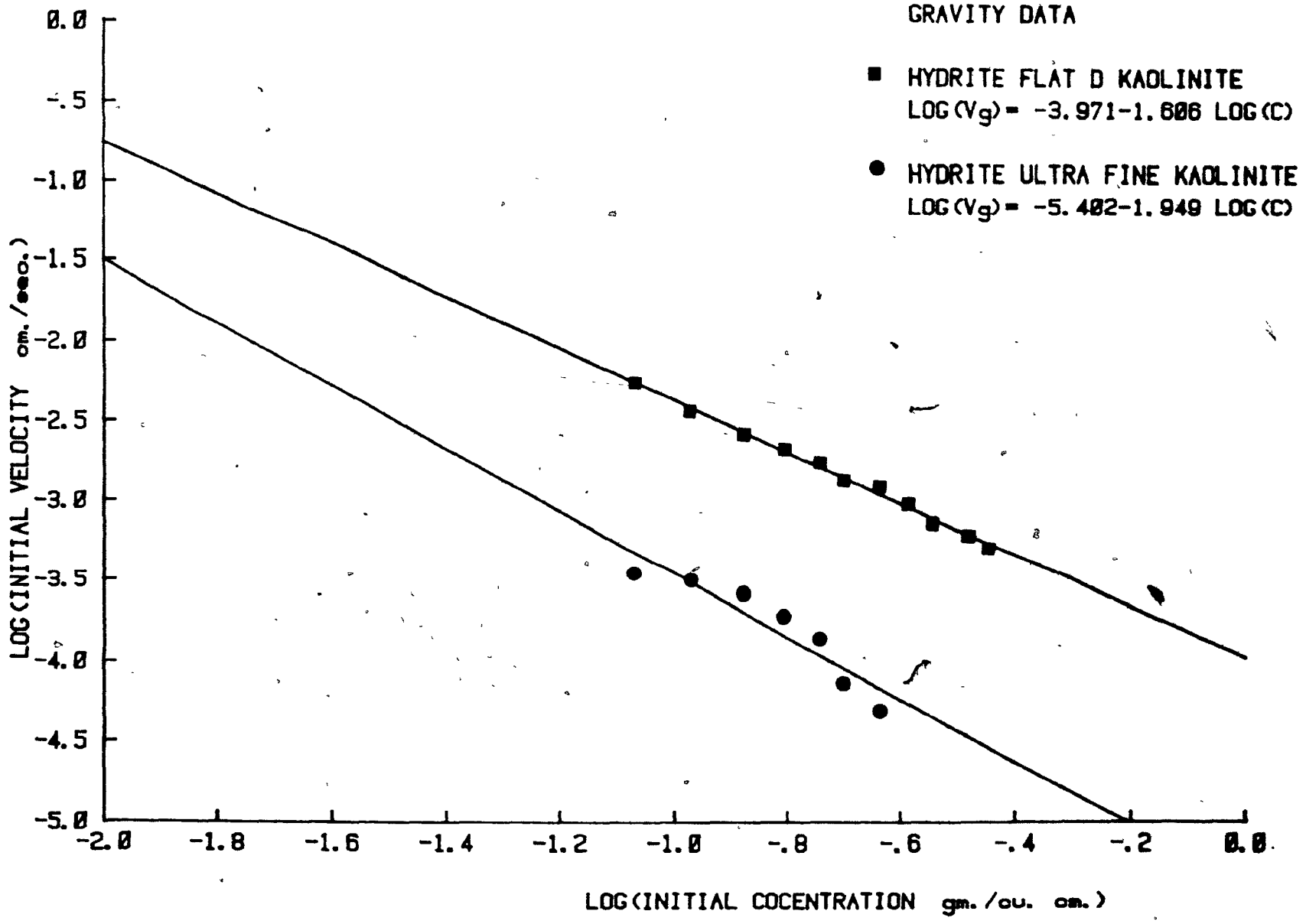

FIGURE 4-13 FLOC DIAMETER WITH CONCENTRATION

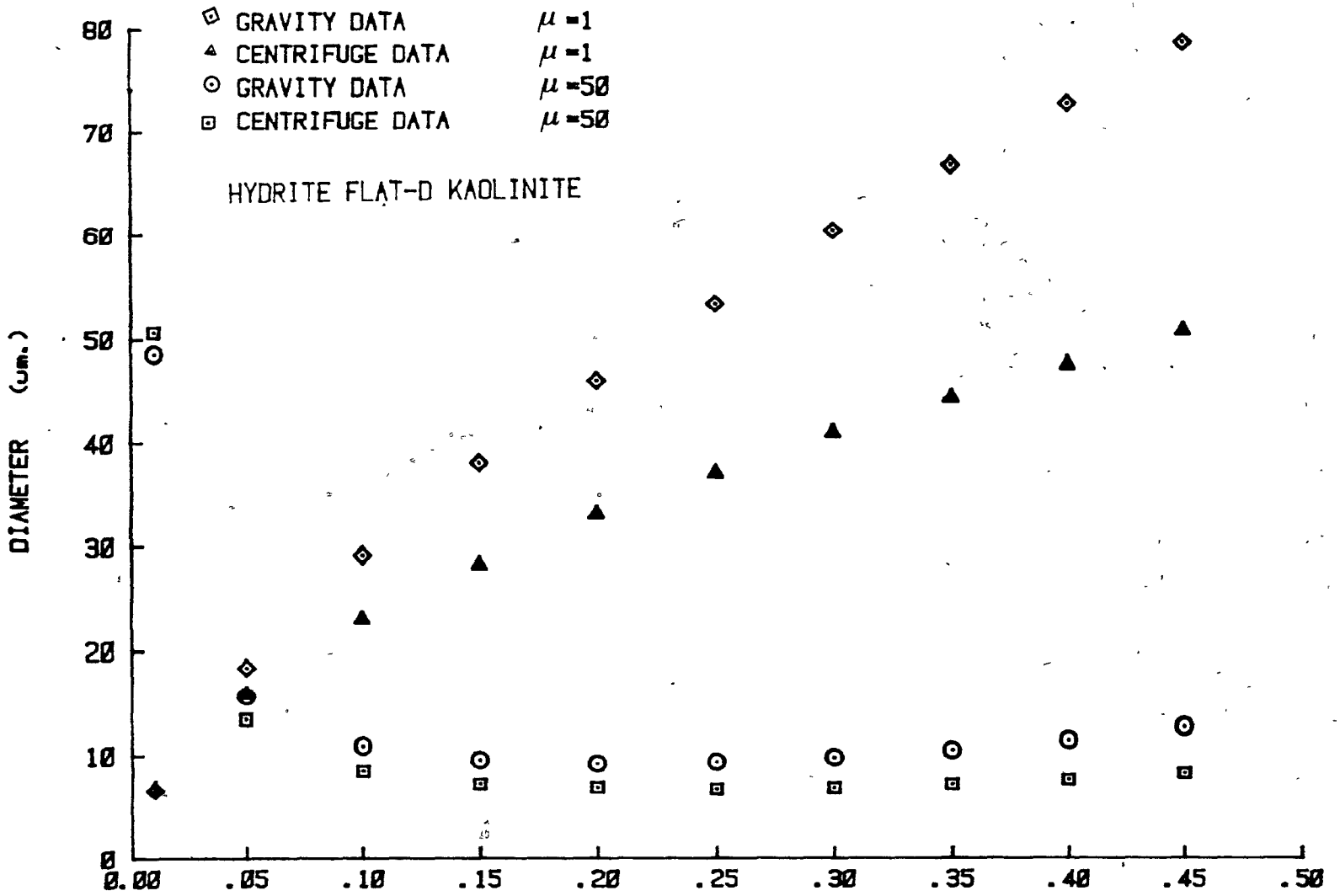

centrifuge data. With increasing concentration, the associated initial settling velocity decreases, and the equivalent diameter increases exponentially.

At viscosity at rate of shear 50 sec^{-1}, the equivalent diameters calculated from gravity data are higher than those calculated from centrifuge data. The figure also shows that the equivalent diameter is independent of concentration, having an average value of 11 μm from gravity data, and 9 μm from centrifuge data. These diameters obtained from the modified Stokes calculation can then be compared with the D_{50} value of 4.5 μm, determined from the standard hydrometer test. This discrepancy may be due to the fact that the true rate of shear is unknown. If it were possible to determine the viscosity of suspension at the true rate of shear, it would be possible to obtain the initial settling velocity of suspension, using D_{50} value from the hydrometer test.

4.1.4 Sediment Volume

The results of Hydrite Flat D kaolinite show that, no matter what the initial concentration was, the final concentration, at the end of zone settling was approximately 0.8 gm/cm^3 in centrifuge tests, while in gravity tests, the final concentration was approximately 0.70 gm/cm^3. These values are not constant, but over long periods of time, will increase due to late sedimentation, compression or consolidation. These values of concentration with time

were calculated with the assumption that the change of concentration with depth is uniform at any interval time, as shown in Figs. 4.14-16. The higher values of final concentration in centrifuge tests indicate that the final volume becomes more compacted due to the applied force.

4.1.5 Comparison of Results of Phase 1 with Other Investigators

Richardson and Zaki have proposed a correlation explaining hindered settling of non-flocculated mono-dispersed smooth spheres. This correlation, which is most accepted by workers in the field, is expressed as follows:

$$V = V_o E^n \qquad (2.1)$$

where V is the hindered settling velocity of a suspension

V_o is the settling velosity of a particle at infinite dilution

E is the porosity (i.e. the free area available for the flow of the displaced liquid in any cross-section within the suspension

$$= \frac{V_{suspension} - V_{solid}}{V_{suspension}} \qquad (4.5)$$

$$= 1 - \frac{C}{P}$$

where C is initial concentration gm/cm^3

P is density of solid gm/cm^3

n is power term in Richardson and Zaki = 4.65

FIGURE 4-14 CONCENTRATION Vs. CENTRIFUGE TIME

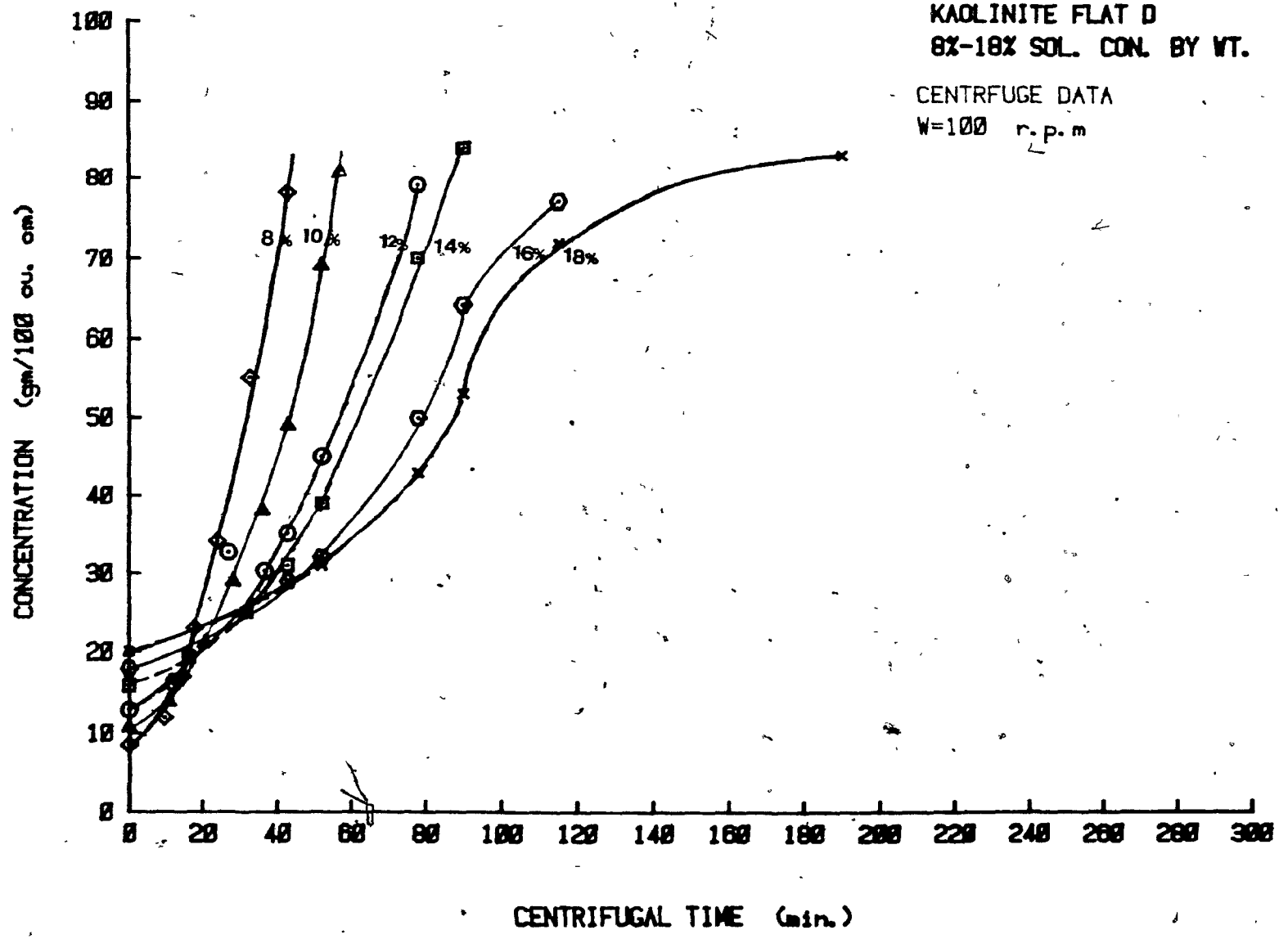

FIGURE 4-15 CONCENTRATION Vs. CENTRIFUGE TIME

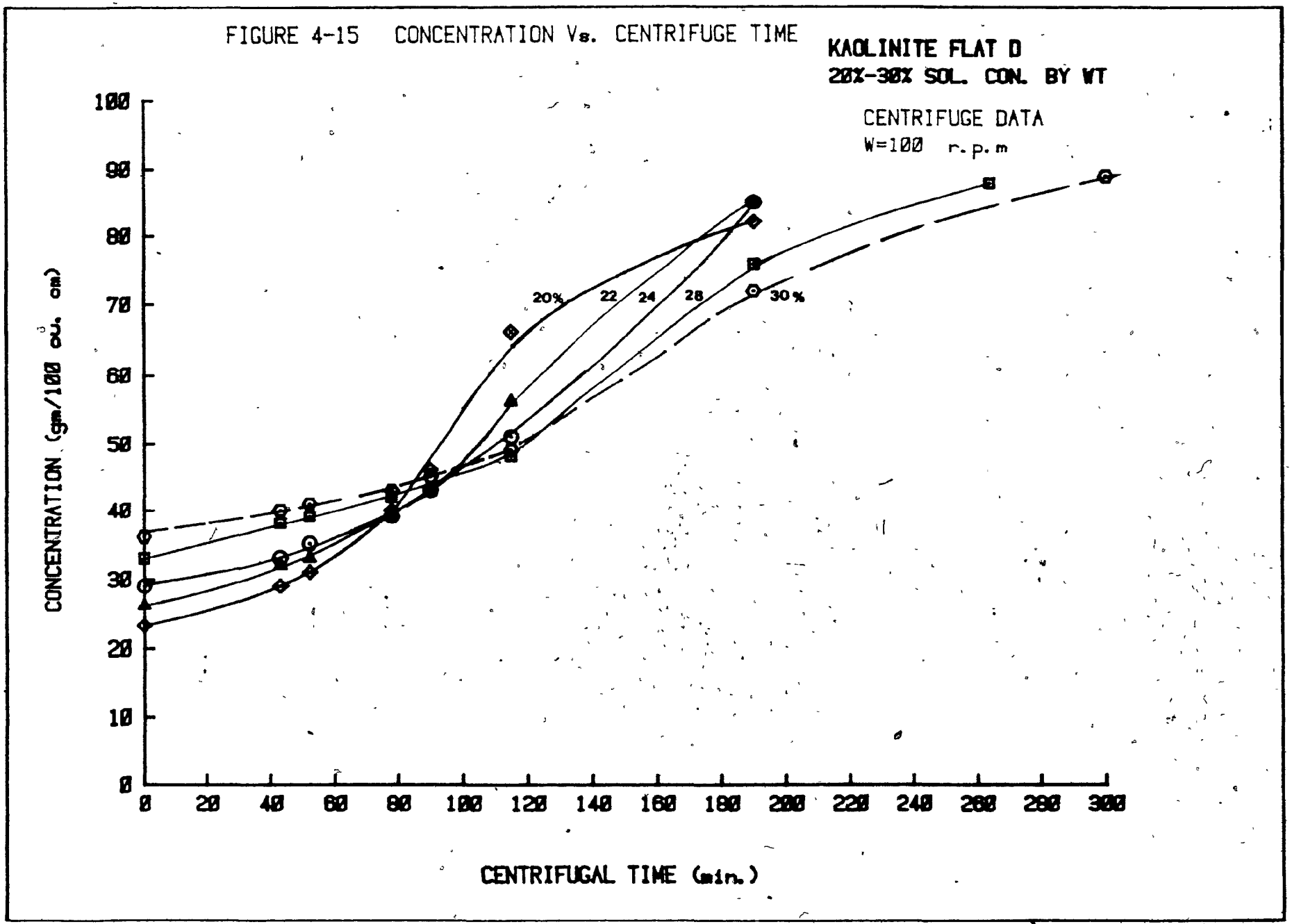

FIGURE 4-16 CONCENTRATION Vs. GRAVITY TIME

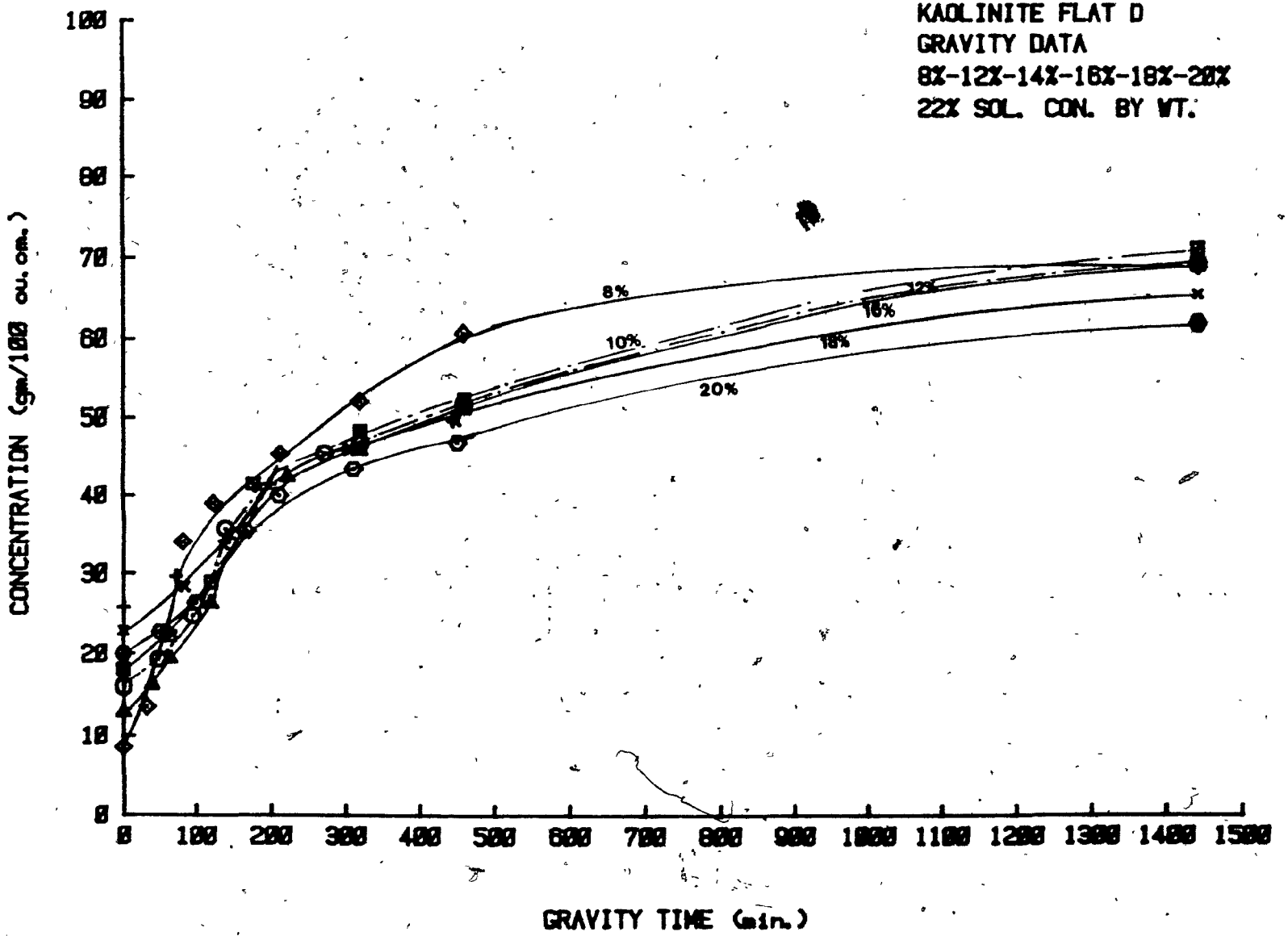

Several experimental studies have shown that the value of the power n exceeds 4.65 for non-spherical and/or rough non-flocculated particles in the Stokes regime. For example, in the case of alumina powder having a mean diameter of 5.5 microns, the value of n was found to be 10.5 (see Table 4.1). Davies and Richardson (1966) summarized the results obtained from several workers, as shown in Table 4.1.

TABLE 4.1 Compilation of values of n for various materials based on Richardson and Zaki formulation

Author	dp (micron)	Materials	Method	Index Measured n	Index Predicted
Jottrand (1952)	20-110	sand/water	fluidization	5.6	4.65
Lewis and Bowerman (1949)	68.8 86	porous catalyst/ organic liquids	fluidization fluidization	8.3	4.65
Richardson and Meikle (1961)	5.5	aluminum/water calgon	sedimentation	10.5	4.65
Whitemore (1957)	194 139 97 65	methyl methacrylate/ Aq.Pb $(NO_3)_2$ + glycerol	sedimentation	6.9 7.5 8.3 9.5	4.65 4.65 4.65 4.65

The above table indicates that there is a tendency for the value of n to increase for small diameter particles. In order to accommodate the value of Richardson and Zaki (n=4.65) normally associated with large smooth spheres, Richardson and Meikle (1961) and Fouda and Capes (1979) introduced a modified hindered settling equation of the form

$$V = V_o (1-KC)^{4.65} \qquad (4.6)$$

where K = hydrodynamic volume factor

C = solid concentration

This modification assumes the presence of immobile liquid surrounding the particle. The presence of the liquid film increases the effective concentration of the particles, and thereby decreases the settling velocity of the suspension.

In the latest communications of Fouda and Capes (1979) and in Epstein (1979), it was suggested that the hydrodynamic volume factor can be estimated by the relationship

$$K \cong \frac{0.6}{1 - E_b} \qquad (4.7)$$

where E_b is the void fraction of the settled bed. In other words, if a suspension is allowed to settle, then the final settled bed voidage can be used to estimate K.

The Richardson and Zaki equation can then be written in the form

$$V = V_o \left(1 - \frac{C}{P}\right)^n \qquad (4.8)$$

To include the effect of hydrodynamic volume, the density of the suspension after final settlement is reached, has to be considered. For Hydrite Flat D kaolinite, the final concentration was approximately 0.7 gm/cm^3; the calculated value of P, based on this concentration, was 1.77 gm/cm^3; similarly, P value for Hydrite Ultra Fine was 1.3712 gm/cm^3 (Yong and Sethi, 1978). These two values of the density were used in the Richardson and Zaki equation

Plotting log V versus log (1- C/P) for the two materials yields straight lines whose slopes give the exponent values in Richardson and Zaki's equation, as shown in Fig. B.31-32, and whose intercept gives the settling velocity of a particle at infinite dilution. Table 4.2 shows the results of this calculation for both tested materials, as well as the values of single particle velocity based on Stokes' law.

TABLE 4.2 Results of Hydrite Flat D and Hydrite Ultra Fine Kaolinite (based on Richardson and Zaki formulation)

Material	Particle Size (micron)	Value of n	$V_o \times 10^{-3}$ cm/sec Infinite Dilution	Correlation Coefficient R^2	Test Data	V_o based on Stokes Law* cm/sec
Hydrite Flat D	4.5	12.056	7.1184	0.952	gravity	1.7861×10^{-3}
" "	4.5	13.743	24.623	0.928	centri-fuge	9.650×10^{-3}
Hydrite UF	0.3	16.957	1.288	0.950	gravity	7.742×10^{-6}
" "	0.3	14.83	3.9345	0.942	centri-fuge	4.18×10^{-5}

* for single particle

Table 4.3 shows the analysis based on Steinour's equation, which is in the form

$$V = V_o \, E^2 \, 10^{-A(1-E)} \qquad (4.9)$$

where A = empirical constant in Steinour's equation

= 1.82

Plotting log V/E^2 versus (1-E), (Fig. B.33-34), yields a straight line, whose slope is A and whose intercept gives the settling velocity of the particle in infinite dilution. Table 4.3 shows the values of A and V_o calculated on the basis of Steinour's equation, and the velocity of single particles calculated on the basis of Stokes' law.

TABLE 4.3 Results of Hydrite Flat D and Hydrite Ultra Fine Kaolinite (based on Steinour formulation)

Material	Particle Size (micron)	Value of A	$V_o \times 10^{-3}$ cm/sec	Correlation Coefficient R^2	Test Data Fo	V_o based on Stokes Law* cm/sec
Hydrite Flat D	4.5	-5.29	7.8077	0.944	gravity	1.7861×10^{-3}
Hydrite Flat D	4.5	-6.2	27.50	0.918	centri-fuge	9.650×10^{-3}
Hydrite UF	0.3	-7.31	1.4194	0.929	gravity	7.742×10^{-6}
Hydrite UF	0.3	-6.33	4.394	0.939	centri-fuge	4.18×10^{-5}

* for single particles

The large values for n obtained from Richardson and Zaki's equation, and also the high values of A obtained from Steinour's equation, may be attributed to the presence of the double layer, which becomes more significant as the particle concentration increases, and the particle size decreases. It should be noted in this connection that the D_{50} for Hydrite Flat D kaolinite is 4.5 microns, and for Hydrite Ultra Fine kaolinite is 0.3 micron. The values for n & A calculated for Hydrite Ultra Fine kaolinite are

higher than those calculated for Hydrite Flat D kaolinite; this difference may be attributed to the different characteristics of the material.

4.2 RESULTS OF PHASE 2

4.2.1 Establishment of Settleability Coefficient

This part of the study was conducted in order to determine the settleability coefficient (see Appendix A). The settleability coefficient can be defined as the settling velocity of the particles per unit force imposed, i.e.

$$S = \frac{v}{w^2 r} \quad sec^{-1} \qquad (4.10)$$

where S = settleability coefficient in sec^{-1}

v = particle velocity in cm/sec

$w^2 r$ = centrifugal acceleration in cm/sec^2

In an effort to determine the settleability coefficient, seven different concentrations (16%, 20%, 24%, 27%, 30% and 33% (by weight)) were considered and a series of tests were conducted at different rotational speeds (w).

Figure 4.17 shows the height of suspension as a function of centrifuge time, at different rotational speeds, for a given concentration. Five rotational speeds in increasing magnitude were used for each of the seven concentrations considered. Due to instrument limitations encountered in pre-setting the centrifuge at a desired rotational speed, the five individual speeds used for a

FIGURE 4-17 SETTLING CURVES

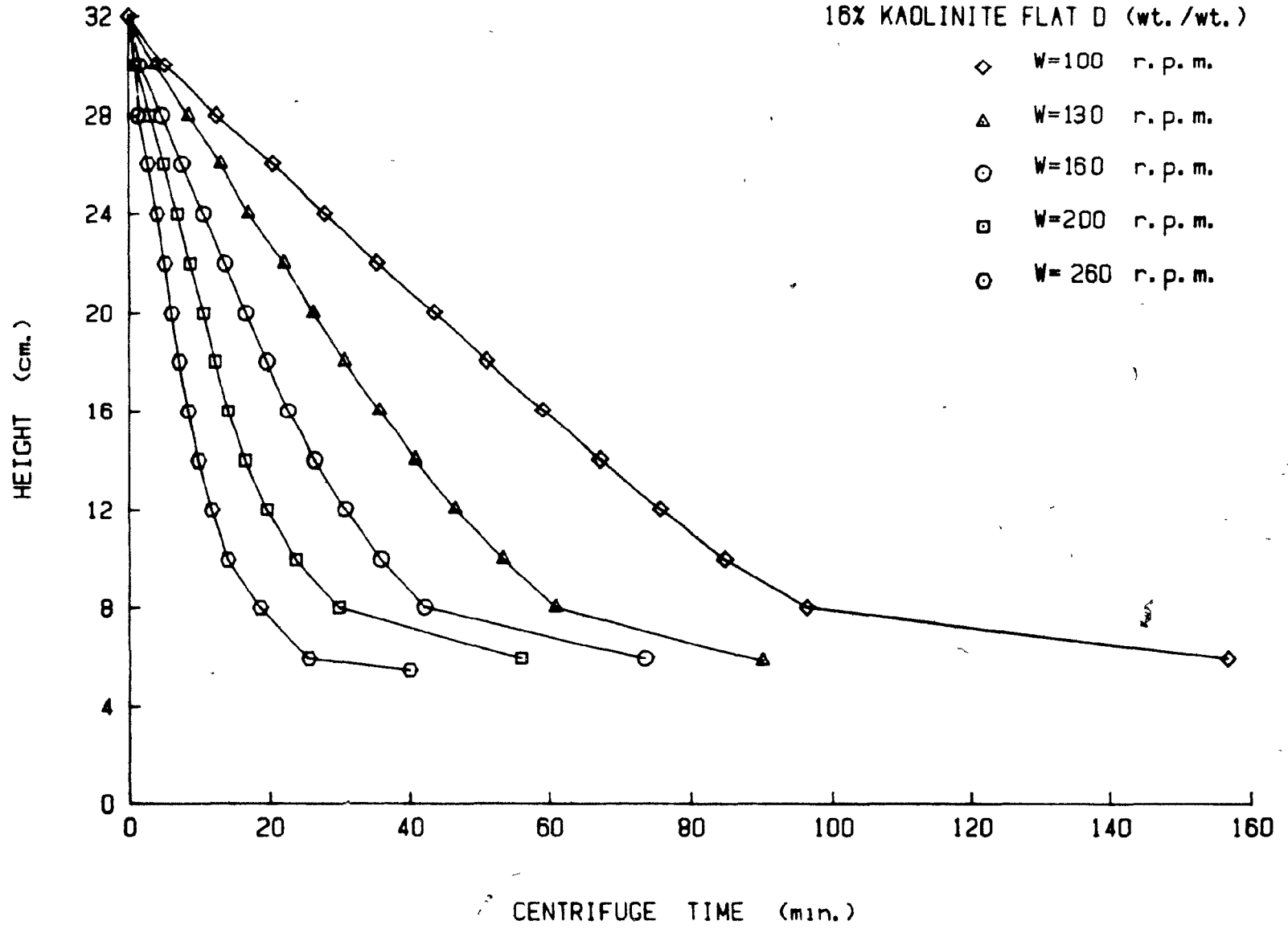

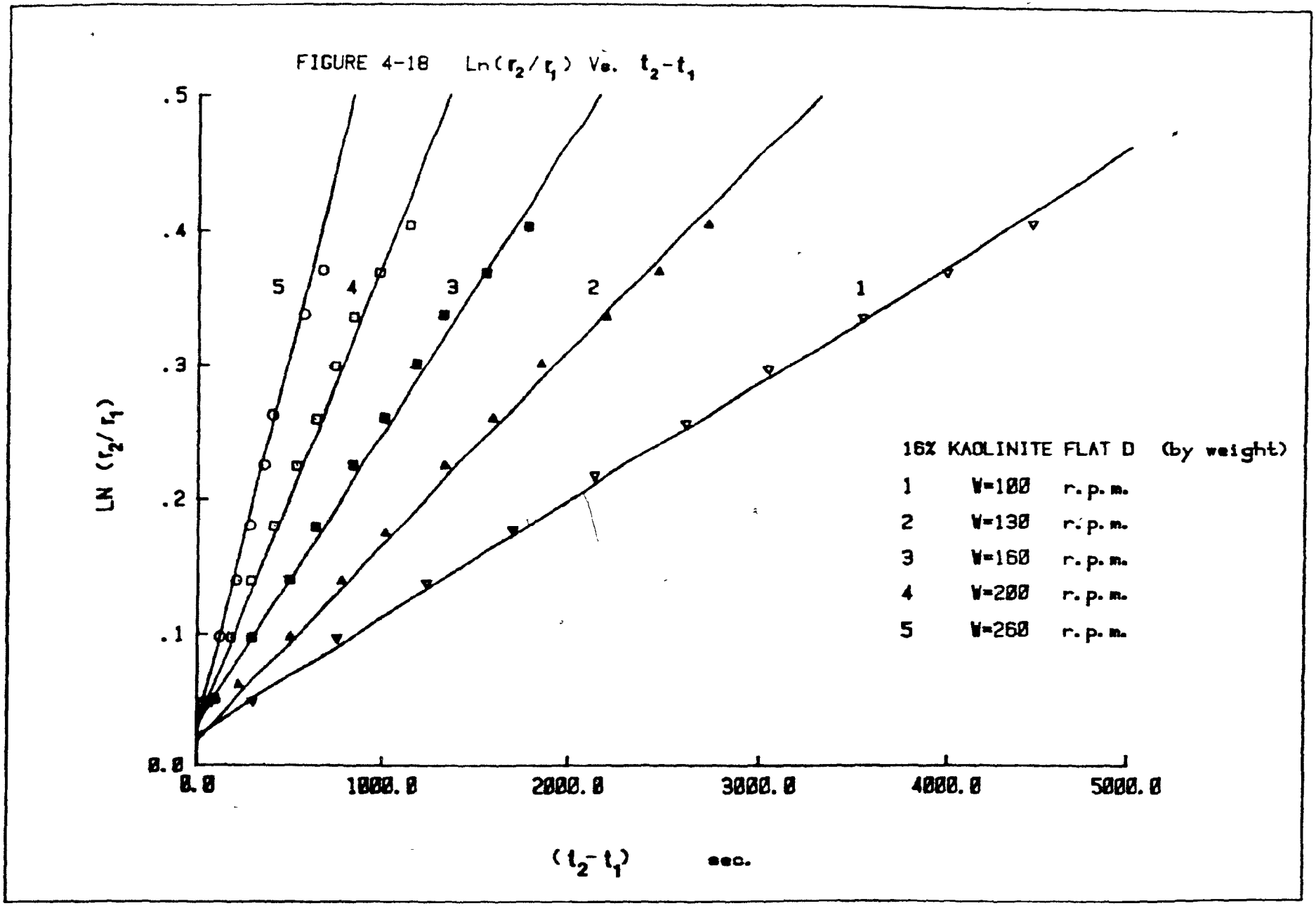
FIGURE 4-18 Ln(r2/r1) Vs. t2-t1
.5
.4
.3
.2
.1
0.0
LN (r2/r1)
5
4
3
2
1
0.0
1000.0
2000.0
3000.0
4000.0
5000.0
(t2-t1) sec.
16% KAOLINITE FLAT D (by weight)
1 W=100 r.p.m.
2 W=130 r.p.m.
3 W=160 r.p.m.
4 W=200 r.p.m.
5 W=260 r.p.m.

given concentration were somewhat different from those used for other concentrations. For example, the rotational speeds for the 16% suspension were 100, 130, 160, 200 and 260 r.p.m. while those for the 20% suspension were 100, 150, 160, 205 and 235 r.p.m. respectively.

The suspensions being tested were treated as previously described in Section 3.2, and for each test run, the position of the interface as a function of centrifuge time was recorded for each rotational speed. Figure 4.17 indicates that with increasing rotational speed, the rate of subsidence increases.

For each test at a given rotational speed, a relationship between $Ln(r_2/r_1)$ and (t_2-t_1) yields a straight line.

where r_1 = the distance from the center of rotation to the initial height of the suspension at time t_1

r_2 = the distance from the center of rotation to the new position of the interface at time t_2

The slope of the straight line is w^2S, and since w, the rotational speed is known, the value of S, the settleability coefficient can be determined.

Figure 4.18 shows the relationship between $Ln\ (r_2/r_1)$ and (t_2-t_1) for the five rotational speeds measured for each concentration considered. It should be noted that $Ln\ (r_2/r_1)$ versus (t_2-t_1) always yielded a linear relationship at all the rotational speeds and concentrations examined. The graphs also show a small intercept which may be attributed

to a small vibration of the tested tube. Due to the movement of the solid particles toward the bottom of the tested tube, the centre of gravity of suspension moves towards the bottom, while the centre of gravity of the second tube, filled with tap water, remains at the same position during the test.

The slope of each of the lines in Fig. 4.18 gives w^2S at different rotational speeds (w). Since w is known for each test run, S can be subsequently determined.

From the definition of settleability coefficient ($S = v/w^2r$), the associated centrifugal acceleration can be calculated for any observed settling velocity of the interface (v), at any rotational speed, as long as the settleability coefficient is known.

Figure 4.19 shows the relationship between the settleability coefficient and the associated centrifugal acceleration (w^2r). The figures indicate that the relationship between settleability coefficient and centrifugal acceleration is linear and parallel to the w^2r - axis, and that the settleability coefficient decreases with increasing concentration. The linear relationship between the settleability coefficient (S) and the associated centrifugal acceleration (w^2r) suggests that the settleability coefficient for a given concentration is independent of the applied force. That is, no matter what the value of w^2r, S will remain the same at the given concentration. This

FIGURE 4-19 SETTLEABILITY COEFFICIENT VERSUS CENTRIFUGAL ACCELERATION

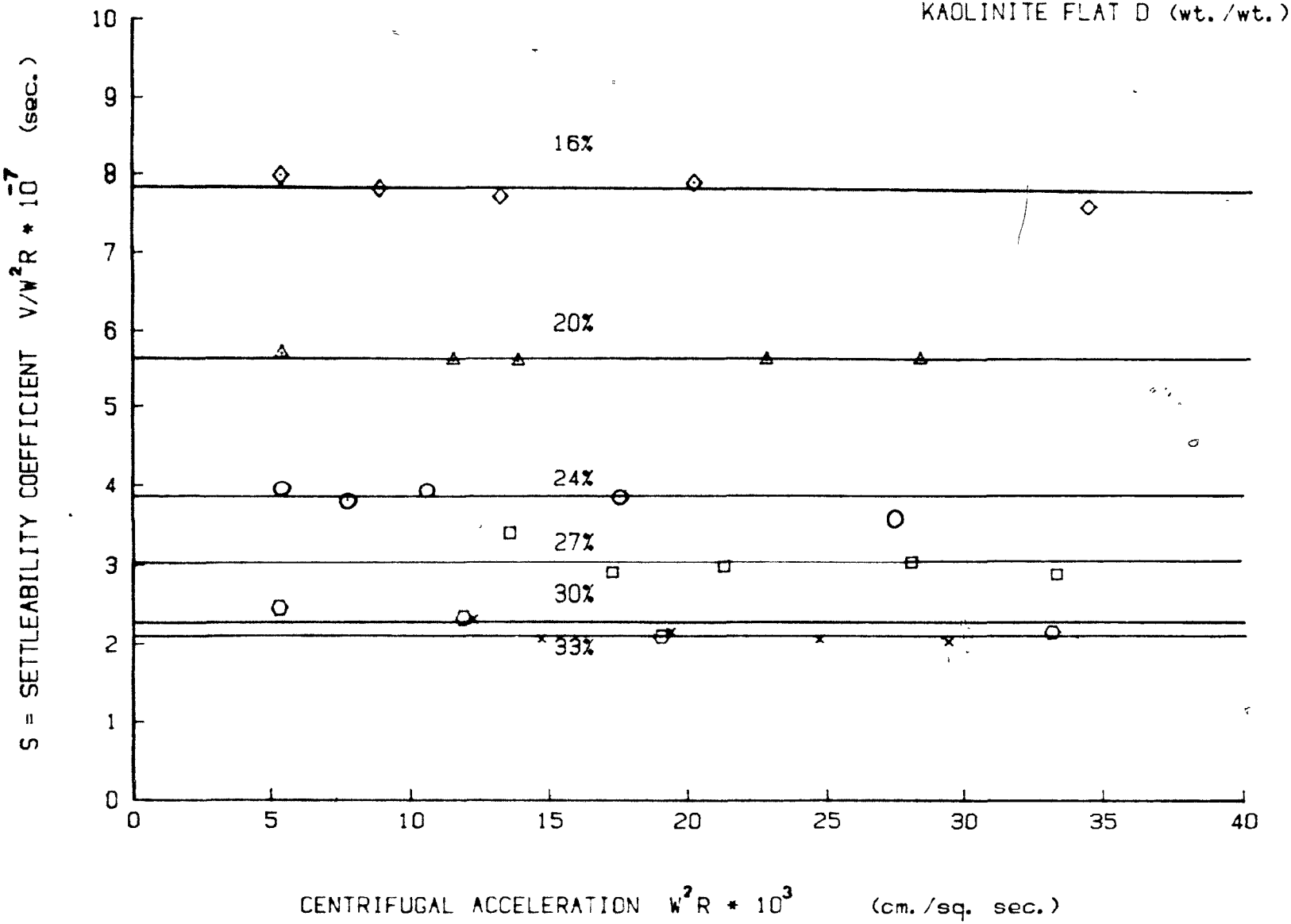

indicates that v, the settling velocity of the interface, increases or decreases in direct proportion to respective increases or decreases of the centrifugal acceleration.

Figure 4.20 shows the effect of viscosity at rate of shear 50 sec^{-1} on the settleability coefficient. It is seen that, at any value of the imposed force, the settling velocity of the interface is inversely proportional to the viscosity.

4.2.2 Relationship Between Settling Velocity and Applied External Force

Figures 4.21-26 show the relationship between the observed settling velocity of the interface and the associated centrifugal acceleration, calculated from the relationship

$$w^2 r = v/S$$

after the settleability coefficient has been determined for each rotational speed. These results are shown for the following six concentrations: 16%, 20%, 24%, 27%, 30% and 33% (by weight). The settling velocity of the interface, under the influence of gravity, which may be considered equal to $w^2 r = 980$ cm/sec^2, has also been plotted for each concentration for the sake of comparison. Each graph shows a linear relationship between the settling velocity of the interface and the associated centrifugal acceleration. It is seen that, at low concentrations (16% by weight),

FIGURE 4-20 SETTLEABILITY COEFFICIENT TIMES VISCOSITY Vs CENTRIFUGAL ACCELERATOIN

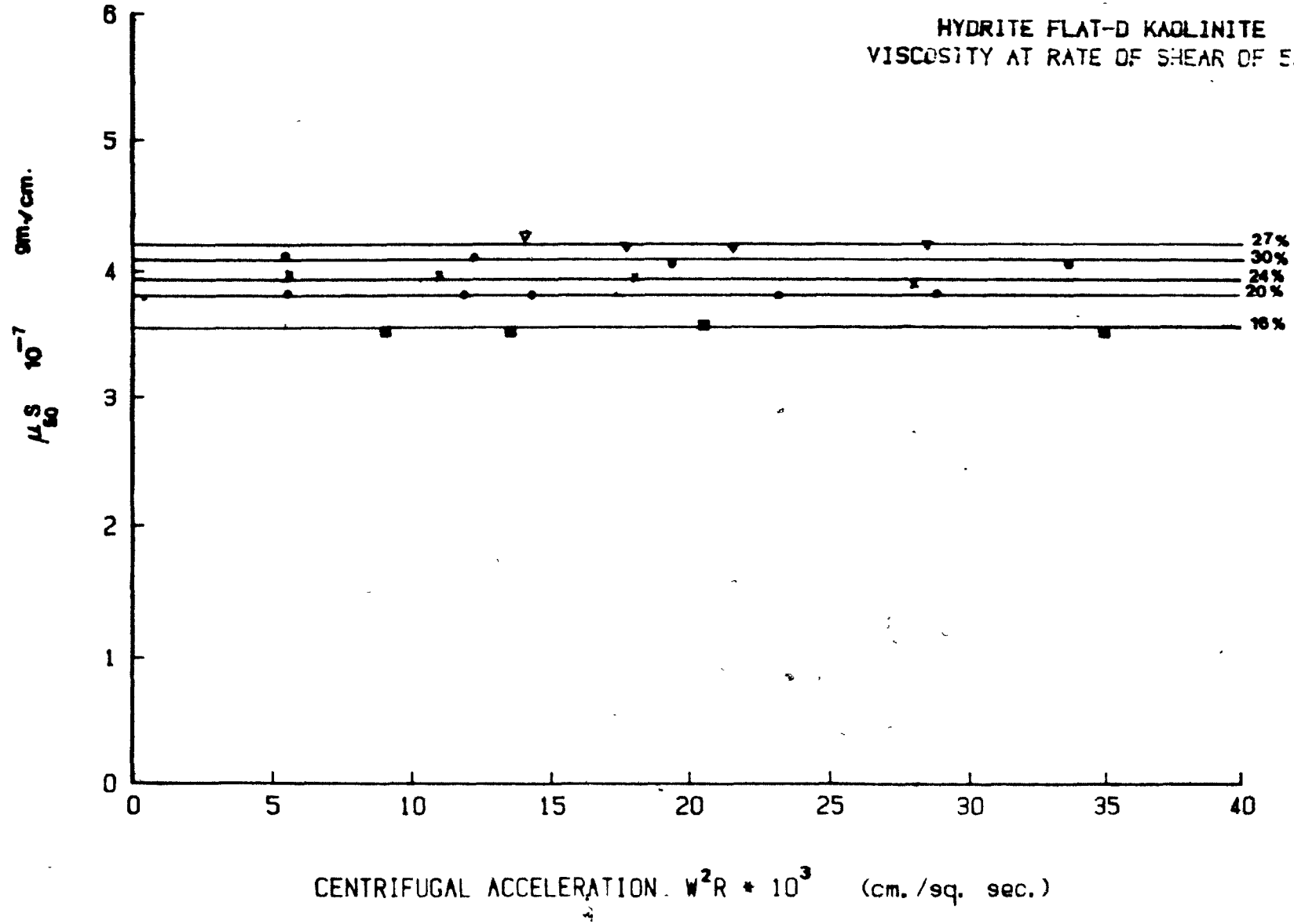

FIGURE 4-21 INITIAL SETTLINIG VELOCITY Vs. ACCELERATION

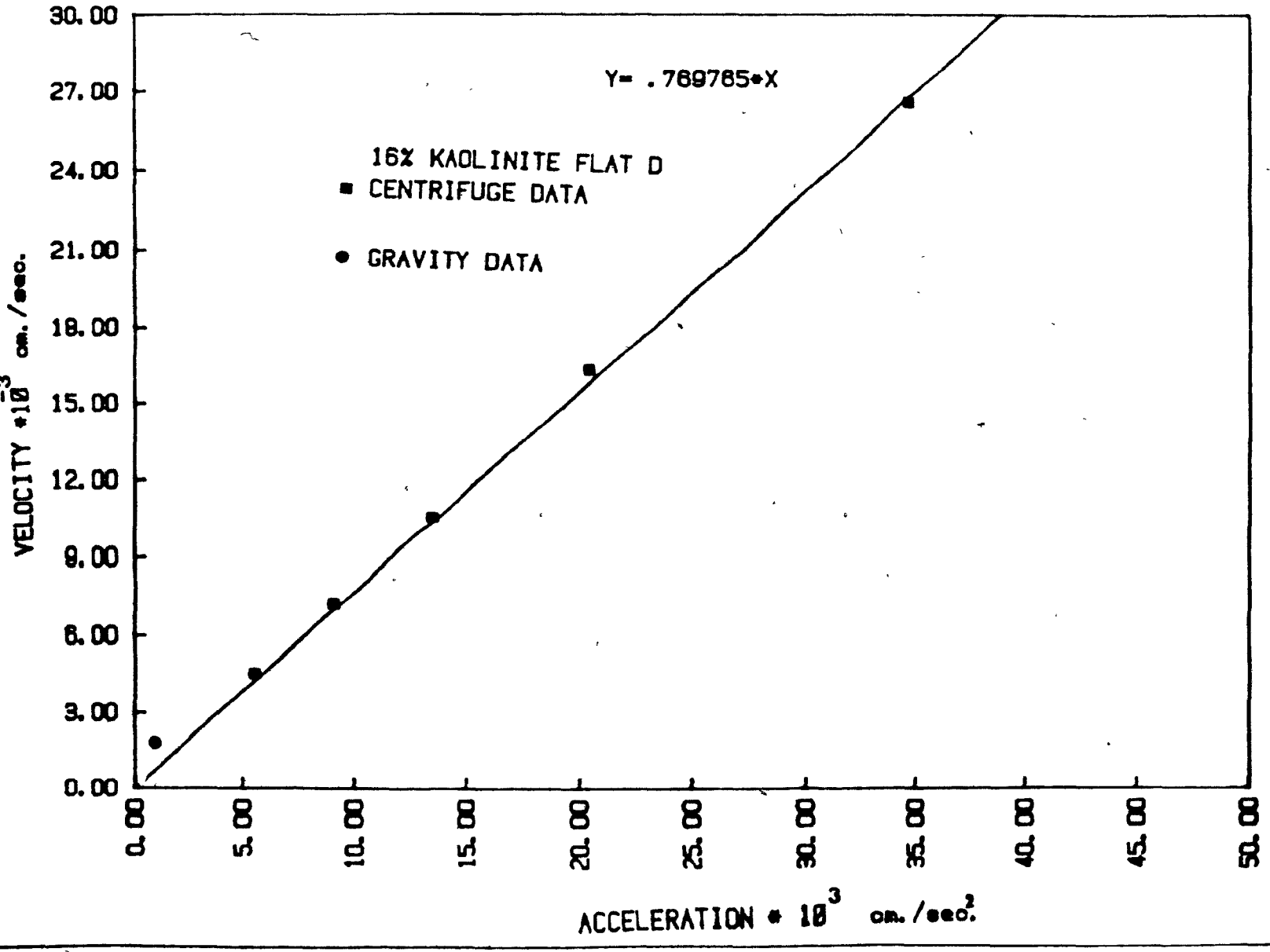

FIGURE 4-22 INITIAL SETTLINIG VELOCITY Vs. ACCELERATION

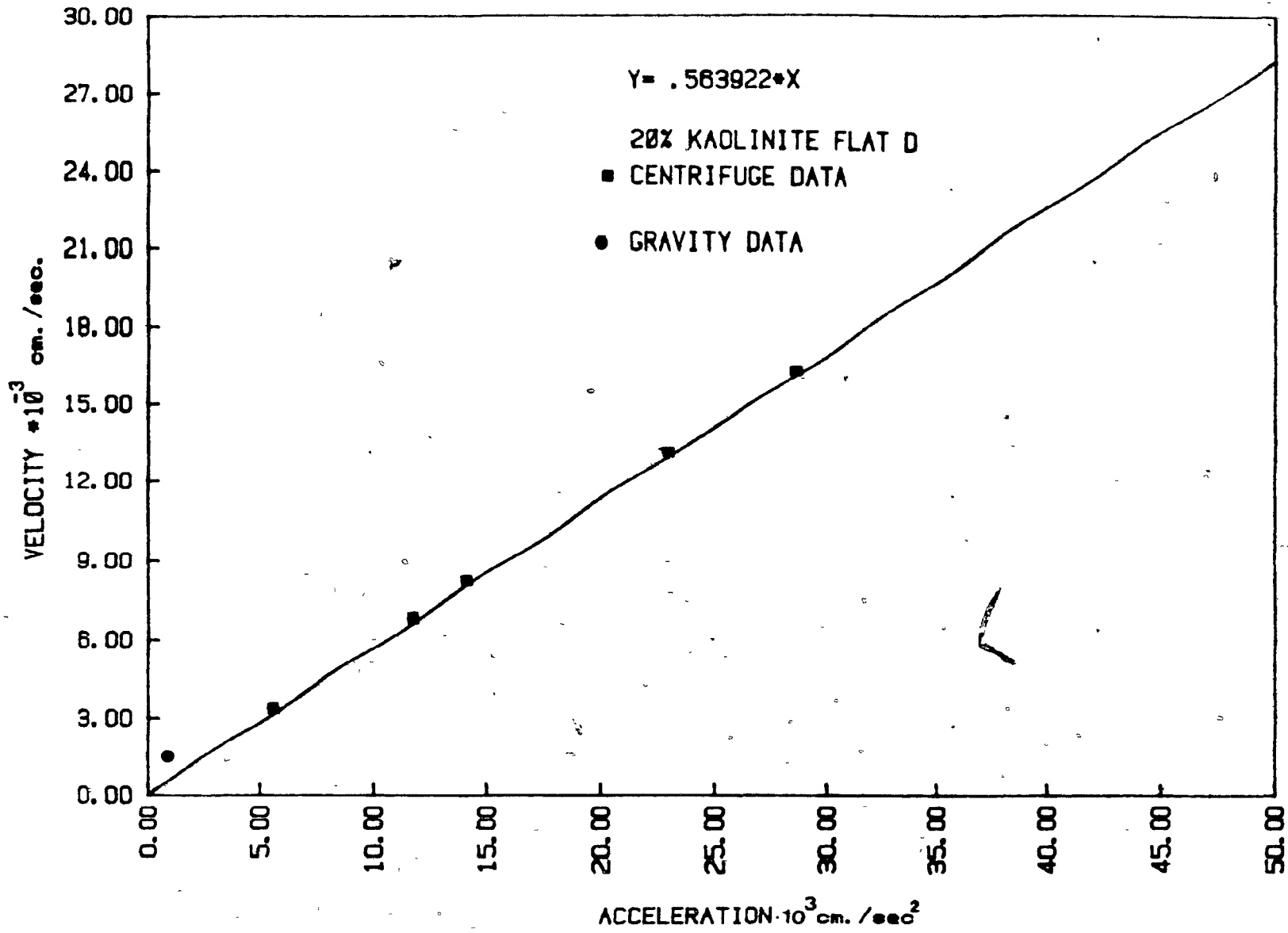

FIGURE 4-23 INITIAL SETTLINIG VELOCITY Vs. ACCELERATION

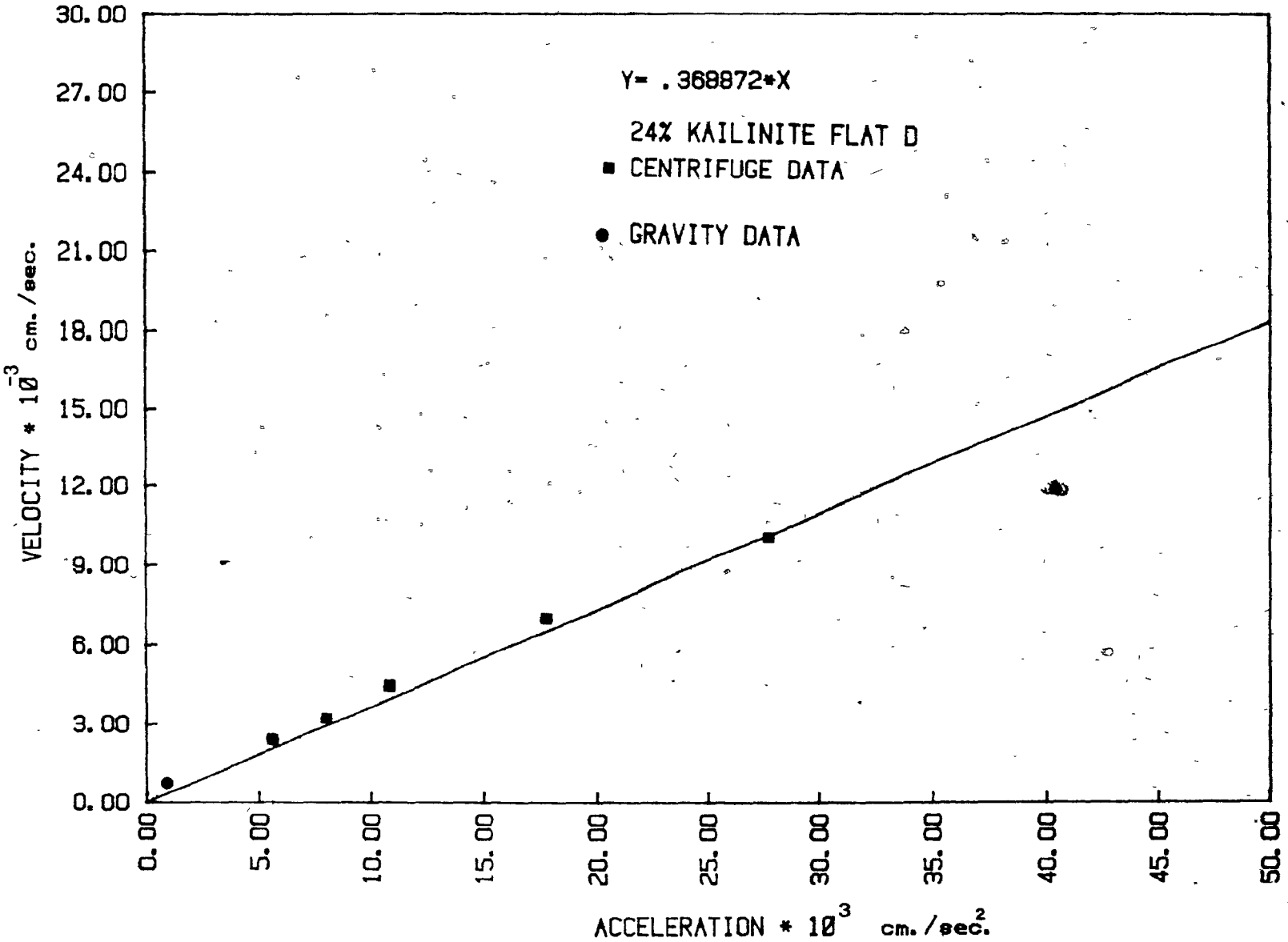

FIGURE 4-24 INITIAL SETTLINIG VELOCITY Vs. ACCELERATION

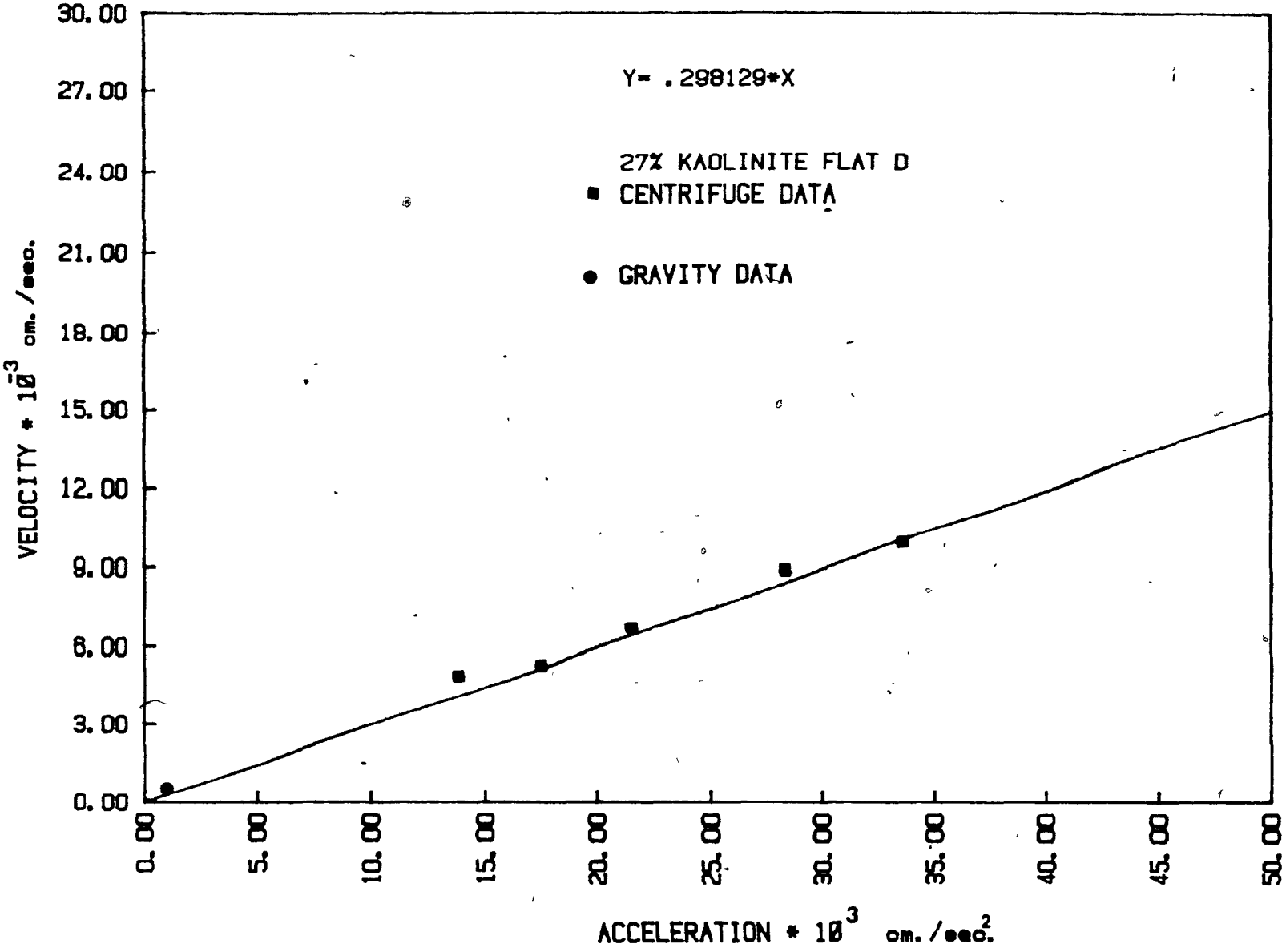

FIGURE 4-25 INITIAL SETTLINIG VELOCITY Vs. ACCELERATION

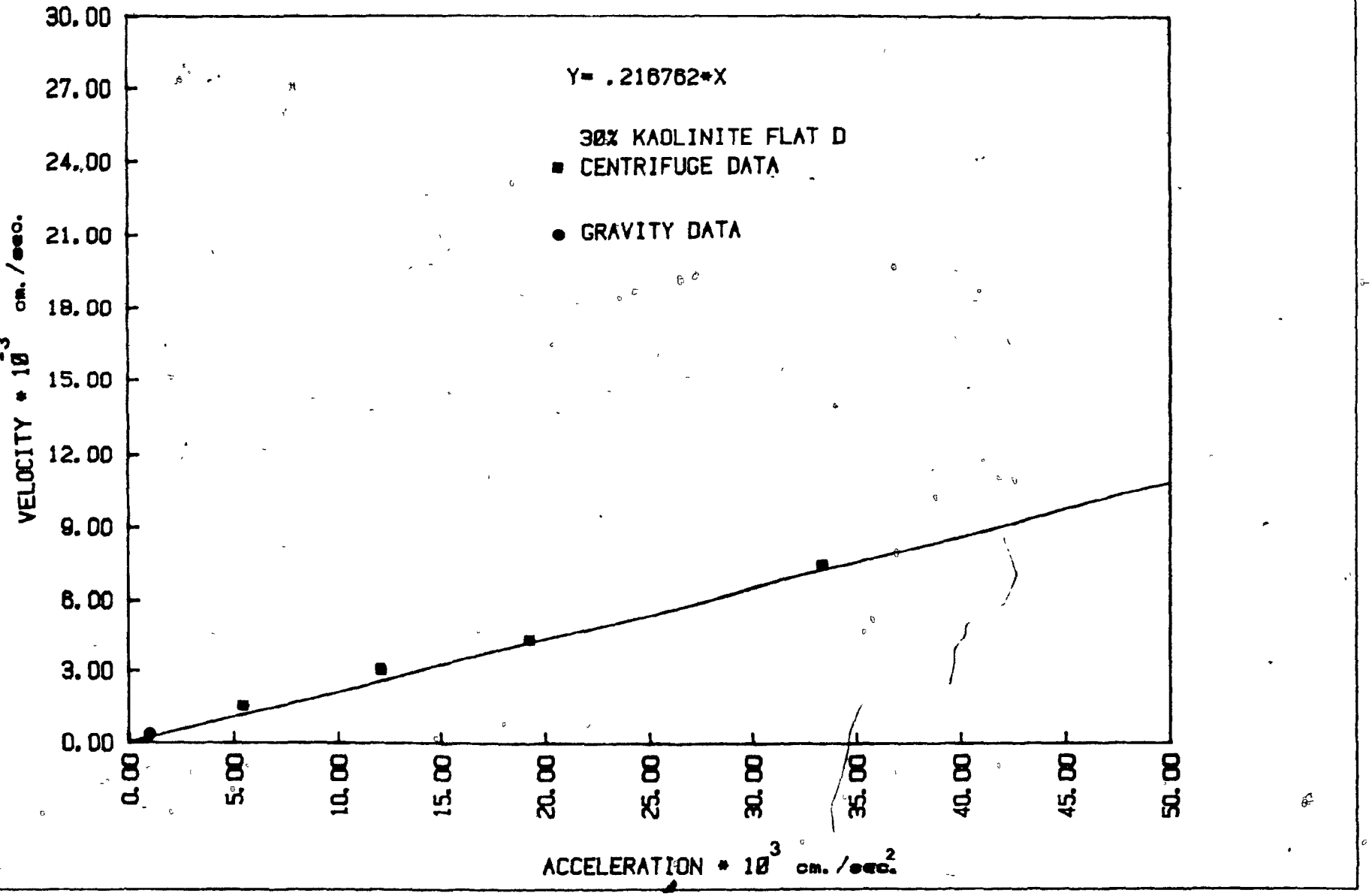

FIGURE 4-26 INITIAL SETTLINIG VELOCITY Vs. ACCELERATION

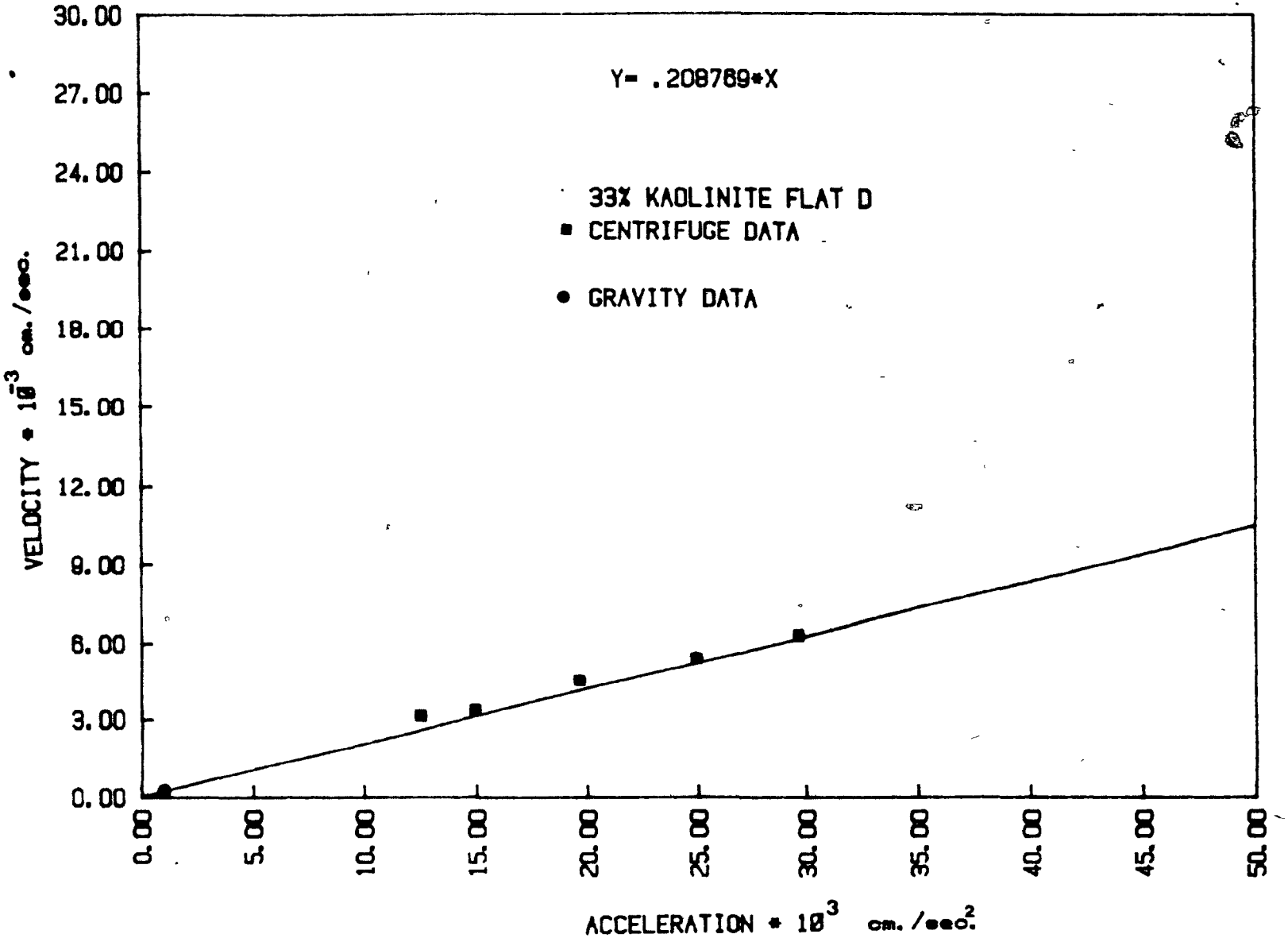

the settling velocity of the interface, under the influence of gravitational acceleration, is higher than that which would have been obtained from extrapolating the settling velocity - centrifugal acceleration line. With increasing concentration (20%, 24% and 27% by weight), the gravitational settling velocity gets closer to the extrapolated line. At the highest concentration investigated, (33% by weight), the gravitational settling velocity was lower than the extrapolated line.

Figure 4.27 shows the relationship between the settleability coefficient and the initial concentration, for both centrifuge and gravity data. It is seen that in the range of concentration up to ≈ 0.4 gm/cm^3, the settleability coefficients derived from gravity data are higher than those derived from centrifuge data. The equations describing these relationships are power functions for both centrifuge and gravity data, thus;

$$S_c = 0.452\ C^{-1.687} \qquad (4.11)$$

$$S_g = 0.152\ C^{-2.908} \qquad (4.12)$$

where S_c = the settleability coefficient calculated from centrifuge data in sec

S_g = the settleability coefficient calculated from gravity data in sec.

and C = initial concentration gm/cm^3

FIGURE 4-27 SETTLEABILITY COEFFICIENT Vs. INITIAL CONCENTRATION

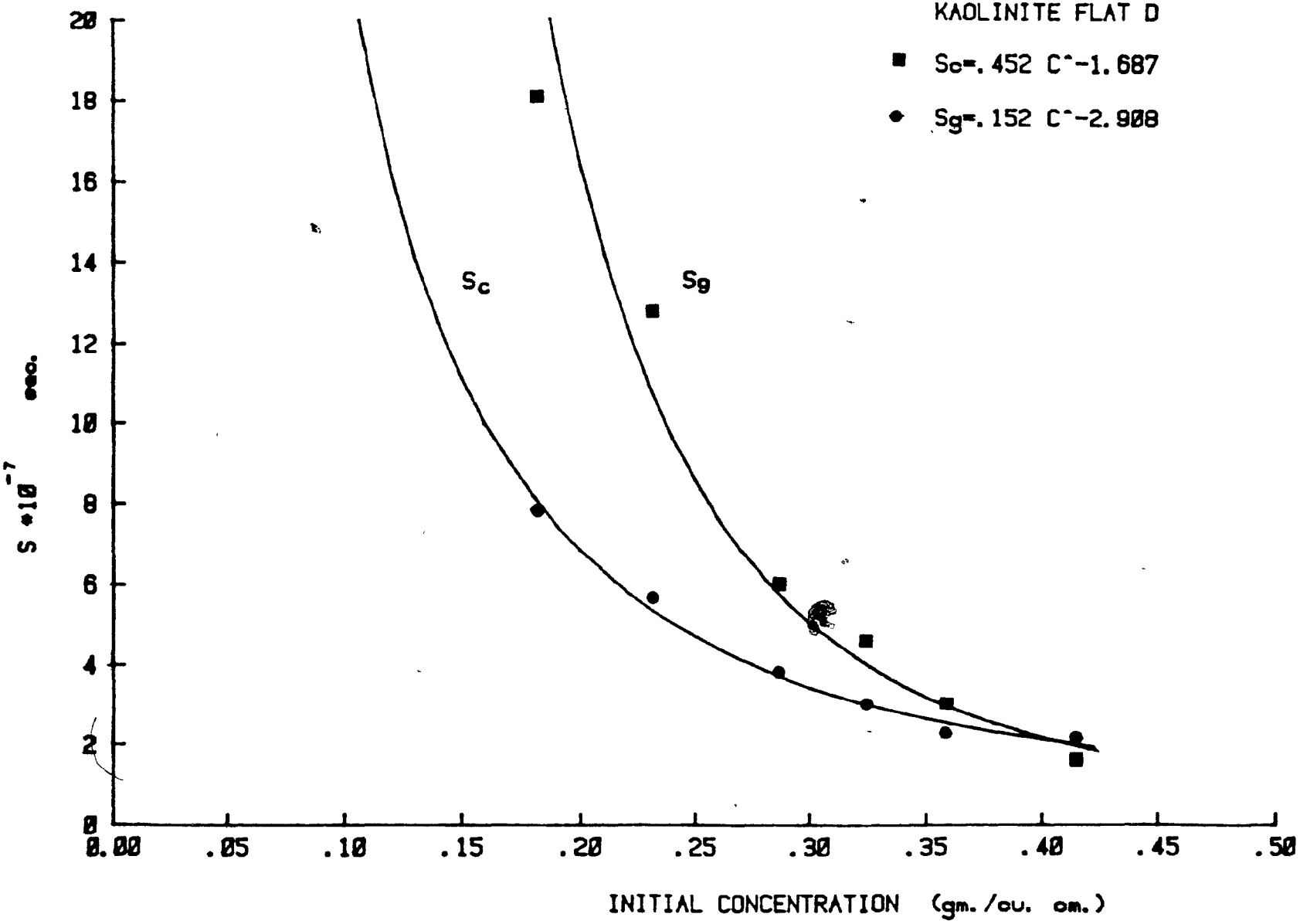

4.2.3 Effect of External Force on Particle-Size Distribution

A possible explanation for the higher settling velocity observed in the gravity settling tests, as compared with the corresponding values extrapolated from the centrifuge tests to an acceleration $w^2r = 980$ cm/sec^2, may be due to the segregation of the particles. In order to further examine this point, a series of experiments were performed:

- In the first series, six different suspensions of concentrations ranging from 16% to 33% (by weight) were subjected to gravitational settling.
- In the second series, a suspension of concentration 16% (by weight) was subjected to four rotational speeds ranging from 130-260 r.p.m.
- In the third series, four different suspensions, of concentrations ranging from 16% to 33% were all subjected to a single rotation speed of 160 r.p.m. Also, a suspension of concentration of 27% was subjected to a speed of 130 r.p.m. (see Appendix B).

For all concentrations, the particle size distribution was monitored by the sedigraph 5000 D, except for the 27% suspension, which was monitored by the standard hydrometer test (see Appendix B).

The aim of these tests is to facilitate the comparison between the behaviour of solid particles under the influence

of both centrifuge and gravity forces. Three samples were withdrawn from each tested tube after complete settling of the solid particles. The three samples were from different positions in the tube, namely, 1.0 cm below the top of the formed sediment, in the middle of the formed sediment, and 1.0 cm above the bottom of the formed sediment respectively. The samples were extracted using a pipette with internal diameter 10 mm . It was decided to take the samples after complete settling of the solid particles; if, at any stage of the test, the centrifuge had been stopped gradually by reducing the rotational speed, the solid particles would have propagated upward again, and it would have been difficult to determine the correct concentration at any level of the suspension.

Series 1

Figures 4.28-29 show the results of particle size analysis on samples taken from gravity tests at each concentration. The particle size distributions, for any three samples taken from a single tube subjected to gravity, are not significantly different. It is possible to conclude that, after turning the tube end over end 8-10 times, and running the test, the particles aggregate to form a floc, and the composition of each floc remains the same without any signficant segregation, until the final sediment is formed. Also, the main particle size diameter (D_{50}) is close to 4.5 microns, which is in agreement with the main particle

FIGURE 4-28 GRAIN SIZE DISTRIBUTION

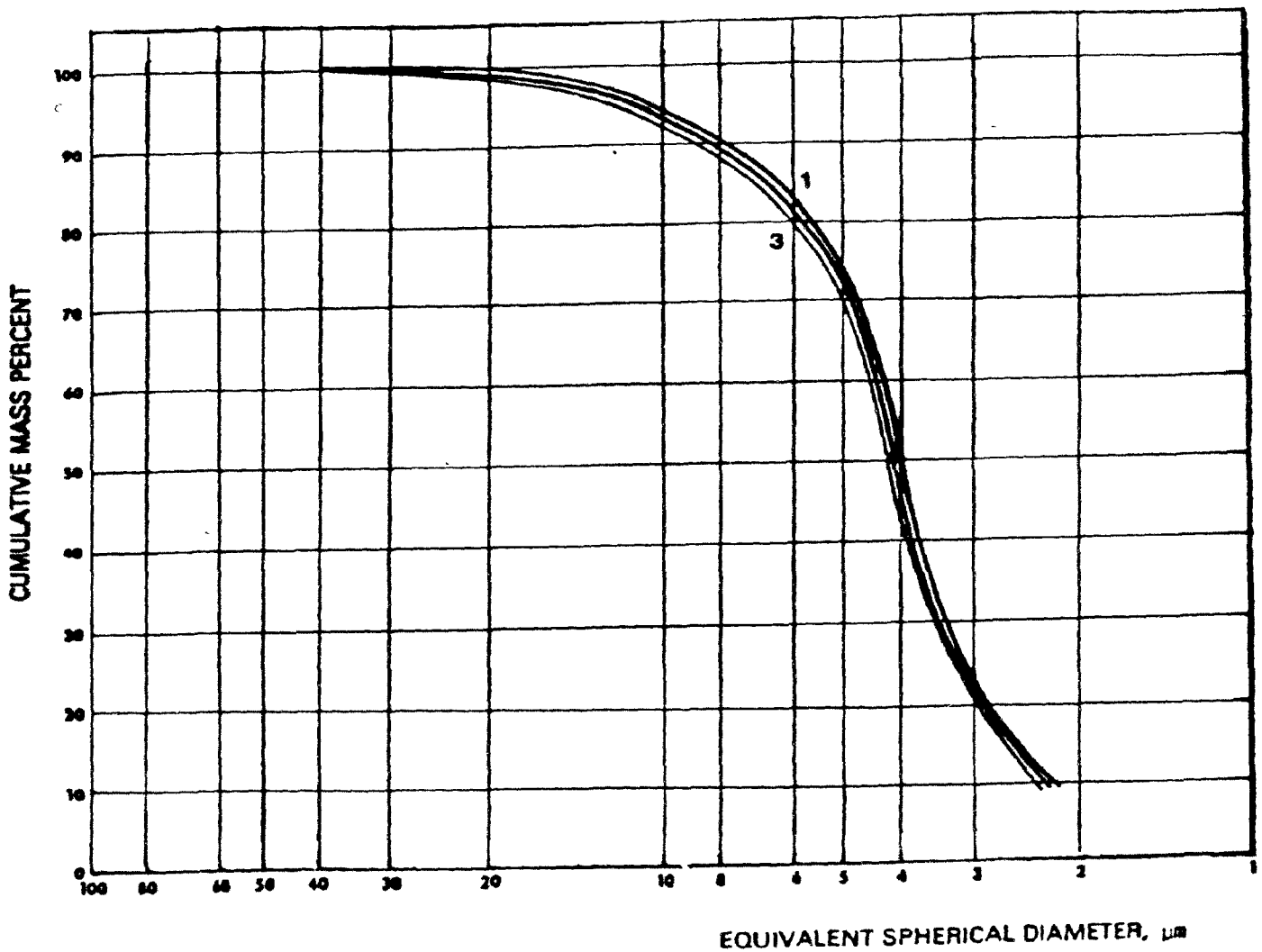

20% KAOLINITE FLAT-D

GRAVITY DATA

1 SAMPLE 1.0 cm. BELOW THE TOP OF THE SEDIMENT.

2 SAMPLE FROM THE MIDDLE OF THE SEDIMENT

3 SAMPLE 1.0 cm. FROM THE BOTTOM OF THE SEDIMENT

FIGURE 4-29 GRAIN SIZE DISTRIBUTION

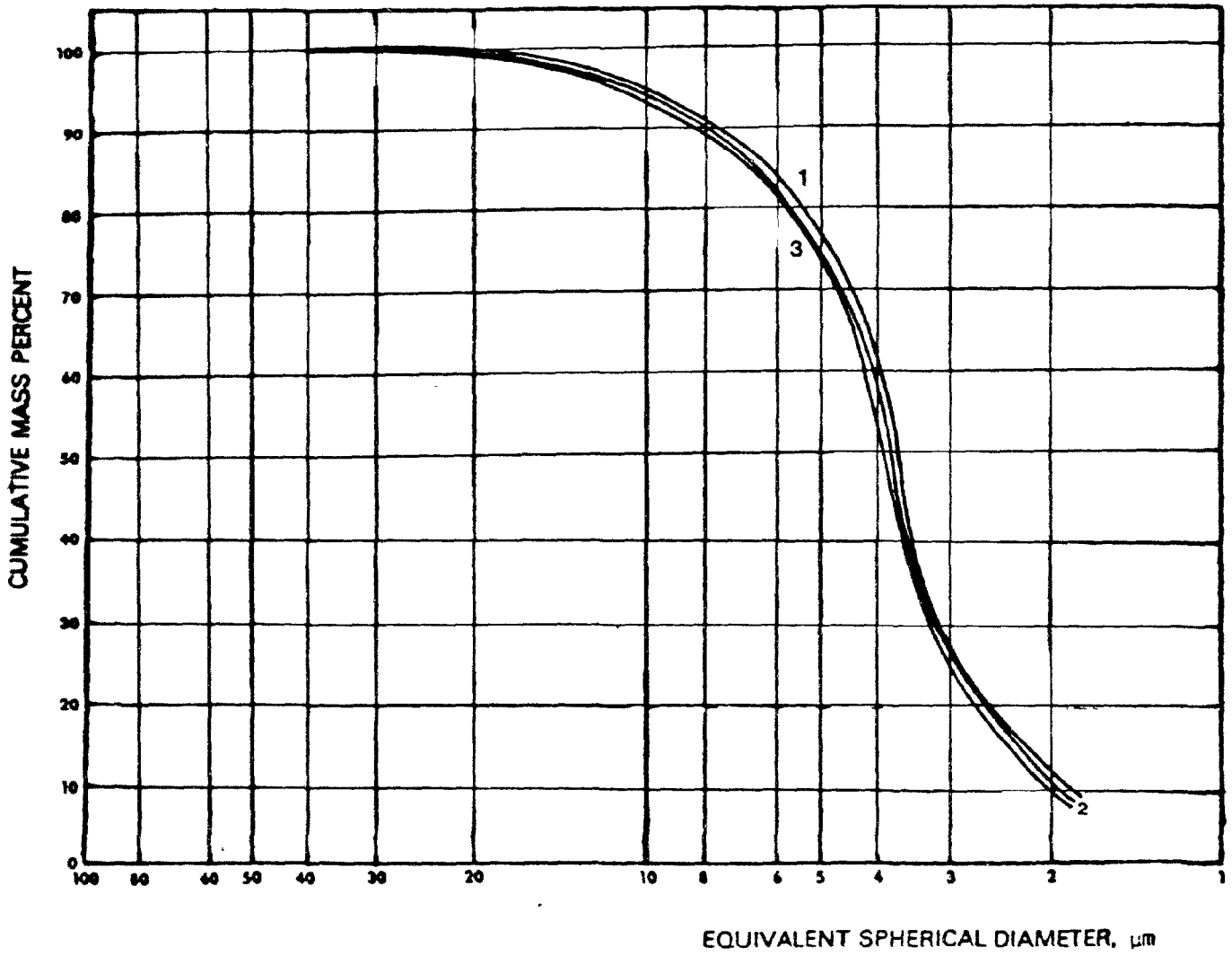

30% KAOLINITE FLAT-D

GRAVITY DATA

1 SAMPLE 1.0cm. BELOW THE TOP OF THE SEDIMENT

2 SAMPLE FROM THE MIDDLE OF THE SEDIMENT

3 SAMPLE 1.0cm. FROM THE BOTTOM OF THE SEDIMENT

size diameter calculated from the standard hydrometer test (Fig. 3.2).

Series 2

The particle size analysis of samples taken from centrifuge tests is different. To facilitate the comparison between the tests, the particle size analysis was plotted on a probability scale, as shown in Figs. 4.30-36. The values of D_{10}, D_{50}, D_{60}, Cu, percent finer less than 40 μm, percent finer less than 4 μm and percent finer less than 1.0 μm are given in each graph. Table 4.4 shows the summary of the particle size analysis for a concentration 16% (by weight) at the four different rotational speeds.

At rotational speed of 130 r.p.m., percent finer less than 4 μm is highest at the top, and decreases from top to bottom. Similarly percent finer less than 1.0 μm is also highest at the top and decreases from top to bottom. The same results are obtained at the other rotational speeds (160, 200 and 260 r.p.m.). Thus, at any rotational speed, the percent finer at the top of the formed sediment is higher than at the middle of the formed sediment, which in turn is higher than at the bottom of the formed sediment.

The same results can be looked at in a different way. The percent finer, obtained from the top position, decreases monotonically with increasing rotational speed; the situation is not as clear for a sample taken from the middle or

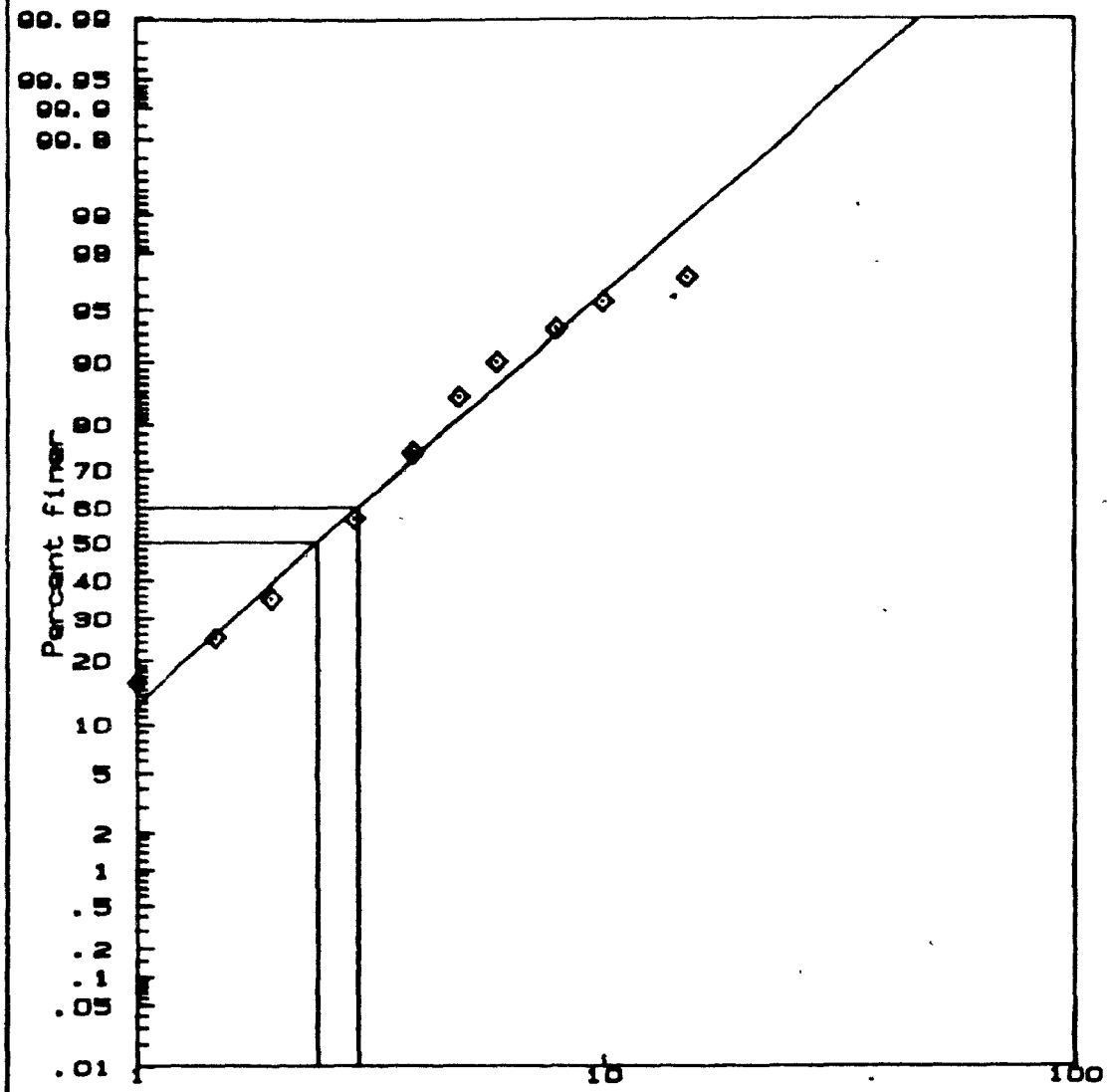

16% KAOLINITE FLAT D
CENTRIFUGE DATA
W=130 r.p.m.
SAMPLE 1.0 cm. BELOW
THE TOP OF THE SEDIMENT

PARTICLE SIZE ANLYSIS

D10	=	.81 micron
D50	=	2.50 micron
D60	=	3.05 micron
Cu	=	3.36 (Cu = D60/D10)

%CLAY (< 40micron) = 99.97776
%CLAY (< 4 micron) = 72.46694
%CLAY (< 1 micron) =12.33546

FIGURE 4-30 GRAIN SIZE DISTRIBUTION

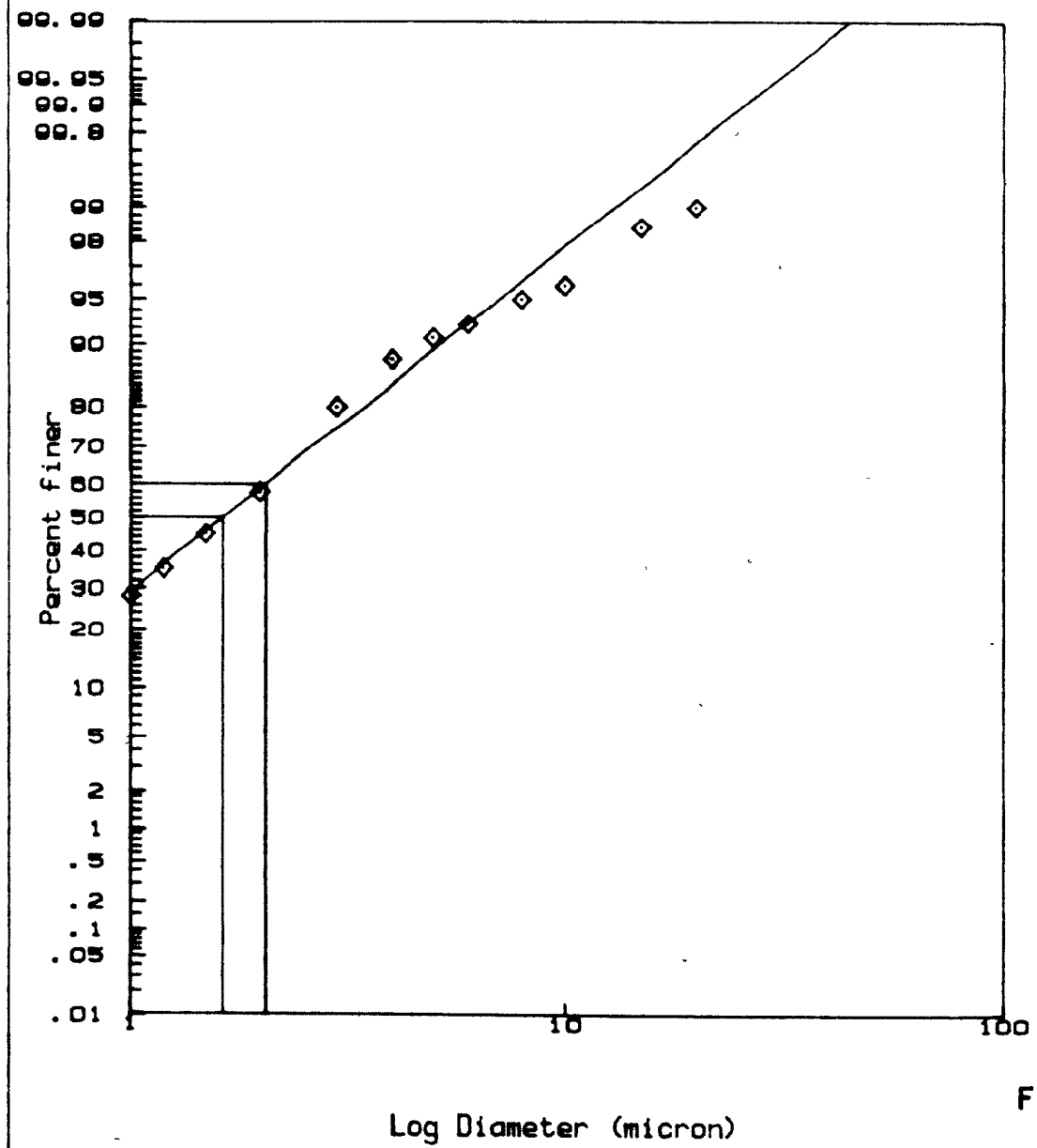

16% KAOLINITE FLAT D
CENTRIFUGE DATA
W=160 r.p.m.
SAMPLE 1.0 cm. BELOW
THE TOP OF THE SEDIMENT

PARTICLE SIZE ANLYSIS

D10	=	.53 micron
D50	=	1.64 micron
D60	=	2.06 micron
Cu	=	3.92 (Cu = D60/D10)

%CLAY (< 40micron) = 99.98321
%CLAY (< 4 micron) = 84.10538
%CLAY (< 1 micron) =28.81058

FIGURE 4-31 GRAIN SIZE DISTRIBUTION

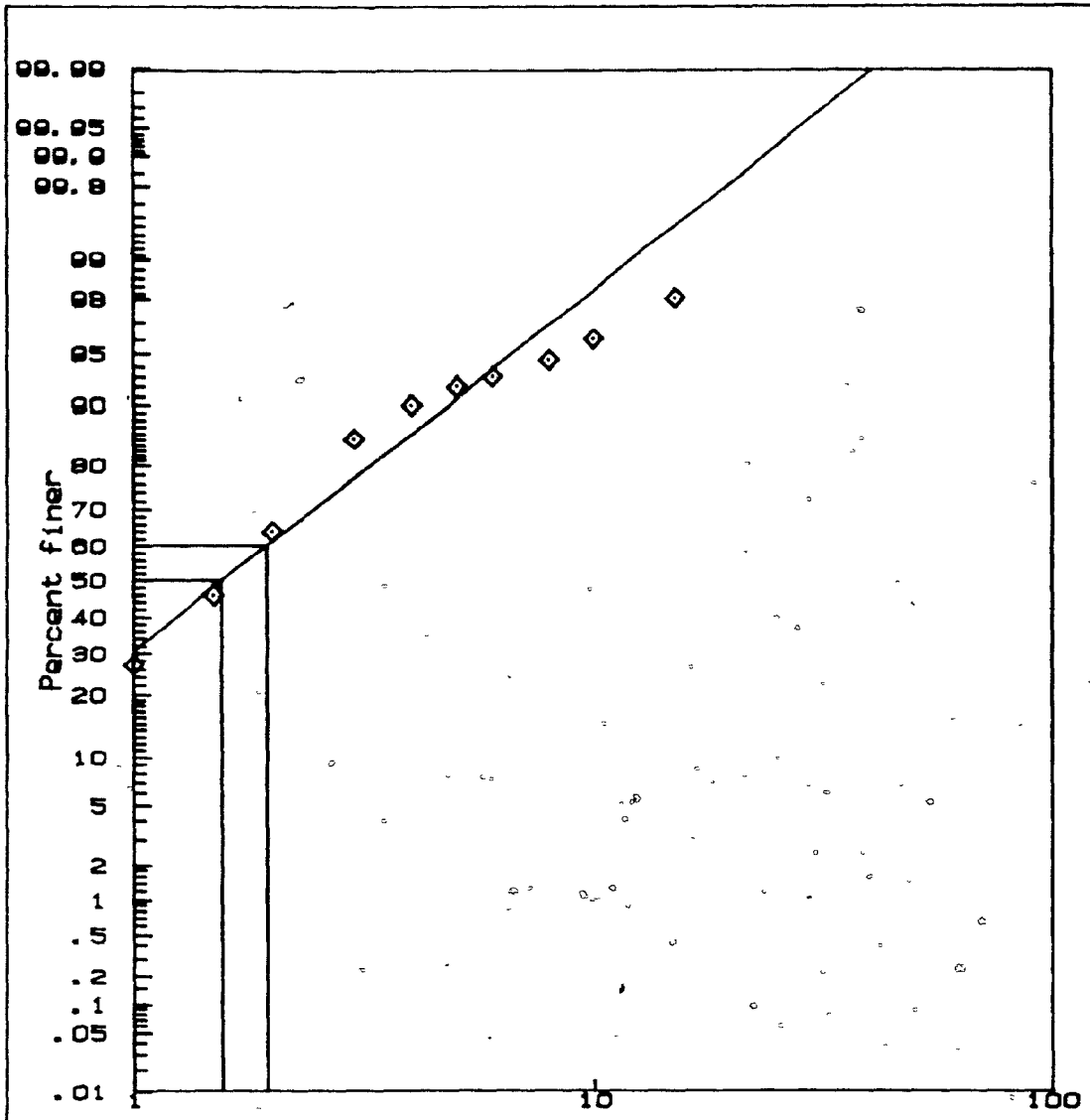

16% KAOLINITE FLAT D
CENTRIFUGE DATA
W=200 r.p.m.
SAMPLE 1.0 cm. BELOW
THE TOP OF THE SEDIMENT

PARTICLE SIZE ANLYSIS

D10	=	.50 micron
D50	=	1.56 micron
D60	=	1.95 micron
Cu	=	3.87 (Cu = D60/D10)

%CLAY (< 40micron) = 99.98853
%CLAY (< 4 micron) = 85.80349
%CLAY (< 1 micron) =30.80081

FIGURE 4-32 GRAIN SIZE DISTRIBUTION

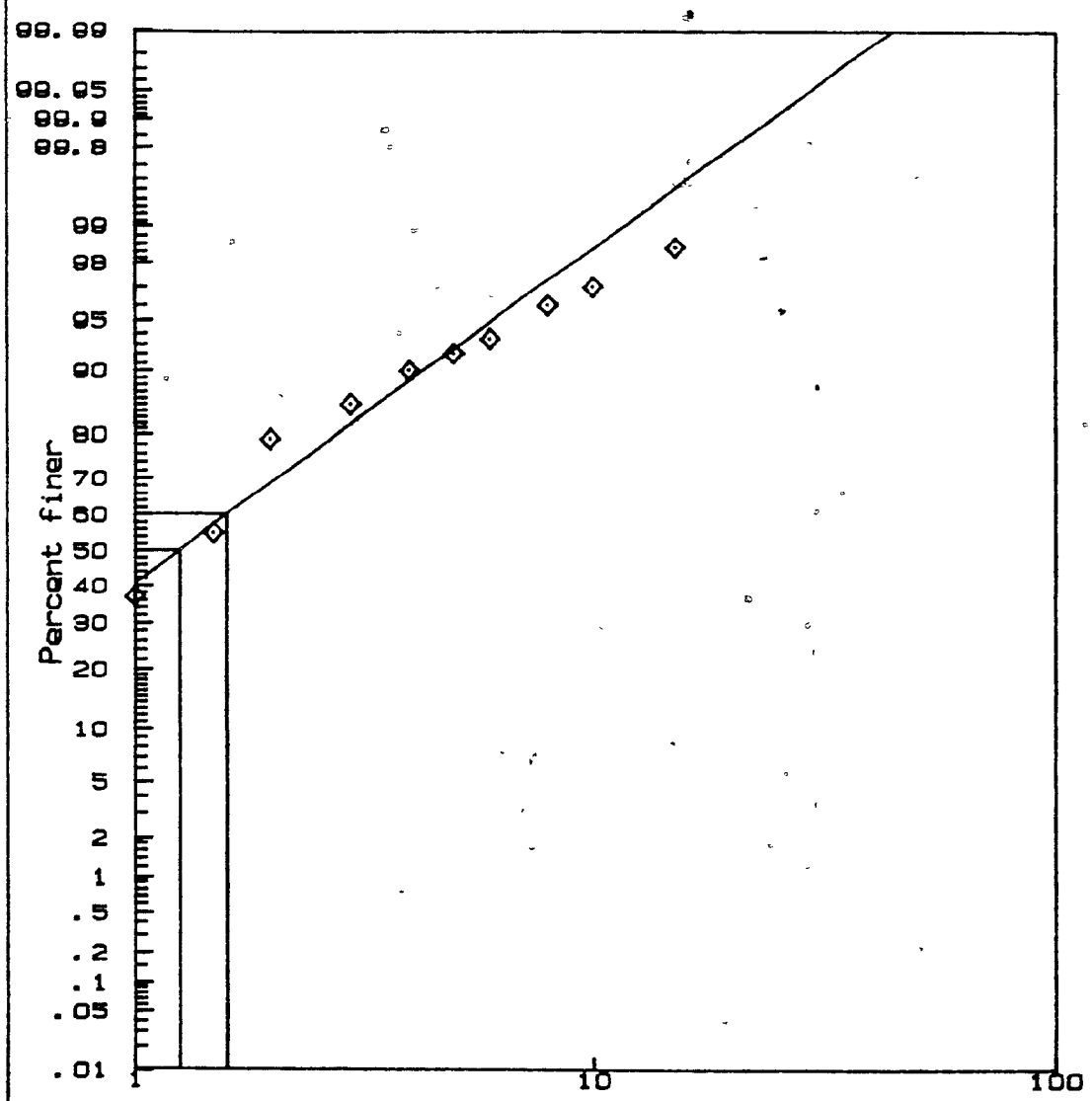

16% KAOLINITE FLAT D
CENTRIFUGE DATA
W=260 r.p.m.
SAMPLE 1.0 cm. BELOW
THE TOP OF THE SEDIMENT

PARTICLE SIZE ANLYSIS

D10	=	.37 micron
D50	=	1.25 micron
D60	=	1.60 micron
Cu	=	4.37 (Cu = D60/D10)

%CLAY (< 40micron) = 99.98437
%CLAY (< 4 micron) = 88.63476
%CLAY (< 1 micron) =40.67264

FIGURE 4-33 GRAIN SIZE DISTRIBUTION

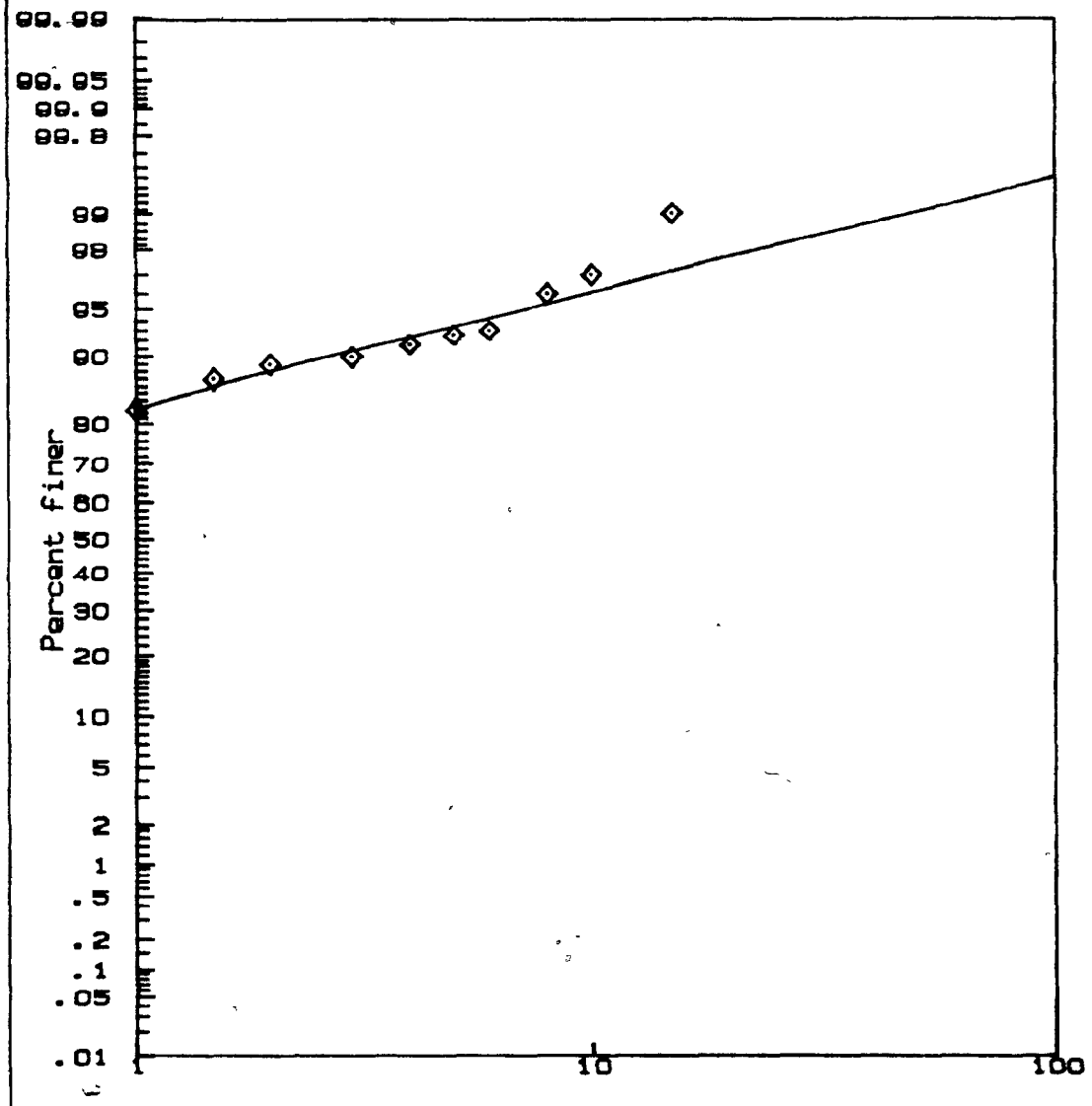

20% KAOLINITE FLAT D
CENTRIFUGE DATA
W=160 r.p.m.
SAMPLE 1.0 cm. BELOW
THE TOP OF THE SEDIMENT

PARTICLE SIZE ANLYSIS

D10 = .00 micron
D50 = .07 micron
D60 = .15 micron
Cu = 74.76 (Cu = D60/D10)

%CLAY (< 40micron) = 98.78200
%CLAY (< 4 micron) = 92.39492
%CLAY (< 1 micron) =82.61108

FIGURE 4-34 GRAIN SIZE DISTRIBUTION

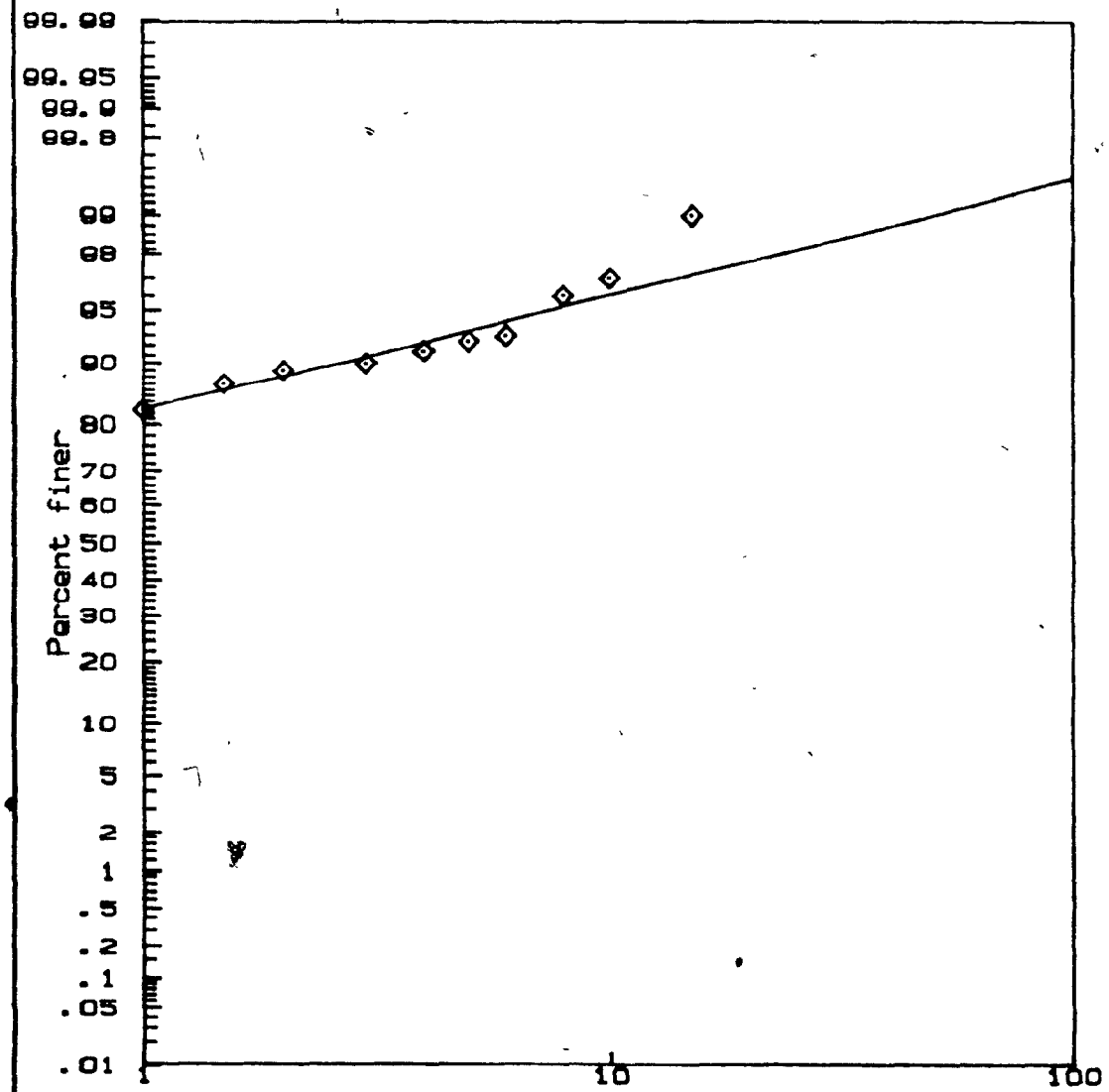

24% KAOLINITE FLAT D
CENTRIFUGE DATA
W=160 r.p.m.
SAMPLE 1.0 cm. BELOW
THE TOP OF THE SEDIMENT

PARTICLE SIZE ANLYSIS

D10 = .00 micron
D50 = .07 micron
D60 = .15 micron
Cu = 74.76 (Cu = D60/D10)

%CLAY (< 40micron) = 98.78200
%CLAY (< 4 micron) = 92.39492
%CLAY (< 1 micron) =82.61108

FIGURE 4-35 GRAIN SIZE DISTRIBUTION

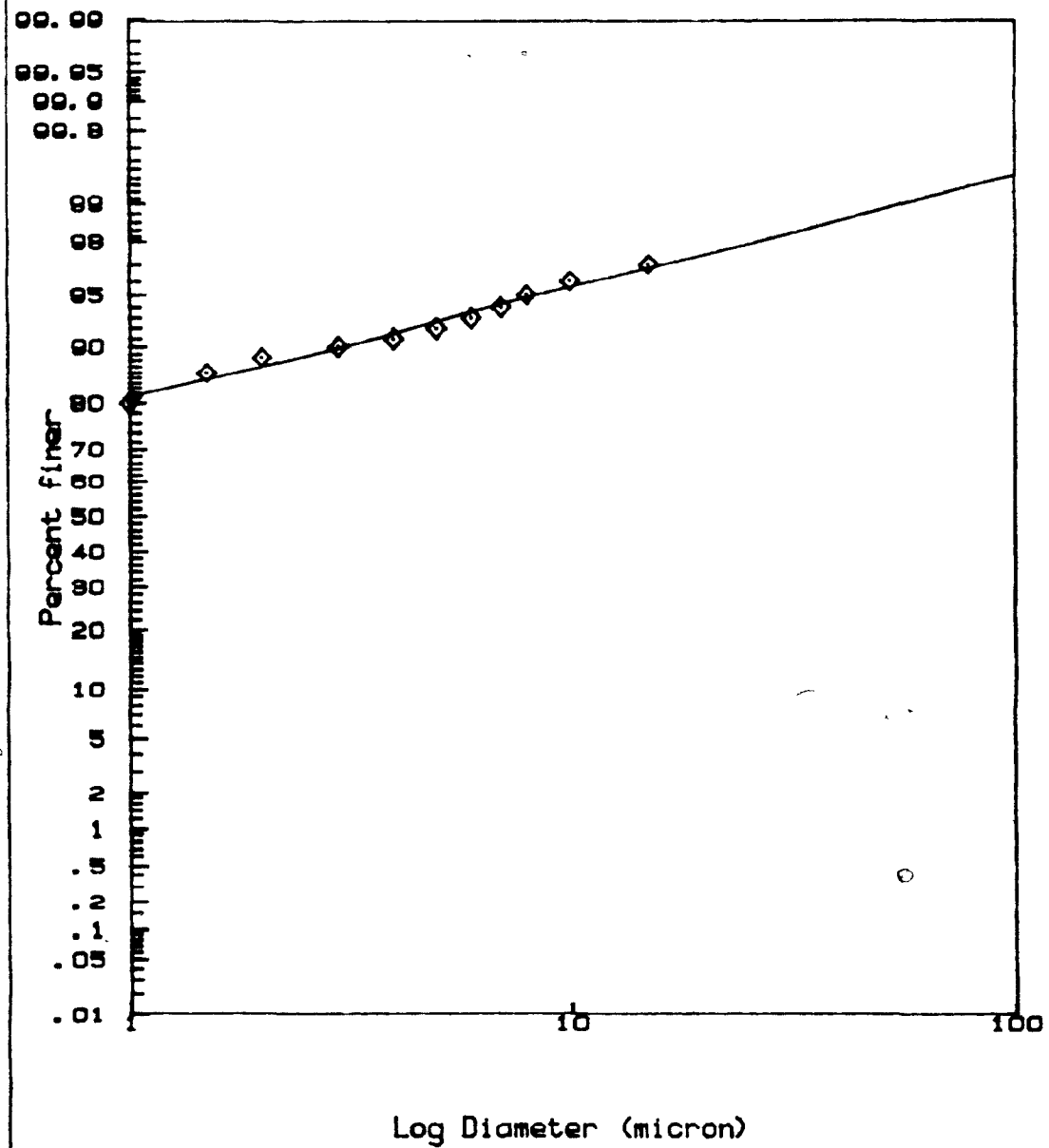

33% KAOLINITE FLAT D
CENTRIFUGE DATA
W=160 r.p.m.
SAMPLE 1.0 cm. BELOW
THE TOP OF THE SEDIMENT

PARTICLE SIZE ANLYSIS

D10 = .00 micron
D50 = .08 micron
D60 = .17 micron
Cu = 74.61 (Cu = D60/D10)

%CLAY (< 40micron) = 98.60107
%CLAY (< 4 micron) = 91.58911
%CLAY (< 1 micron) =81.17833

FIGURE 4-36 GRAIN SIZE DISTRIBUTION

TABLE 4.4 Particle size analysis for concentration 16% (wt/wt) at different rotational speeds and different depths

Rotational Speed (w) r.p.m.	Size μm	Sample 1.0 cm below the top of the sediment %	Sample from the middle of of the sediment %	Sample 1.0 cm above the bottom of the sediment %
130	<40	99.98	99.98	99.91
	< 4	72.47	56.34	31.38
	< 1	12.34	3.12	0.39
160	<40	99.98	99.88	99.67
	< 4	84.11	65.4	46.34
	< 1	28.81	11.67	3.74
200	<40	99.99	99.96	99.97
	< 4	85.8	71.6	50.87
	< 1	30.8	13.93	2.03
260	<40	99.98	99.98	99.17
	< 4	88.63	65.27	25.3
	< 1	40.67	6.51	0.62

the bottom: hence the percent finer does not appear to relate in a simple way with the rotational speed.

Table 4.5 shows the values of D_{10}, D_{50} and D_{60}, for concentration 16% (by weight), at different rotational speeds. The results indicate that, at any rotational speed, the values of D_{10}, D_{50} and D_{60}, as determined from samples taken at the top, are smaller than the corresponding values obtained from either the middle or the bottom of the sediment; in turn, the values of D_{10}, D_{50} and D_{60} from the middle are smaller than the corresponding values taken from the bottom.

For samples taken from the top, it is seen that, as the speed of rotation increases, the values of D_{10}, D_{50} and D_{60} decrease monotonically (thus, at speed 130 r.p.m, D_{50} = 2.5 μm, and at speed 260 r.p.m., it decreases to 1.25 μm).

Again it is not possible to find a simple relation between the D values and the speed of rotation, when these values are obtained from samples extracted from the middle and the bottom of the tubes.

The effect may be attributed to the error resulting from passing the pipette through different layers of the formed sediment; it is possible that different sizes of particles are picked up in this way. This may explain the absence of a simple relationship between the speed of rotation on the one hand, and the percent finer and the D

TABLE 4.5 Particle size analysis for concentration 16% (wt/wt) at different rotational speeds and different depths

Rotational Speed (w) r.p.m	Equivalent Particle Diameter	Sample 1.0 cm below top of the sedimment	Sample from the middle of the sediment	Sample 1.0 cm above the the bottom of the sediment
130	D_{10}	0.91	1.49	2.41
	D_{50}	2.5	3.59	5.45
	D_{60}	3.05	4.27	6.4
160	D_{10}	0.53	0.93	1.51
	D_{50}	1.64	2.83	4.31
	D_{60}	2.06	3.54	5.32
200	D_{10}	0.5	0.85	1.67
	D_{50}	1.56	2.48	3.94
	D_{60}	1.95	3.07	4.68
260	D_{10}	0.37	1.18	2.51
	D_{50}	1.25	3.01	6.58
	D_{60}	1.6	3.62	7.98

values (obtained from samples extracted from the middle and the bottom of the tubes) on the other hand. With regard to the amount of sample withdrawn, which is approximately 1-2 cm^3, it is possible to assert that results related to samples taken from the top of the sediment are more accurate than those relating to samples from either the middle or the bottom of the formed sediment.

Series 3:

Tables 4.6-7 show the particle size analysis for each concentration (16%, 20%, 24%, and 33% by weight) at a constant rotational speed of 160 r.p.m. The percent finer for any sample extracted at the top is highest, and decreases from top to bottom. Also, the values of D_{10}, D_{50} and D_{60} at the top of the sediment are smallest and increase from top to bottom. Tables 4.6-7 also show that the percent finer and the values of D_{10}, D_{50} and D_{60} for the top samples do not vary significantly at concentrations higher than 20% (by weight). On the other hand, in the case of samples taken from the middle and bottom of the tubes, some variation is observed in the values of the percent finer and in the D values; however, no systematic relation could be deduced.

TABLE 4.6 Particle size analysis at the same rotational speed (w = 160 r.p.m.) with changing initial concentrations at different depths

Conc. wt/wt	Size μm	Sample 1.0 cm below the top of the sediment %	Sample from the middle of the sediment %	Sample 1.0 cm above the bottom of the sediment %
16%	<40	99.98	99.88	99.67
	< 4	84.11	65.4	46.34
	< 1	28.81	11.67	3.74
20%	<40	98.78	99.99	99.87
	< 4	92.4	72.6	40.97
	< 1	82.61	5.86	0.72
24%	<40	98.78	99.99	99.99
	< 4	92.4	77.44	59.7
	< 1	82.61	9.5	2.08
33%	<40	98.6	99.99	99.99
	< 4	91.59	63.25	41.41
	< 1	81.18	1.67	0.42

TABLE 4.7 Particle size analysis at the same rotational speed (w = 160 r.p.m.) with changing initial concentrations at different depths

Conc. wt/wt	Equivalent Particle Diameter	Sample 1.0 cm below the top of the sedi-ment	Sample from the middle of the sedi-ment	Sample 1.0 cm above the bottom of the sedi ment
16%	D_{10}	0.53	0.93	1.51
	D_{50}	1.64	2.83	4.31
	D_{60}	2.06	3.54	5.32
20%	D_{10}	0.0	1.2	2.07
	D_{50}	0.07	2.72	4.61
	D_{60}	0.15	3.21	5.41
24%	D_{10}	0.0	1.02	1.58
	D_{50}	0.07	2.41	3.45
	D_{60}	0.15	2.86	4.02
33%	D_{10}	0.0	1.61	2.17
	D_{50}	0.08	3.31	4.53
	D_{60}	0.17	3.82	5.24

Conclusions:

1. The results of the first series of tests indicate that no significant segregation occurs in experiments conducted under gravity, and that, independently of concentration.

2. The results of the second series of tests indicate that segregation occurs in experiments conducted under centrifugal force. For a given concentration, the segregation increases with increasing rotational speed; it is also highest at the top of the sample, and decreases from the top to the bottom of the sample.

3. The results of the third series indicate that the segregation is independent of concentration, for concentration higher than 20% (by weight)

CHAPTER 5

SUMMARY AND CONCLUSIONS

The purpose of this study was to evaluate experimentally the applicability of the centrifuge as a tool to determine the settling characteristics of suspensions. The centrifuge test is proposed as a substitute for a technique used in conventional laboratory batch column tests (i.e. settling of the suspension under the influence of gravity force) to determine the relationships between settling velocities and concentration of suspension. The centrifuge test can be completed in a few hours, yielding information which would take days or even weeks to obtain from gravity tests. Two suspension materials were used: Hydrite Flat D Kaolinite and Hydrite Ultra Fine Kaolinite.

These two types of suspension tests were conducted to study the effect of concentration on settling velocities at a constant rotational speed of 100 r.p.m., as well as the effect of concentration on settling velocities under the influence of gravity force (i.e. no centrifugal force was employed).

In Hydrite Flat D studies, the validity and/or applicability of the centrifuge test was evaluated through its ability to predict accurately the settleability coefficient of the suspension, at different rotational speeds, and at different concentrations; this predicted settleability coefficient was then compared to that obtained from gravity tests.

In Hydrite Flat D studies, a further evaluation of the centrifuge technique was carried out; it involved the determination of particle size distribution, at different concentrations and rotational speeds. The results were compared to particle size distributions measured from gravity tests carried out at the same concentrations.

5.1 STUDIES OF PHASE 1

5.1.1 Studies of Hydrite Flat D

The results of phase one studies of Hydrite Flat D indicated that the relationship between the initial settling velocity of the suspensions and their initial concentration, in the range of 8%-30% (by weight) (as determined by Coe and Clevenger's initial rate method) was found to conform very closely to the following equations:

1. For centrifuge tests at constant rotational speed of 100 r.p.m.

$$V_c = 0.196 \times 10^{-3} \times C^{-1.858} \qquad (4.1)$$

where V_c = initial settling velocity under the influence of centrifugal force (at rotational speed of 100 r.p.m.) in cm/sec

C = initial concentration in gm/cm^3

2. For gravity tests (i.e. absence of centrifugal force)

$$V_g = 0.107 \times 10^{-3} C^{-1.605} \qquad (4.3)$$

where V_g = initial settling velocity under the influence of gravitational force in cm/sec

C = initial concentration in gm/cm^3

From the above two equations, the theoretical relationship between settling velocity, at a constant rotational speed of 100 r.p.m., and settling velocity, under the influence of gravity at any concentration in the range of 8%-30% may be described as:

$$\frac{V_g}{V_c} = 0.5459\ C^{0.253} \qquad (5.1)$$

From the above equation, it is found that the settling velocities in a centrifugal field are approximately 1.3 to 3.47 times larger than the corresponding settling velocities under the influence of gravity. The lower ratio refers to the lowest concentration (8%) while the highest ratio refers to the highest concentration (30%). At the same time, the imposed centrifugal force at the rotational speed of 100 r.p.m. was approximately 5.4 times larger than the gravitational force.

Thus, the equation governing the motion of the particles in a centrifugal field, viz,

$$V_c = (R.C.F.)\ V_g \qquad (2.11)$$

where V_c = settling velocity under the influence of centrifugal force

V_g = settling velocity and the gravity force

R.C.F.= relative centrifugal force

is not satisfactory. This may be attributed to the fact

that the particles moving through a centrifuge tube are passing through a zone of higher force where they are being accelerated, and their velocity is less than that calculated from equilibrium conditions.

Ambler (1961) pointed out that the law of conservation of momentum predicts that the rotational velocity of the particle will lag behind the rotational speed of the centrifuge and its fluid, if the particle is relatively heavy.

5.1.2 Studies of Hydrite Ultra Fine

The results of phase one studies of Hydrite Ultra Fine indicated that the relationship between initial settling velocity and initial concentration, in the range 8%-20% (by weight) (as determined by Coe and Clevenger's initial rate method) was found to conform very closely to the following equations:

a. For centrifuge test at a constant rotational speed of 100 r.p.m.

$$V_c = 0.02 \times 10^{-3} \times C^{-1.819} \qquad (4.2)$$

b. For gravity test (i.e. absence of centrifuge field)

$$V_g = 0.03965 \times 10^{-4} \times C^{-1.9494} \qquad (4.4)$$

The relationship between settling velocity at a constant rotational speed (100 r.p.m.) and settling velocity under gravity for any concentration between 8%-20% (by weight) may then be described by:

$$\frac{V_g}{V_c} = 0.19825 \times C^{0.1304} \qquad (5.2)$$

5.2 STUDIES OF PHASE 2

The material used in these studies was Hydrite Flat D kaolinite. The results of six sets of centrifugal tests, on suspensions of different concentrations (16%, 20%, 24%, 27%, 30% and 33% by weight) were compiled. Five rotational speeds were applied to each concentration considered.

The results of each set of tests indicated that the observed settling velocity of the interface is proportional to the force imposed, i.e.

$$V_c \propto w^2 r$$

or
$$\frac{V_c}{w^2 r} = S_c = \text{constant} \qquad (4.10)$$

where V_c = the observed settling velocity of the interface in cm/sec

$w^2 r$ = centrifugal acceleration in cm/sec^2

S_c = settleability coefficient in sec.

In other words, the settleability coefficient for each concentration considered is independent of the rotational speed or radius of rotation. It means that, on increasing or decreasing the rotational speed, the centrifugal acceleration increases or decreases; at the same time, the observed settling velocity of the interface also increases or decreases, to keep the ratio between the observed settling velocity and the associated centrifugal

acceleration constant. The settleability coefficient depends on the concentration; it decreases with increasing concentration.

At each concentration considered, the plot of the observed settling velocity of the interface, versus the associated centrifugal acceleration, yields a straight line, whose slope gives the settleability coefficient. This straight line was then extrapolated towards the origin, to obtain an estimate of the settling velocity corresponding to an acceleration given by

$$w^2 r = 980 \text{ cm/sec}^2$$

which is the acceleration due to gravity.

On superposing the settling velocity, as determined from the gravity tests, onto the corresponding graph, it was found that at low concentrations (16% by weight), the "gravitational" settling velocity was higher than the "centrifugal" settling velocity, obtained by extrapolation. The difference between the "gravitational" settling velocity and the extrapolated "centrifugal" settling velocity, was found to decrease with increasing concentration of the suspension. For the highest concentration of suspension (33% by weight), the "gravitational" settling velocity even falls below the extrapolated "centrifugal" settling velocity.

The relationship between the settleability coefficient and the concentration in the centrifugal field can be described by:

$$S_c = 0.452\ C^{-1.687} \qquad (4.11)$$

where S_c = settleability coefficient in sec.

C = initial concentration in gm/cm^3

while the relationship describing the settleability coefficient as a function of concentration in the gravitational field is

$$S_g = 0.152\ C^{-2.908} \qquad (4.12)$$

The observed discrepancy in the values of settling velocities as observed in gravity tests on the one hand, and in the centrifuge tests, on the other hand, may be due to segregation of the particles; in the gravity field, no significant segregation occurred while in the centrifugal field, there was segregation of the particles.

In order to check this hypothesis, it was necessary to determine the particle size distribution. For this purpose, three samples were picked up from three different levels of the tubes (viz, 1.0 cm below the top, at the middle, and 1.0 cm above the bottom of the formed sediment) in both gravity and centrifuge tests; the process was repeated for five concentrations (16%, 20%, 25%, 27% and 33% by weight).

The results are illuminating. In samples subjected to gravitational settling, the particle size distribution indicated no significant differences in the average size of particles between the top and the bottom of the formed

sediment. On the other hand, the results of centrifuge tests are more complex. The following could be observed:

1. For a constant concentration (16% by weight) and for all tests in samples taken 1.0 cm below the formed sediment, the percent of finer increases with increasing rotational speed (in the range 130 to 260 r.p.m) and the equivalent diameter of particles decreases with increasing rotational speed. In samples withdrawn 1.0 cm from the bottom of the formed sediment, the percent of finer decreases with increasing rotational speed and the equivalent diameter increases with increasing rotational speed. Thus, in the centrifugal tests, the imposed force causes segregation of particles. Increasing the rotational speed increases this segregation.

2. For the fixed rotational speed (160 r.p.m.) in samples taken 1.0 cm below the top, for all concentrations tested (16% - 33% by weight), the percent of finer increases with increasing concentration, up to a concentration of 20% (by weight), and thereafter becomes independent of the concentration.

A theory, proposed by Kynch (1952) explains the so-called hindered settling zone; it was developed by assuming that all particles are equi-sized. Furthermore, it seems reasonable to suggest that the theory is valid only above some minimum concentration.

The present results indicate that, for a kaolinite suspension in a centrifugal field, the Kynch theory is not applicable. It is found that increasing the centrifugal force causes the segregation of the solid particles, in spite of the tendency of the particles to agglomerate, due to both Brownian motion and surface charge; thus, these two influences are countered by the higher centrifugal force.

On the other hand, the behaviour of kaolinite suspensions in a gravitational field is in agreement with the Kynch assumption, and the condition of equi-sized particles is satisfied; this can be seen from the grain size distribution.

CONCLUSIONS

The present study on the sedimentation of kaolinite suspensions was calculated under both centrifugal and gravitational force. From this study, the following conclusions can be drawn:

1. The equation governing the settling velocity of a suspension is given by:

$$V_c = (R.C.F.)\ V_g$$

where: V_c = settling velocity of the interface under the influence of centrifugal force

R.C.F. = relative centrifugal force acting on solid particles

V_g = settling velocity under the influence of gravitational force.

This equation was found to not be applicable to suspensions of kaolinite at low solid concentrations (< 16% wt/wt); but could be applicable to suspensions of kaolinite at high concentrations, where segregation is less of a problem.

2. For a kaolinite suspension, under the influence of a centrifugal force, the settling velocity of the interface (V_c) is proportional to the imposed

centrifugal force. The ratio between the settling velocity of the interface (V_c), and the imposed centrifugal force is constant. The constant is called the "settleability coefficient (S)". The settleability coefficient is a characteristic of the system; it depends on the solids concentration and the nature and size of the flocs, but does not depend on the imposed centrifugal force.

3. For a kaolinite suspension, the application of Stokes' law to calculate the floc diameter in the hindered settling zone, using the viscosity of the supsension at shear rate of 50 sec^{-1} shows that:
   a. the floc diameter does not depend on the initial solids concentration
   b. the floc diameter is twice (D_{50}) the particle size calculated from standard hydrometer tests.

4. For kaolinite suspensions, the values of n and A (the constants in the Richardson and Zaki equation, and in the Steinour equation respectively) determined from the present investigation, are higher than the corresponding values determined by all previous investigators. The higher values may be attributed to the surface activity of kaolinite particles.

REFERENCES

Ambler, C.M. (1952) "The evaluation of Centrifuge Performance", Chemical Engineering Progress Journal, Vol. 48, No. 3, pp. 150-154

Ambler, C.M. (1961) "The Fundamentals of Separation, Including Sharples 'Sigma values' for Predicting Equipment Performance", Industrial and Engineering Chemistry Journal, Vol. 53, pp. 430-433

Anderson, A.A. and Sparkman, J.E. (1959) "Review - Sedimentation Theory", Chemical Engineering, p.

Ayres, E.E. Jr. (1917) "The Effect of Centrifugal Force on Colloidal Solutions", American Institute of Chemical Engineers, Transaction, Vol. IX, pp. 203-231

Behn, V.C. (1957) "Settling Behaviour of Wastes Suspenstions", Proceedings American Society of Civil Engineers, Vol. 83, No. SA5, Proc. Paper 1423

Bingeman, J.B. (1955) "Preliminary Selection of Centrifugal Equipment", Chimical Engineering Progress, pp. 272-277

Bond, A.W. (1960) "Behaviour of Suspensions", Proceedings American Society of Civil Engineers, Vol. 86, No. SA3, pp. 57-85

Bond, A.W. (1961) "The Behaviour of Suspensions", Journal Institution of Water Engineers, Vol. 15, pp. 494

Brugger, K. (1976) "Centrifugal Sedimentation and Brownian Motion" Powder Technology Journal, Vol. 14, pp. 187-188

Coe, H.S. and Clevenger, G.H. (1916) "Methods for Determining the Capacity of Slime-Settling Tanks", Transactions American Institute of Mining Engineers, Vol. 55, pp. 356-384

Coulson, J.M., Richardson, J.F. (1960) "Chemical Engineering" Pergamon, Oxford, Vol. 2, pp. 510

Davies, J. and Richardson, J.F. (1966) "Gas Interchange Between Bubbles and the Continuous Phase in a Fluidized Bed", Treactions, Institution of Chemical Engineers, Vol. 44, pp. 293

Davies, L., Dollimore, D. and McBride, G.B. (1977) "Sedimentation of Suspensions: Simple Methods of Calculating Sedimentation Parameters", Powder Technology Journal, Vol. 16, pp. 45-49

Douglas, E. and Yong, R.N. (1981) "Interparticle Forces, Coagulation and Fabric of Partially Hydrolized Kaolinite", 2nd World Congress of Chemical Engineers, Montreal, Canada, Vol. 3, pp. 364-370

Eckenfelder, W.W. and Melbinger, N. (1957) "Settling and Compaction Characteristics of Biological Sludges", Sewage and Industrial Wastes, Vol. 29, pp. 1114-1122

Elton, G.A.H. and Hirschler, F.G. (1954) "Electroviscosity in Dilute Heterodisperse Suspensions", Brit. J. Appl. Phys., Suppl. No. 3, pp. 560

Epstein, N. (1979) "Hydrodynamic Particle Volume Factor and Settled Bed Volume", Canadian Journal of Chemical Engineering, Vol. 57, pp. 383.

Escritt, L.B. (1952) "Facts and Fallacies of Sedimentation", Surveyor, Vol. 111, pp. 203, Abstract Sewage and Industrial Wasts, Vol. 25, pp. 120 (1953)

Fitch, E.B. (1958) "Sedimentation Process Fundamentals", Biological Treatment of Sewage and Industrial Wastes, Vol. II, Reinhold, New York, pp. 159-170

Fouda, A.E. and Capes, C.E. (1979) "Hydrodynamic Particle Volume and Fluidized Bed Expansion", Canadian Journal of Chemical Enginering, Vol. 57, pp. 120

Hawksley, P.G.W. (1951) "The Effect of Concentration on the Settling of Suspensions and Flow Through Porous Media", Some Aspects of Fluid Flow, Arnold, London

Jottrand, R. and Appl, J. (1952) Chem. (Suppl. Issue 1), 2, S'17

Kalinske, A.A. (1953) "Settling Rate of Suspensions in Solids Contact Units", Proc. American Society of Civil Engineers, Vol. 76, pp. 186

Kynch, G.J. (1952) "A Theory of Sedimentation", Transactions Faraday Society, Vol. 48, pp. 166-176

Lauzon, R.V. and Reid, K.I.G. (1979) "New Rheological Model Offers Field Alternative", The Oil and Gas Journal, Vol. 77, pp. 51-57

Lewis, W.K. Gilliland, E.R. and Bauer, W.C. (1949) "Characteristics of Fluidized Particles", Industrial and Engineering Chemistry, Vol. 41, Pt. 1, pp. 1104

Loeffer, A.L. and Ruth, B.F. (1959) "Particulate Fluidisation and Sedimentation of Spheres", Journal Americal Institute of Chemical Engineers,

Michaels, A.S. and Bolger, J.C. (1962) "Settling Rates and Sediment Volumes of Flocculated Suspensions", Industrial and Engineering Chemistry Fundamentals, Vol. 1, No. 1

Miller, D.G. (1964) "Sedimentation - A Review of Published Work", Water and Water Engineering, Vol. 68, pp. 52

Oliver, D.R. (1961) "The Sedimentation of Closely Sized Spherical Particles", Chemical Engineering Society, Vol. 15, pp. 230

Pavlik, R.E. and Sansone, E.B. (1973) "The Effect of 'Electroviscosity' on Liquid Sedimentation Analysis", Powder Technology Journal, Vol. 8, pp. 159-164

Richardson, J.F. and Meikle, R. (1961) "Sedimentation and Fluidization Part III, The Sedimentation of Uniform Fine Particles and of Two Component Mixtures of Solids", Transactions - Institution of Chemical Engineers, Vol. 39, pp. 348

Richardson, J.F., and Zaki, W.N. "Sedimentation and Fluidization, Part 1-4", Transactions Institution of Chemical Engineers, Vol. 32, pp. 35 (1954); Vol. 36, pp. 270, (1958); Vol. 39, pp. 348 (1961); Vol. 39, pp. 357 (1961).

Robinson, C.S. (1926) "Some Factors Affecting Sedimentation", Industrial and Engineering Chemistry, Vol. 18, pp. 869

"Sedigraph 5000 D", Instruction Manual - Particle Size Analyzer - Micromeritics Instrument Corporation (1975) 5680 Goshen Springs Road, Norcross, Georgia, 30071 U.S.A.

Shanannon, P.T., Dehaas, R.D., Stroupe, E.P. and Tory, E.M. (1964) "Batch and Continuous Thickening", I & Ec Fundamentals, Vol. 3, No. 3, pp. 250

Steinour, H.H. (1944) "Rate of Sedimentation: Part 1, Non-flocculated Suspension of Uniform Spheres; Part 2, Suspensions of Uniform Size Angular Particles; Part 3, Concentrated Flocculated Suspensions of Powders", Industrial and Engineering Chemistry, Vol. 36, pp. 618, pp. 840, pp. 901

Stokes, G.G. (1845) "On the Theories of the Internal Friction in Motion and of the Equilibrium and Motion of Elastic Bodies", Transactions Cambridge Philosophical Society, Vol. 8, pp. 287

Stokes, G.G. (1851) "On the Effect of the Internal Friction of Fluids on the Motion Pendulum", Transaction Cambridge Philosophical Society, Vol. 9, pp. 8

Stokes, G.G. (1901) "Mathematical and Physical Papers", Transactions Cambridge Philosophical Society, Vol. 9, pp. 8

Svarovsky, L. (1977) "Solid-Liquid Separation", Chemical Engineering Series, Butterworths

Talmadge, W.B. and Fitch, E.B. (1955) "Determining Thickener Unit Areas", Industrial and Engineering Chemistry, Vol. 47, pp. 38

Vesilind, P.A. (1977) "Characterizing Sludge for Centrifugal Dewatering", Filtration and Separation, pp. 115

Vesilind, P.A. (1974) "Estimating Centrifuge Capacities", Chemical Engineering, Vol. 81, pp. 7

Vesilind, P.A. (1970) "Estimation of Sludge Centrifuge Performance", Journal of Sanitary Engineering Division, ASCE, Vol. 97, SA3

White, M.J.D. and Lockyear, C.F. (1978) "A Novel Method for Assessing the Thickenability of Sludges", Ninth International Conference on Water Pollution Research, Stockholm, Vol. 10, pp. 33-43

Whitmore, R.L. (1957) "The Relationship of the Viscosity to the Settling Rate of Slurries", Institute of Fuel Journal, Vol. 30, pp. 238

Work, L.T. and Kohler, A.S. (1940) "Sedimentation of Suspensions", Industrial and Engineering Chemistry, Vol. 32, pp. 1329

Yong, R.N. and Sethi, A.J. (1978) "Mineral Particle Interaction Control of Tar Sand Stability", Journal of Canadian Petroleum Technology, Vol. 17, No. 4, pp. 1-8

Yong, R.N., Sethi, A.J., Ludwig, H.P. and Jorgensen, M. (1979) "Interparticle Motion and Rheology of Dispersive Clays", ASCE Journal of Geotechnical Engineering Division, Vol. 105, pp. 1193-1209

Yong, R.N., Sheeran, D.E., Sethi, A.J. and Erskine, H.L. (1982) "The Dynamics of Tar Sand Tailings", Proceedings Applications of Mechanics, Calgary, pp. 116-120

Yong, R.N., Siu, S.K. and Sheeran, D.E. (1983) "On the Stability and Settling of Suspended Solids in Settling Ponds: Part I Piece-Wise Linear Consolidation Analysis of Sediment Layer", submitted to Canadian Geotechnical Journal.

APPENDIX A

NOMENCLATURE FOR TABLE 2.1

a	a constant in the Rouse equation
b	a constant in the Rouse equation
c	volumetric particle concentraiton (1-E)
C	weight particle concentration
d	diameter of particle
D	diameter of vessel
f	shape constant in Bond's equation
F	a constant in the Kalinske equation
g	acceleration due to gravity
k_1	a constant in the Kalinske equation
k_2	a constant in the Loeffler and Ruth equation
k_3	a constant in the Oliver equation
K	a constant in Steinour's equation
K_1	a constant in the Rouse equation
K_2	a constant in the Robinson equation
K_3	a constant in the Oliver equation
P	a constant in the Kalinske equation
q	wet solids fraction (volume ratio of final settled solids to original suspension)
V_g	rate of fall of suspension relative to fixed horizontal plane
V_t	terminal velocity of particle
V_o	terminal velocity of particle calculated from Stokes law
W_i	Steinour's correction for immobile liquid
n	power term in Richardons's equation

E	porosity of suspension (volume ratio of voids to suspension)
E_c	cross section porosity of suspension (ratio of void area to total area at any cross-section)
$\vartheta(E)$	function of E in Steinour's equation
μ	viscosity of fluid
μ_s	viscosity of suspension
P_f	density of fluid
P_s	density of solid

APPENDIX A

SETTLEABILITY COEFFICIENT (S)

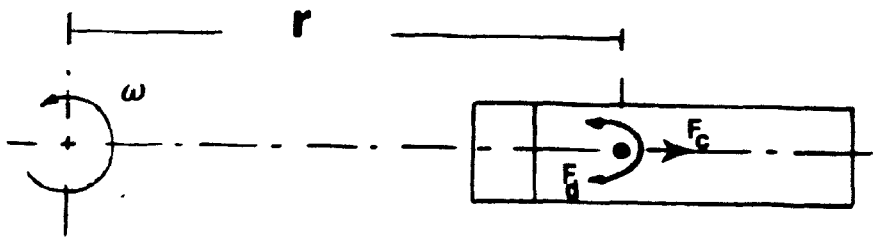

A particle settling under centrifugal force in a test tube

Consider a particle in a solution, held in a rapidly spinning centrifuge. This particle, as it is settling in the centrifugal field, is subjected to two forces, the centrifugal force and the drag force.

If the rotor turns with an angular velocity w (radians per second), the particle experiences a centrifugal force. This force can be described as

$$F_c = w^2 r (P_s - P) V \qquad (A.1)$$

where r = radius from the centre of rotation to the particle (cm)

P_s = density of the particle (gm/cm^3)

P = density of the fluid (gm/cm^3)

V = volume of the particle (cm^3)

The force is balanced by the drag force F_d, which can be written as

$$F_d = C_D \frac{A\ v^2\ P}{2} \qquad (A.2)$$

where A = projected area of the particle (cm^3)

C_D = drag coefficient

v = particle velocity (cm/sec)

Assuming laminar flow (C_D = 24/Reynolds number) and spherical particle shape

$$F_c = F_d \qquad (A.3)$$

can be rearranged to read

$$\frac{v}{w^2 r} = \frac{(P_s - P)\ d^2}{18\ \eta} \qquad (A.4)$$

The term v/w^2r has been used in biology to characterize the stability of single cells in the ultra centrifuge, assuming that the settling velocity of the interface is a function of the solid concentration (as in gravitational thickening). But as the solids move rapidly outward, the radius changes and the centrifugal force on the suspension increases, and the interface velocity could well be influenced by increasing radius during settling.

This problem can be eliminated by recognizing that

$$v = \frac{dr}{dt} \qquad (A.5)$$

$$S = \frac{v}{w^2 r} \qquad (A.6)$$

$$\frac{dr}{dt} = w^2 r\ S \qquad (A.7)$$

Integrating,

$$\text{Ln } \frac{r_2}{r_1} = w^2 S \, (t_2 - t_1) \qquad \text{(A.8)}$$

where r_1, r_2 are the positions of the interface at time t_1 and t_2 respectively.

A graph of Ln (r_2/r_1) versus (t_2-t_1) yields a straight line whose slope is w^2S. Thus S can be determined since the rotational speed is known.

SEDIGRAPH 5000 D PARTICLE SIZE ANALYZER

The use of the sedigraph 5000 D particle size analyzer as a means of determining particle size distribution requires the prior determination of the particle density. The determined particle density is used to calculate the largest permissible particle diameter from the equation:

$$D = \frac{1.837 \times 10^6 \, \mu^2 \, R_e}{P_o \, (P - P_o)} \qquad \text{(A.9)}$$

where D = largest particle diameter in microns - also called the starting diameter

μ = viscosity of fluid in poise

P_o = density of fluid in gm/cm^3

P = density of solid particle in gm/cm^3

R_e = Reynold's number $\tilde{=}$ 0.4

The starting diameter value is then used to obtain an appropriate multiplier; this multiplier determines the rate at which the cell containing the suspension will move downward relative to the X-ray beam. The rate is determined from the equation:

$$\text{Rate (start } \mu\text{m)} = \frac{(205.42)(P-P_o)}{\mu} \, s \, \text{(multiplier)} \qquad \text{(A.10)}$$

The instrument is subsequently adjusted for the given rate obtained from the above equation. The well-mixed suspension in the cell is then allowed to settle, while the cell itself moves downwards with respect to the X-ray beam. A particle size distribution is thereby obtained.

TABLE A.1 Initial Settling Velocity Data from Gravity and Centrifuge Measurements (w = 100 r.p.m.)

Hydrite Flat D Kaolinite

Initial Concentration gm/cm^3	$V_c \times 10^{-3}$ cm/sec	$V_g \times 10^{-3}$ cm/sec
0.0853	18.97	5.533
0.1066	13.183	3.683
0.1324	8.5	2.667
0.1566	6.1	2.183
0.1814	4.383	1.783
0.1996	3.767	1.367
0.2313	2.983	1.25
0.2592	2.5	0.983
0.2863	2.083	0.75
0.3302	1.5	0.633
0.3584	1.35	0.517

TABLE A.2 Initial Settling Velocity Data from Gravity and Centrifuge Measurements (w = 100 r.p.m.)

Hydite Ultra Fine Kaolinite

Initial Concentration gm/cm^3	$V_c \times 10^{-3}$ cm/sec	$V_g \times 10^{-3}$ cm/sec
0.0853	1.675	0.34805
0.1066	1.353	0.318529
0.1324	0.8	0.268518
0.1566	0.632	0.199881
0.1814	0.404	0.1450444
0.1996	0.342	0.0737826
0.2313	0.331	0.0493935

TABLE A.3 Number of Particles per Gram Solid - Based on the Grain Size Distribution for Hydrite Flat D

Diameter μm.	% Finer	Mean Diameter μm	Volume of Single Particle $V \times 10^{-12}$ cm^3	V_T/gm cm^3	Number of Particles/gm* Solid
40-20	3.4	30	14137	0.012977	0.917952×10^6
20-10	12.5	15	1767	0.0477099	2.7×10^7
10-8	7.8	9	382	0.0297709	7.7934×10^7
8-6	10.5	7	180	0.0400763	2.22646×10^8
6-4	15.3	5	65.5	0.0583969	8.91555×10^8
4-2	22	3	20.6	0.0839694	4.07618×10^9
2-1	15.3	1.5	1.8	0.0583969	3.24427×10^{10}
less than 1.0	13.2	less than 1.0	0.53	0.0503816	9.50596×10^{10}

$$* \frac{3.4}{100 \times G_s (2.62)} = 0.012977$$

$$= \text{No. of particles} = \frac{0.012977}{14137 \times 10^{-12}} = .917953 \times 10^6$$

Total No. per gm solid = 1.7279×10^{11}

TABLE A.4 Number of Particles per Gram Solid - Based on the Grain Size Distribution for Hydrite Ultra Fine Kaolinite

Diameter μm	% Finer	Mean Diameter μm	Volume of Single Particle $V \times 10^{-2}$ cm^3	V_T/gm cm^3	Number of Particles per Gram Solid
40-4.8	1.5	22.4	5885	5.81395×10^{-3}	0.987915×10^{6}
4.8-3.5	1.0	4.15	37.4	3.87596×10^{-3}	1.03635×10^{8}
3.5-2.6	1.6	3.05	14.86	6.20155×10^{-3}	4.17328×10^{8}
2.6-1.9	2.9	2.25	8.18	0.0112403	1.37411×10^{9}
1.9-1.5	12.5	1.7	2.57	0.0484496	1.88519×10^{10}
1.5-1	28	1.25	1.02	0.1085271	0.06399×10^{11}
1-.71	37	.855	0.33	0.143411	4.34578×10^{11}
less than .71	15.5	less than .71	0.33	0.06008	1.82051×10^{11}

Total Number per Gram Solid = 6.4378×10^{11}

TABLE A.5 Effect of viscosity at rate of shear of unity for various concentrations on particle diameter- Hydrite Flat D

(Gravity Data)

1. $u_1 = 0.144\ (C \times 100)^{1.462}$ [2]

2. $\log V_g = -3.971 - 1.606 \log C$

3. $D = \sqrt{0.0113378\ \eta\ V_g}$

Concentration gm/cm^3	u_1	V_g cm/sec	D µm
.01	$2.0736\ 10^{-4}$	.1742	6.399
0.05	.022935	.0131357	18.48
.10	.17407	4.3151×10^{-3}	29.18
.15	.56966	2.25×10^{-3}	38.12
.2	1.3211023	1.4175×10^{-3}	46.08
.25	2.5368791	9.90625×10^{-4}	53.38
.3	4.3234385	7.39171×10^{-4}	60.194
.35	6.7854414	5.77069×10^{-4}	66.63
.4	10.02646	4.65685×10^{-4}	72.759
.45	14.148635	3.85427×10^{-4}	78.631

TABLE A.6 Effect of viscosity at rate of shear of unity for various concentrations on particle diameter Hydrite Flat D

(Centrifuge Data)

$$u_1 = 0.144\ (C \times 100)^{1.462} \quad 2$$

$$\text{Log } V_c = -3.706 - 1.858 \log C$$

$$D = \sqrt{2.0996 \times 10^{-3}\ V_c\ \eta}$$

Concentration gm/cm^3	u_1 poise	V_c cm/sec	D μm
0.01	2.0736×10^{-4}	1.02329	6.6747
0.05	.022935	5.1441×10^{-2}	15.738
.1	.17407	1.419×10^{-2}	22.773
.15	.56966	6.6807×10^{-3}	28.267
.2	1.3211023	3.9145×10^{-3}	32.951
.25	2.5368691	2.5859×10^{-3}	37.113
.3	4.3234385	1.8429×10^{-3}	40.901
.35	6.7854414	1.3839×10^{-3}	44.403
.4	10.02646	1.0798×10^{-3}	47.679
.45	14.148635	8.6762×10^{-4}	50.768

TABLE A.7 Effect of viscosity at rate of shear of 50 sec^{-1} for various concentrations on particle diameter Hydrite Flat D

(Gravity Data)

$$\mu_{50} = \frac{1}{0.952 \times e^{-0.039\ Cx100}}$$

Concentration gm/cm^3	μ_{50} poise	V_g cm/sec	D μm
.01	1.1929×10^{-2}	.1742	48.538
.05	1.6297×10^{-2}	.0131357	15.579
.1	2.407×10^{-2}	4.3151×10^{-3}	10.851
.15	3.5551×10^{-2}	2.25×10^{-3}	9.5231
.2	5.2508×10^{-2}	1.4175×10^{-3}	9.1862
.25	7.7553×10^{-2}	9.90625×10^{-4}	9.3329
.3	11.454475×10^{-2}	7.39171×10^{-4}	9.7977
.35	16.918039×10^{-2}	5.77069×10^{-4}	10.52
.4	24.98762×10^{-2}	4.65685×10^{-4}	11.486
.45	36.906×10^{-2}	3.85427×10^{-4}	12.699

TABLE A.8 Effect of viscosity at rate of shear of 50 sec^{-1}. for various concentrations on particle diameter Hydrite Flat D

(Centrifuge Data)

Concentration gm/cm^3	μ_{50} poise	V_c cm/sec	D μm
0.01	1.1929×10^{-2}	1.02329	50.625
.05	1.6297×10^{-2}	5.1441×10^{-2}	13.267
.1	2.407×10^{-2}	1.419×10^{-2}	8.468
.15	3.551×10^{-2}	6.6807×10^{-3}	7.058
.2	5.2508×10^{-2}	3.9145×10^{-3}	6.67
.25	7.7553×10^{-2}	2.5859×10^{-3}	6.489
.3	11.454475×10^{-2}	1.8429×10^{-3}	6.657
.35	16.918039×10^{-2}	1.3839×10^{-3}	7.011
.4	24.98762×10^{-2}	1.0798×10^{-3}	7.527
.45	26.906×10^{-2}	8.6762×10^{-4}	8.199

TABLE A.9 Summary of the centrifugation results for 16% (wt/wt) Hydrite Flat D

w r.p.m.	$w^2S \times 10^{-4}$ sec^{-1}	$S \times 10^{-7}$ sec	$V_c \times 10^{-3}$ cm/sec	$w^2r \times 10^3$ cm/sec^2
100	.8747	7.980	4.280	5.360
130	1.451	7.830	6.980	8.914
160	2.1713	7.734	10.28	13.29
200	3.464	7.890	16.00	20.28
260	5.6423	7.61	26.27	34.52
1 g		18.060	1.77	0.98

$S_{c_{average}} = 7.8088 \times 10^{-7}$ sec

TABLE A.10 Summary of centrifugation results for 20% (wt/wt) Hydrite Flat D

w r.p.m.	$w^2S \times 10^{-4}$ sec^{-1}	$S \times 10^{-7}$ sec	$V_c \times 10^{-3}$ cm/sec	$w^2r \times 10^3$ cm/sec^2
100	.6276	5.723	3.080	5.38
150	1.389	5.630	6.520	11.58
160	1.576	5.614	7.820	13.93
205	2.597	5.635	12.870	22.84
235	3.420	5.650	16.070	28.46
1 g		12.755	1.25	.98

$S_{c_{average}} = 5.6504 \times 10^{-7}$ sec

TABLE A.11 Summary of centrifugation results for 24% (wt/wt) Hydrite Flat D

w r.p.m.	$w^2S \times 10^{-4}$ sec^{-1}	$S \times 10^{-7}$ sec	$V_c \times 10^{-3}$ cm/sec	$w^2r \times 10^3$ cm/sec^2
100	.4327	3.950	2.130	5.40
120	.5975	3.780	2.950	7.80
140	.84262	3.920	4.170	10.64
180	1.362	3.830	6.750	17.61
230	2.0754	3.580	9.85	27.52
1 g		6.00	.59	.98

$S_{c_{average}} = 3.812 \times 10^{-7}$ sec

TABLE A.12 Summary of centrifugation results for 27% (wt wt) Hydrite Flat D

w r.p.m.	$w^2S \times 10^{-4}$ sec^{-1}	$S \times 10^{-7}$ sec	$V_c \times 10^{-3}$ cm/sec	$w^2r \times 10^3$ cm/sec^2
160	9552	3.400	4.63	13.61
180	1.030	2.900	5.02	17.32
200	1.31	2.990	6.37	21.33
230	1 77	3.050	8.583	28.13
250	1 975	2.890	9.62	33.38
1 g		4.592	.450	.98

$S_{c_{average}} = 3.046 \times 10^{-7}$ sec

TABLE A.13 Summary of centrifugation results for 30% (wt/wt) Hydrite Flat D

w r.p.m.	$w^2 s \times 10^{-4}$ sec^{-1}	$s \times 10^{-7}$ sec	$V_c \times 10^{-3}$ cm/sec	$w^2 r \times 10^{3}$ cm/sec^2
100	.2691	2.45	1.3	5.3
150	.57569	2.33	2.78	11.92
190	.82995	2.10	4.00	19.08
250	1.484	2.17	7.18	33.20
1 g		3.06	.30	.98

$$s_{c_{average}} = 2.2625 \times 10^{-7} \text{ sec}$$

TABLE A.14 Summary of centrifugation results for 33% (wt/wt) Hydrite Flat D

w r.p.m.	$w^2 S \times 10^{-4}$ sec^{-1}	$S \times 10^{-7}$ sec	$V_c \times 10^{-3}$ cm/sec	$w^2 r \times 10^3$ cm/sec^2
155	.608	2.31	2.833	12.28
170	.65574	2.07	3.05	14.74
195	.9008	2.16	4.2	19.44
200	1.0978	2.07	5.12	24.75
240	1.286	2.04	6.00	29.47
1 g		1.633	.16	.98

$S_{c_{average}} = 2.13 \times 10^{-7}$ sec

APPENDIX A-21

Derivation of equation 2-7

From

$$Fc = w^2 r\ (P_s - P)\ V \qquad 2\text{-}4$$

$$Fd = C_D\ \frac{A\ v^2\ P}{2} \qquad 2\text{-}5$$

Therefore

$$w^2 r\ (P_s - P)\ V = \frac{C_D\ A\ v^2\ P}{2}$$

it can be rearranged to read

$$\frac{v^2}{w^2 r} = \frac{(P_s - P)\ V.2}{C_D.A.P} \qquad A\text{-}21\text{-}1$$

where;

$$C_D = \frac{24}{R_N} \quad \text{and} \quad R_N = \frac{P_D v}{\mu}$$

Therefore

$$C_D = \frac{24\ \mu}{P_D v} \qquad A\text{-}21\text{-}2$$

Substituting the value of C_D in equation (A-21-1)

$$\frac{v^2}{w^2 r} = \frac{(P_s - P)\ V.2.P.D.v}{24.A.\mu.P}$$

$$= \frac{(P_s - P)\ (\pi\ 6\ D^3).2.P.D.v}{24.(\pi\ 4\ D^2).\mu.P}$$

gives

$$\frac{v}{w^2 r} = \frac{(P_s - P)\ D^2}{18\ \mu} \qquad 2\text{-}7$$

APPENDIX B

FIGURE B.1 VISCOSITY AT GEL STRENGTH Vs. INITIAL CONCENTRATION

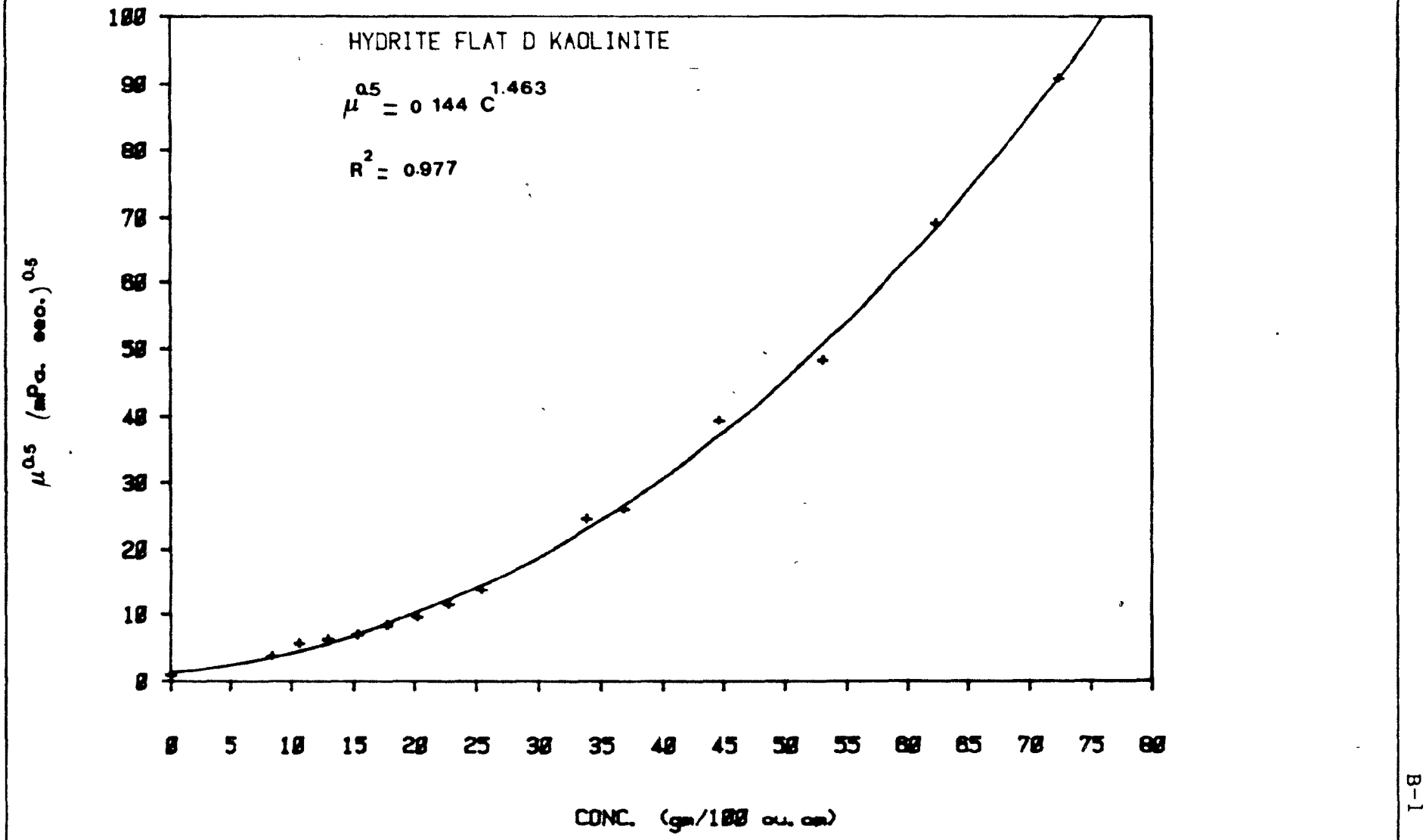

FIGURE B.2 VISCOSITY AT RATE OF SHEAR OF 50 $sec.^{-1}$ Vs. INITIAL COCENTRATION

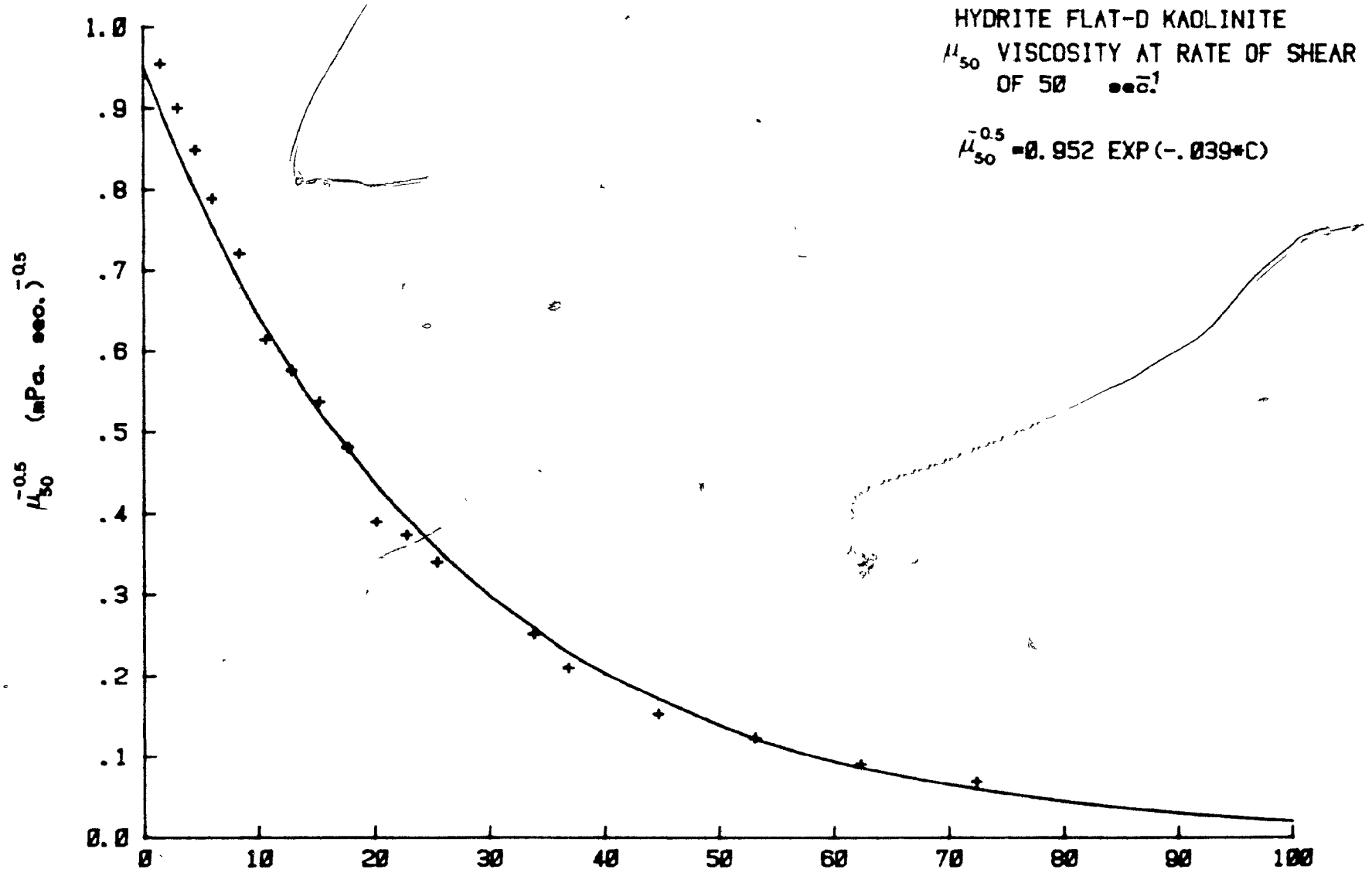

FIGURE B.3 HEIGHT-TIME RELATIONSHIP AT FIVE DIFFERENT ROTATIONAL SPEEDS

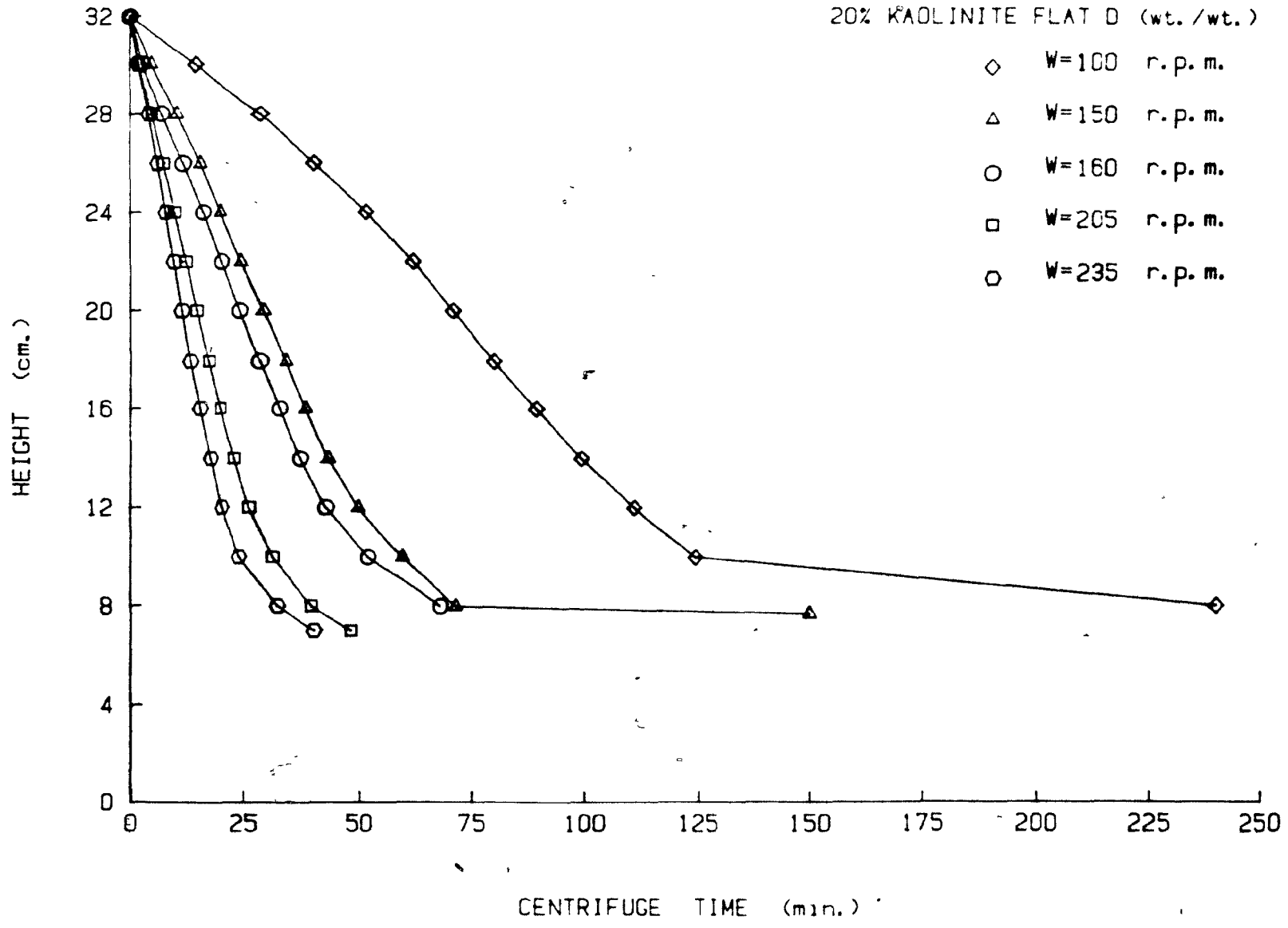

FIGURE B.4 HEIGHT-TIME RELATIONSHIP AT FIVE DIFFERENT ROTATIONAL SPEEDS

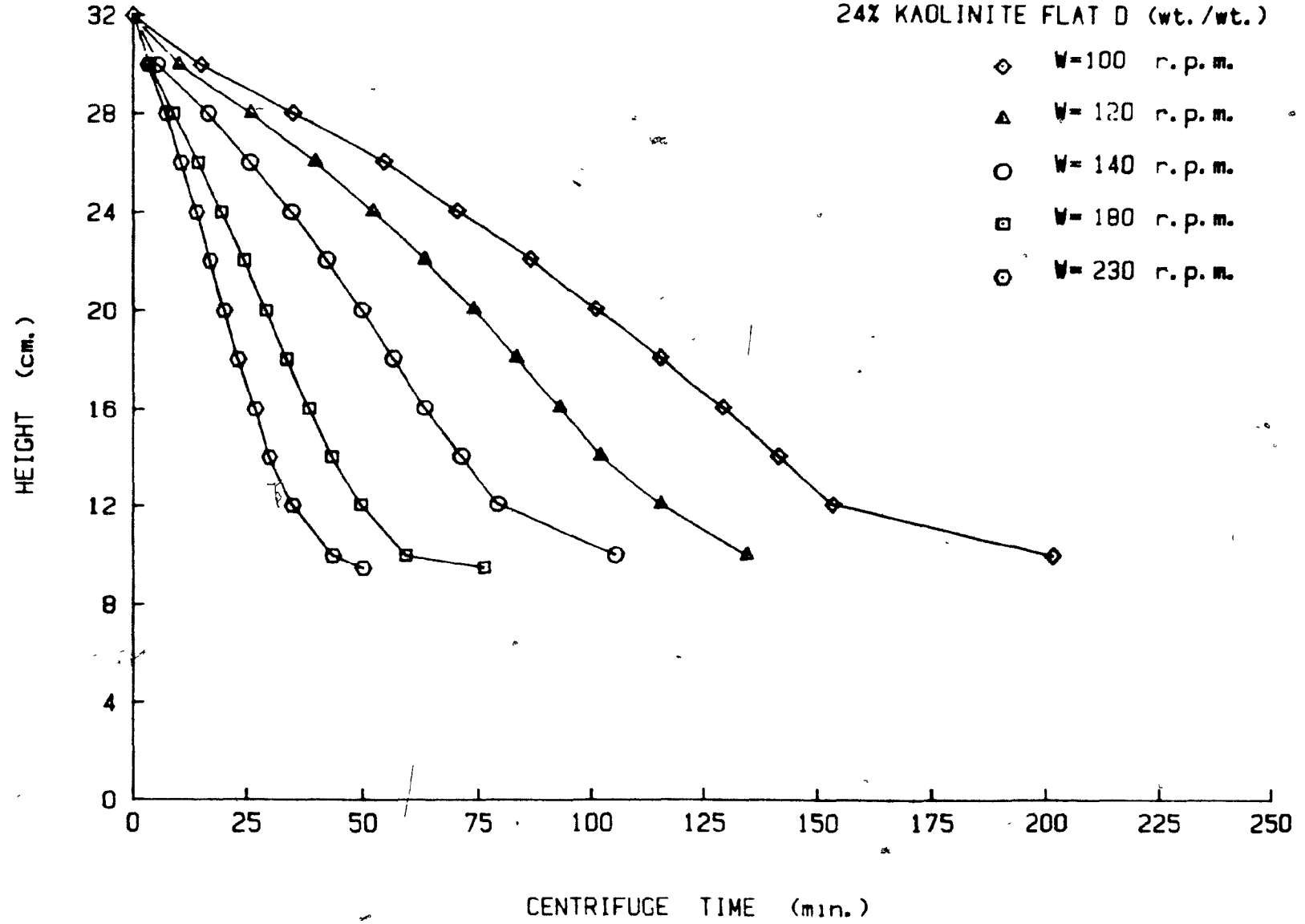

FIGURE B.5 HEIGHT-TIME RELATIONSHIP AT FIVE DIFFERENT ROTATIONAL SPEEDS

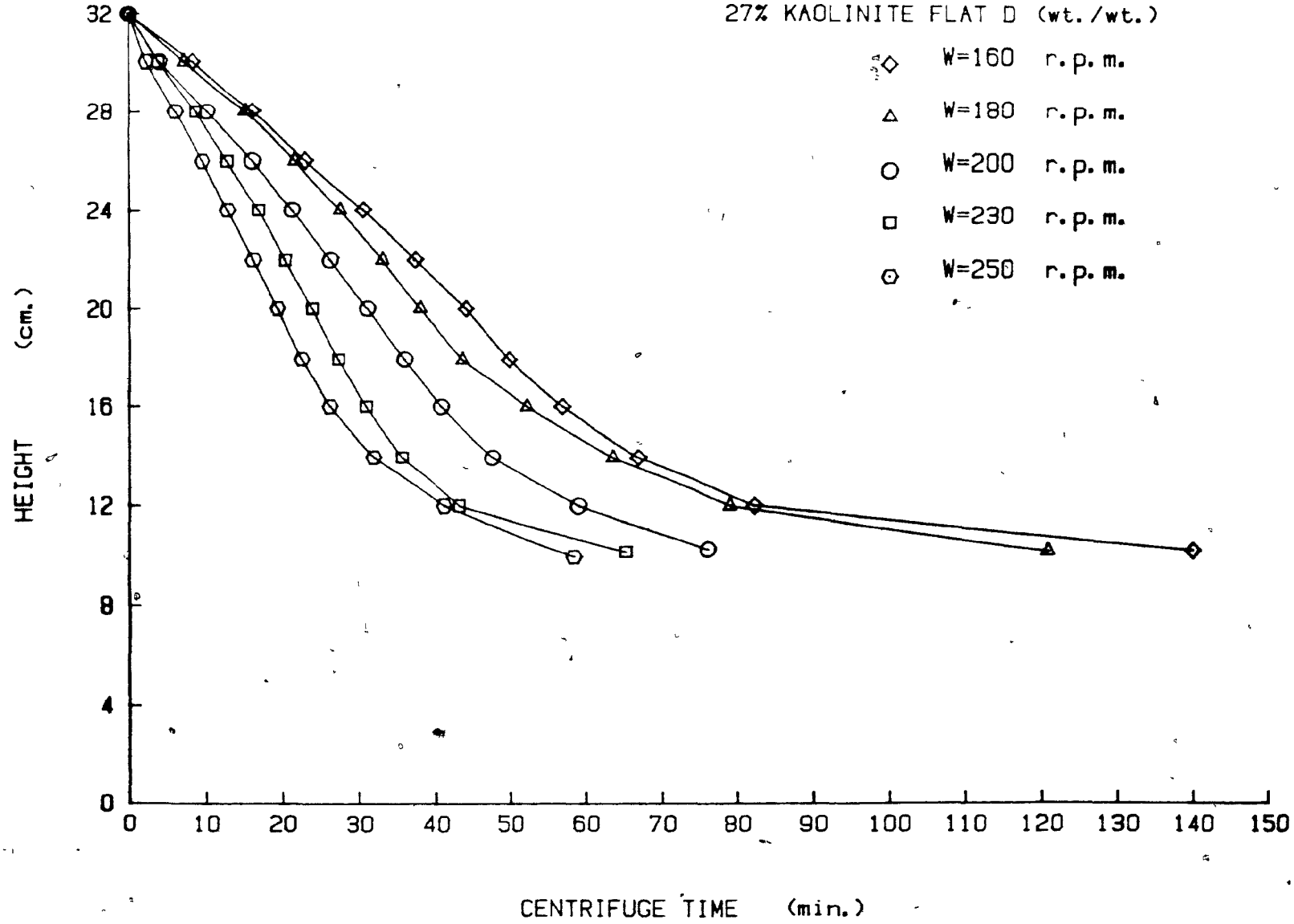

FIGURE 8.6 HEIGHT-TIME RELATIONSHIP AT FIVE DIFFERENT ROTATIONAL SPEEDS

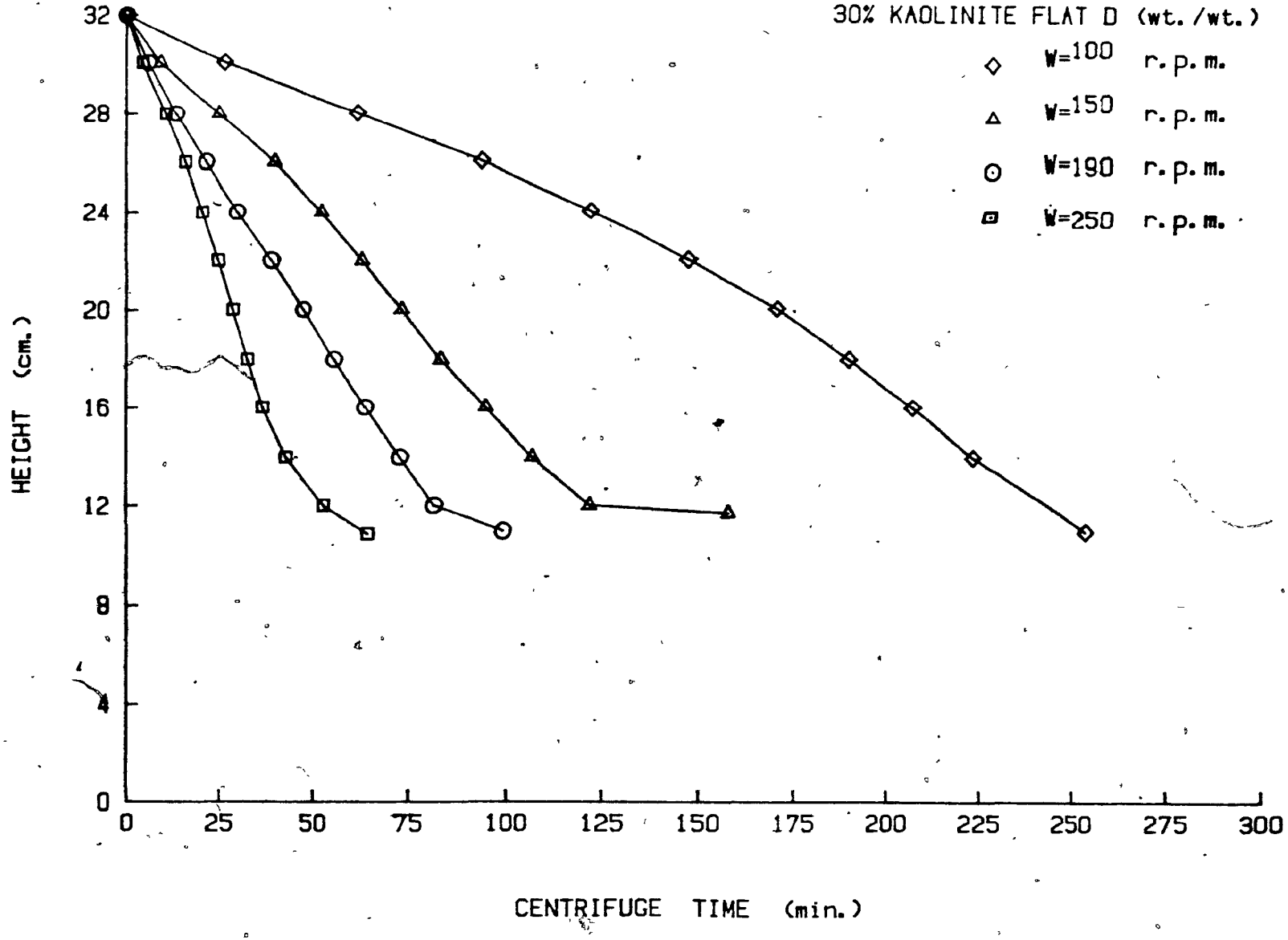

FIGURE B.7 : HEIGHT-TIME RELATIONSHIP AT FIVE DIFFERENT ROTATIONAL SPEEDS

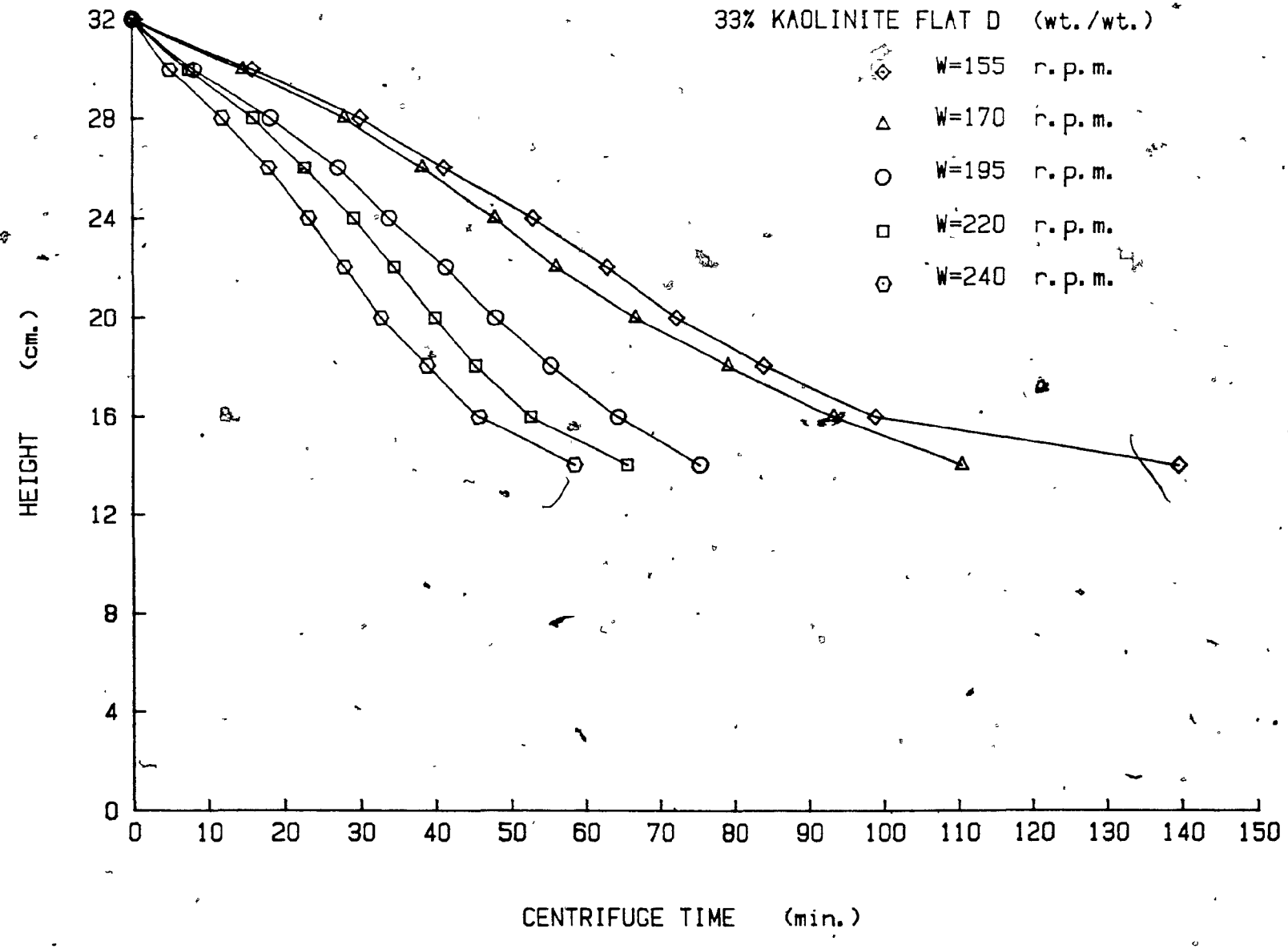

FIGURE B-8 $Ln(r_2/r_1)$ Vs. $t_2 - t_1$ AT FIVE DIFFERENT ROTATONAL SPEEDS

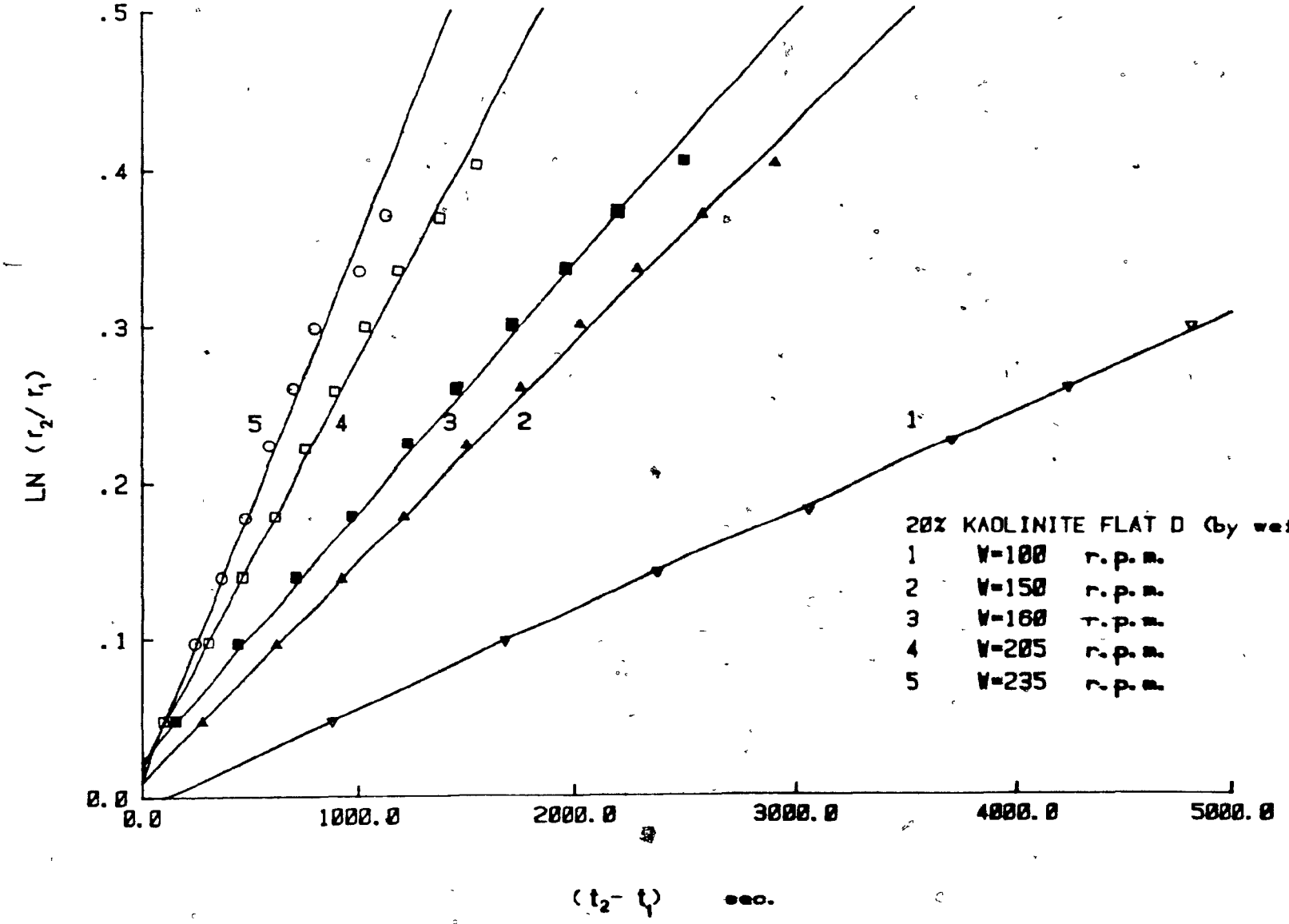

FIGURE B-9 $Ln(r_2/r_1)$ Vs. $t_2 - t_1$ AT FIVE DIFFERENT ROTATIONAL SPEEDS

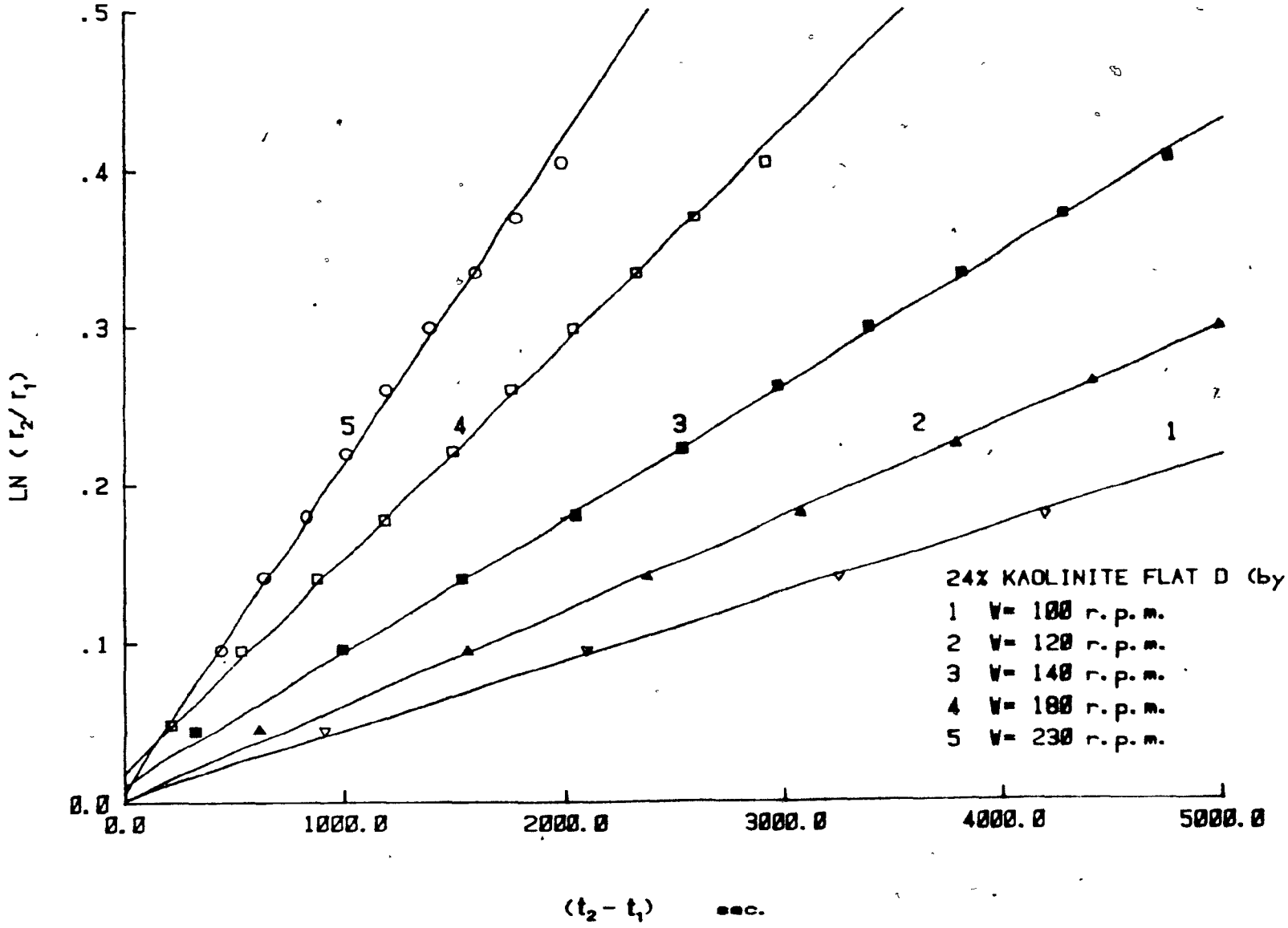

FIGURE B-10 Ln(r_2/r_1) Vs. t_2-t_1 AT FIVE DIFFERENT ROTATONAL SPEEDS

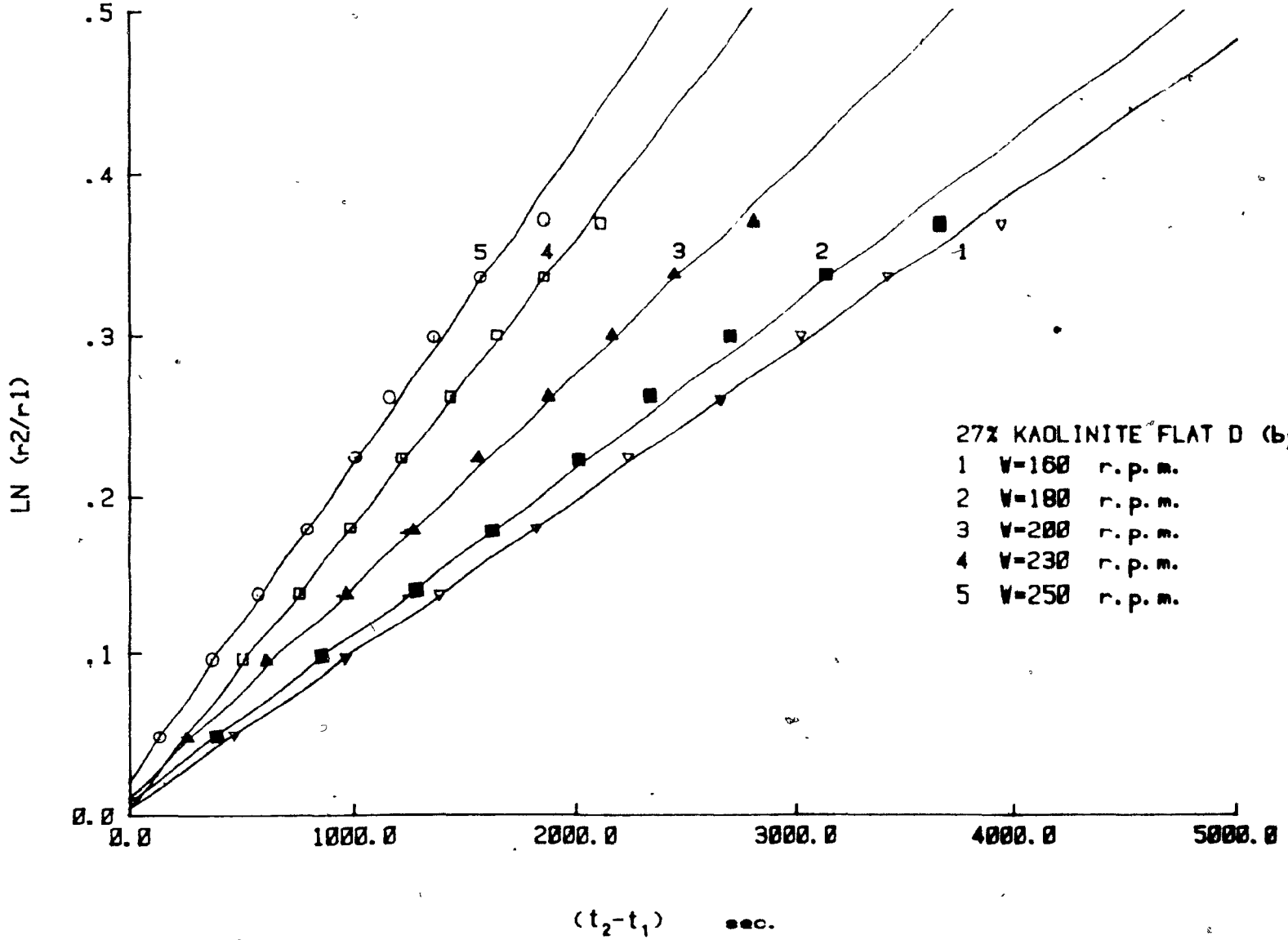

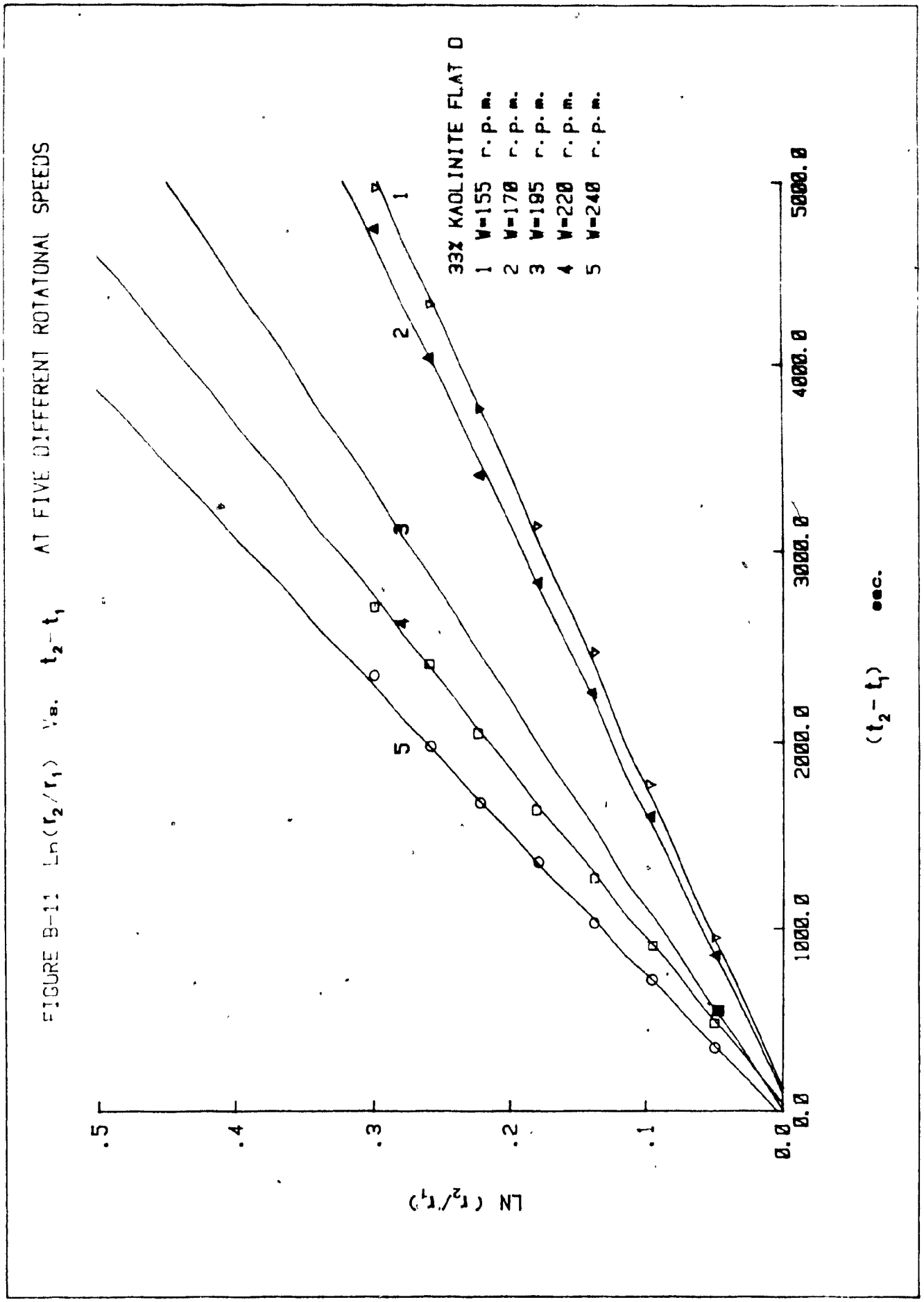

FIGURE B-11 $Ln(r_2/r_1)$ Vs. $t_2 - t_1$ AT FIVE DIFFERENT ROTATIONAL SPEEDS

FIGURE B. 12 GRAIN SIZE DISTRIBUTION

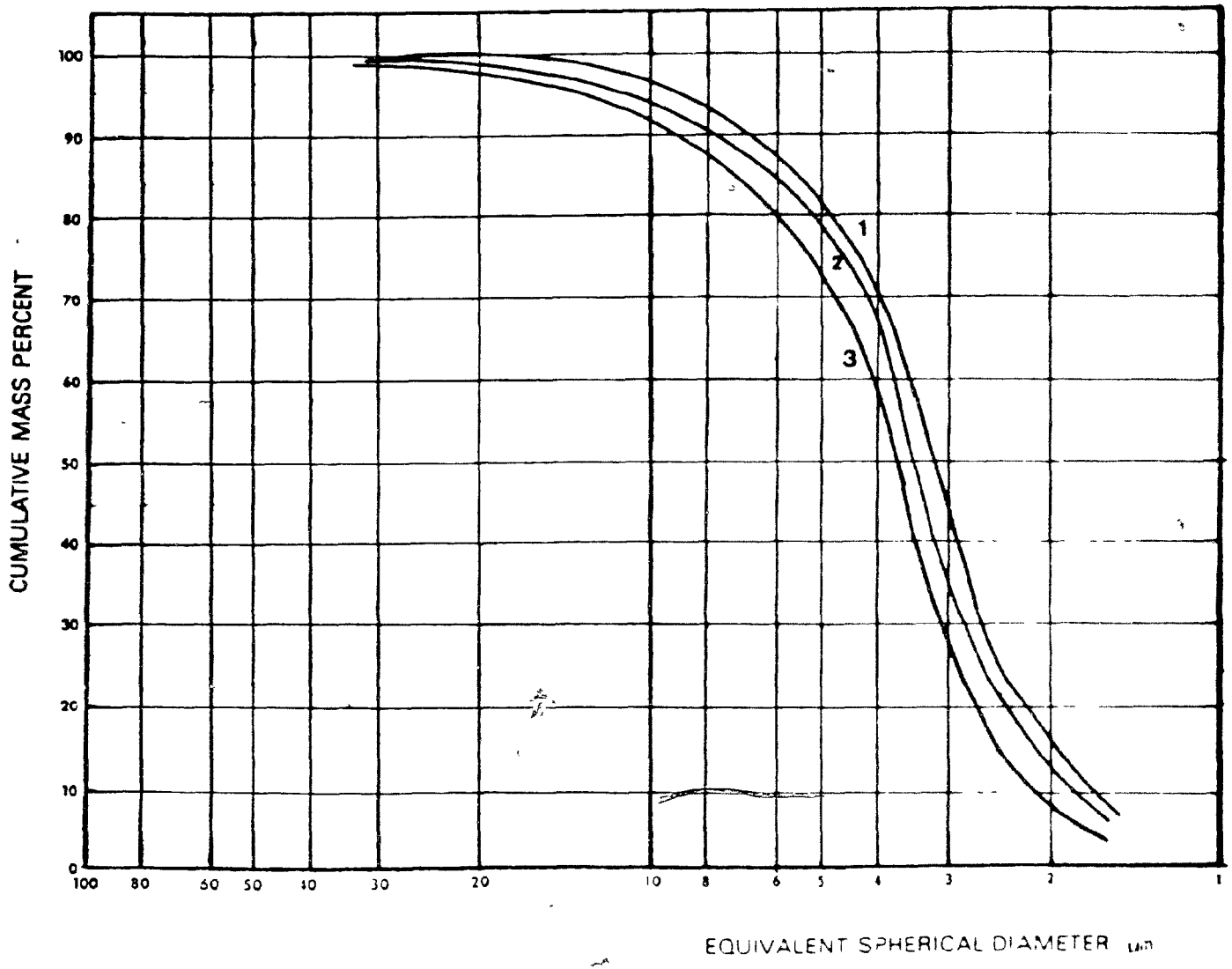

16% KAOLINITE FLAT-D

GRAVITY DATA

1 SAMPLE 1.0 cm. BELOW THE TOP OF THE SEDIMENT

2 SAMPLE FRPM THE MIDDLE OF THE SEDIMEN

3 SAMPLE 1.0 cm. FROM THE BOTTOM OF THE SEDIMENT

FIGURE B.13 GRAIN SIZE DISTRIBUTION

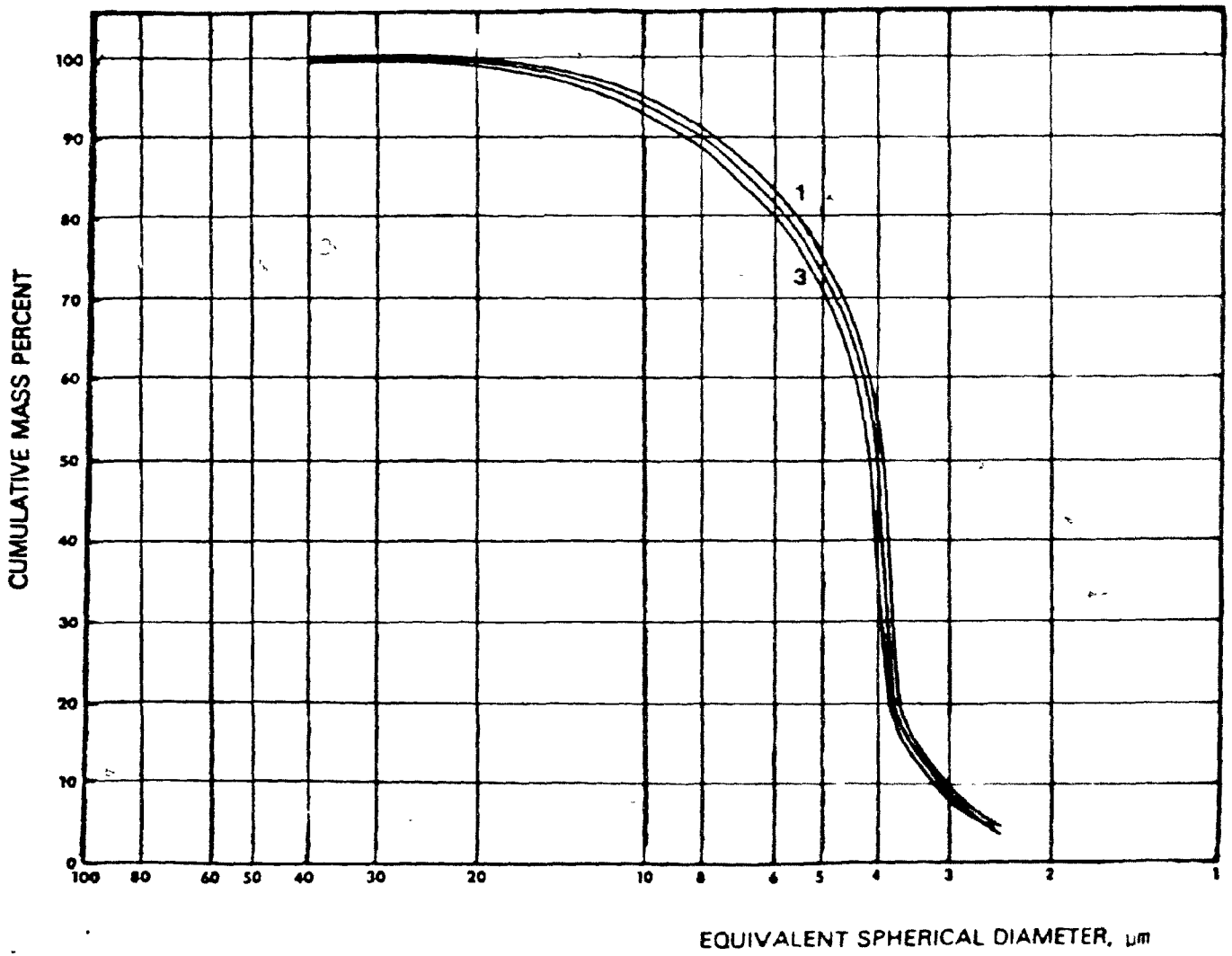

33% KAOLINITE
FLAT-D

GRAVITY DATA

1 SAMPLE 1.0 cm. BELOW THE TOP OF THE SEDIMENT

2 SAMPLE FROM THE MIDDLE OF THE SEDIMENT

3 SAMPLE 1.0 cm. FROM THE BOTTOM OF THE SEDIMENT

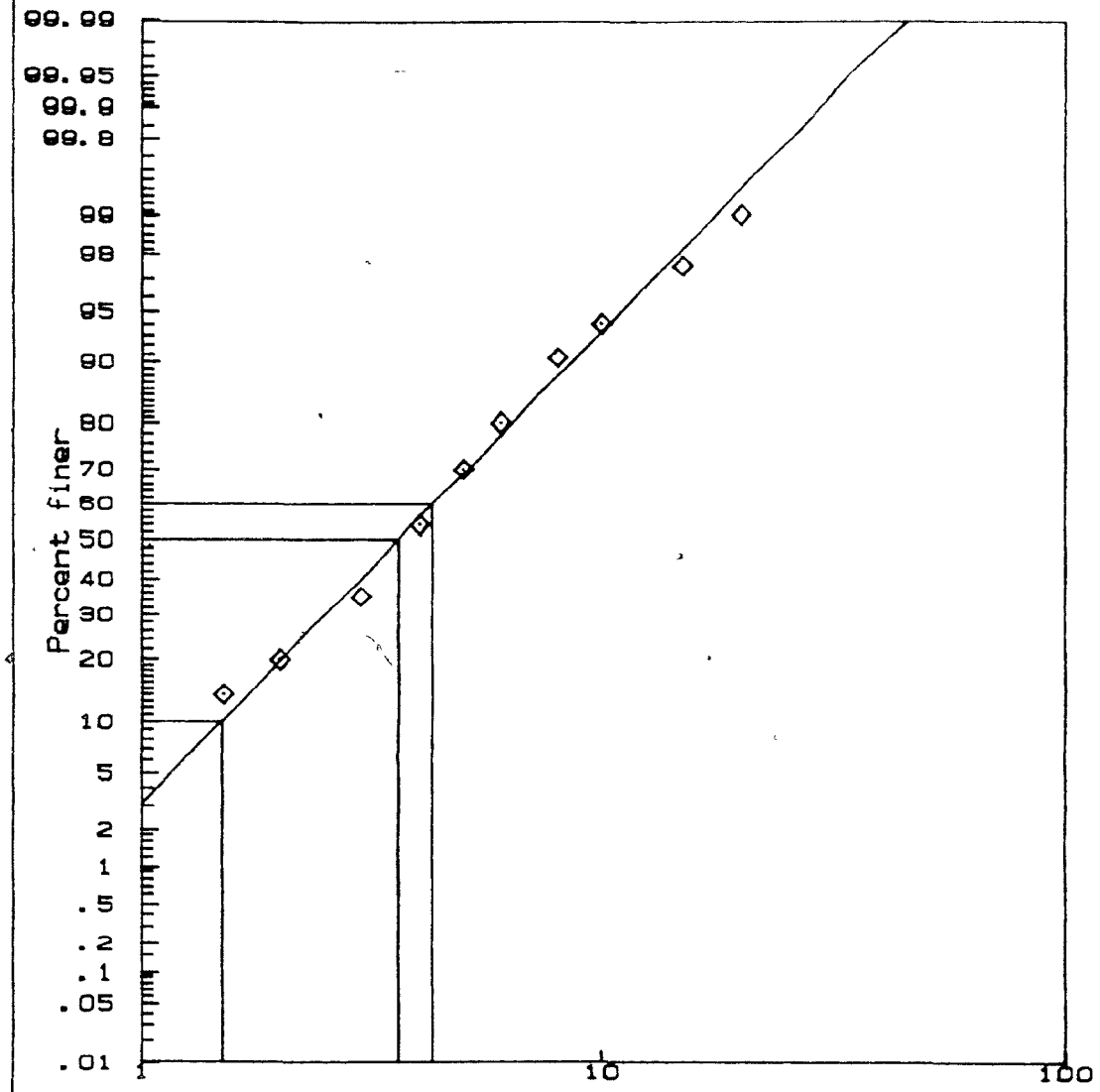

16% KAOLINITE FLAT D
CENTRIFUGE DATA
W=130 r.p.m.
SAMPLE FROM THE MIDDLE
OF THE SEDIMENT

PARTICLE SIZE ANLYSIS

D10	=	1.49 micron
D50	=	3.59 micron
D60	=	4.27 micron
Cu	=	2.86 (Cu = D60/D10)

%CLAY (< 40micron) = 99.97847
%CLAY (< 4 micron) = 56.34038
%CLAY (< 1 micron) = 3.11663

FIGURE B.14 GRAIN SIZE DISTRIBUTION

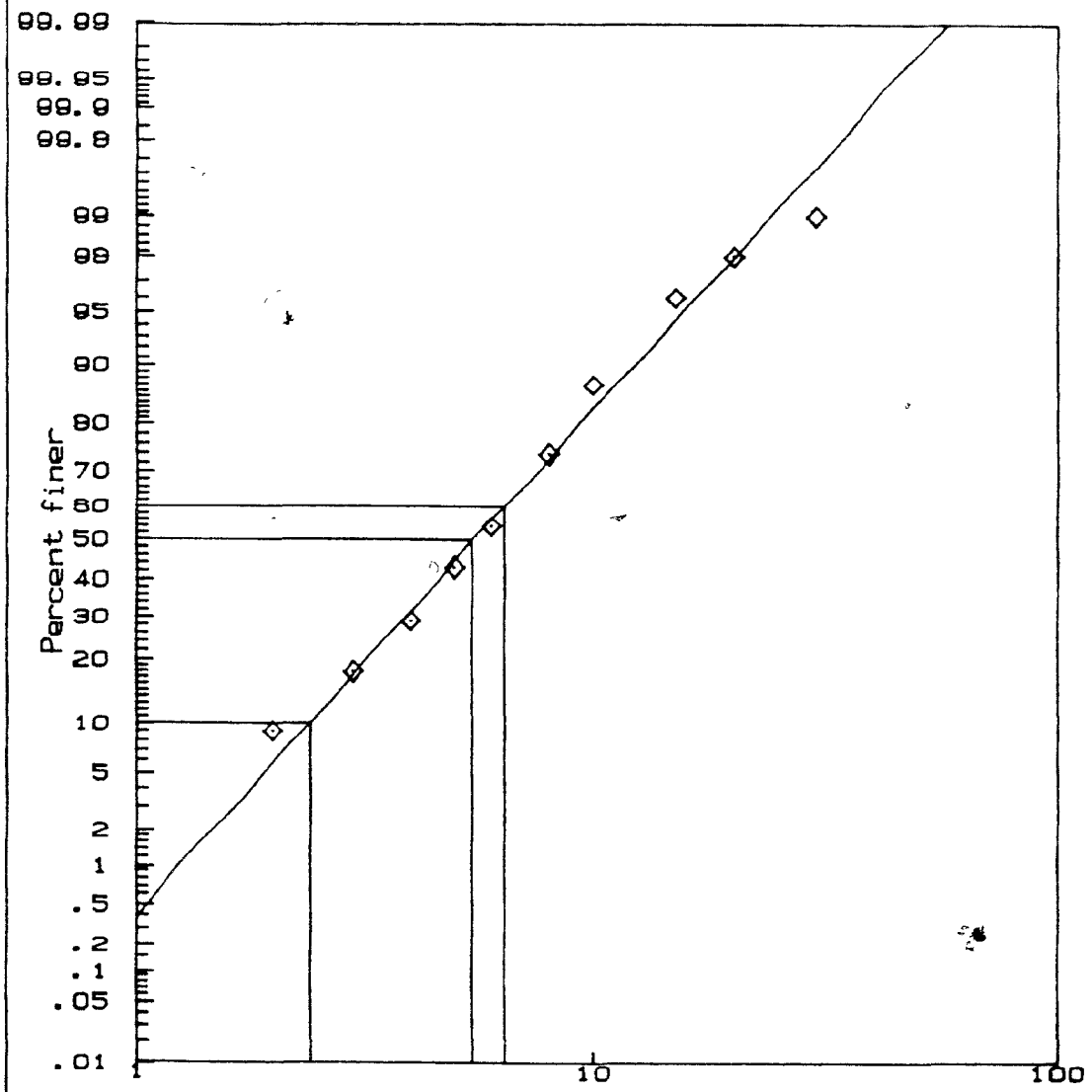

16% KAOLINITE FLAT D
CENTRIFUGE DATA
W=130 r.p.m.
SAMPLE 1.0 cm. FROM THE
BOTTOM OF THE SEDIMENT

PARTICLE SIZE ANLYSIS

D10	=	2.41 micron
D50	=	5.45 micron
D60	=	6.40 micron
Cu	=	2.65 (Cu = D60/D10)

%CLAY (< 40micron) = 99.91437
%CLAY (< 4 micron) = 31.38009
%CLAY (< 1 micron) = .38467

FIGURE B.15 GRAIN SIZE DISTRIBUTION

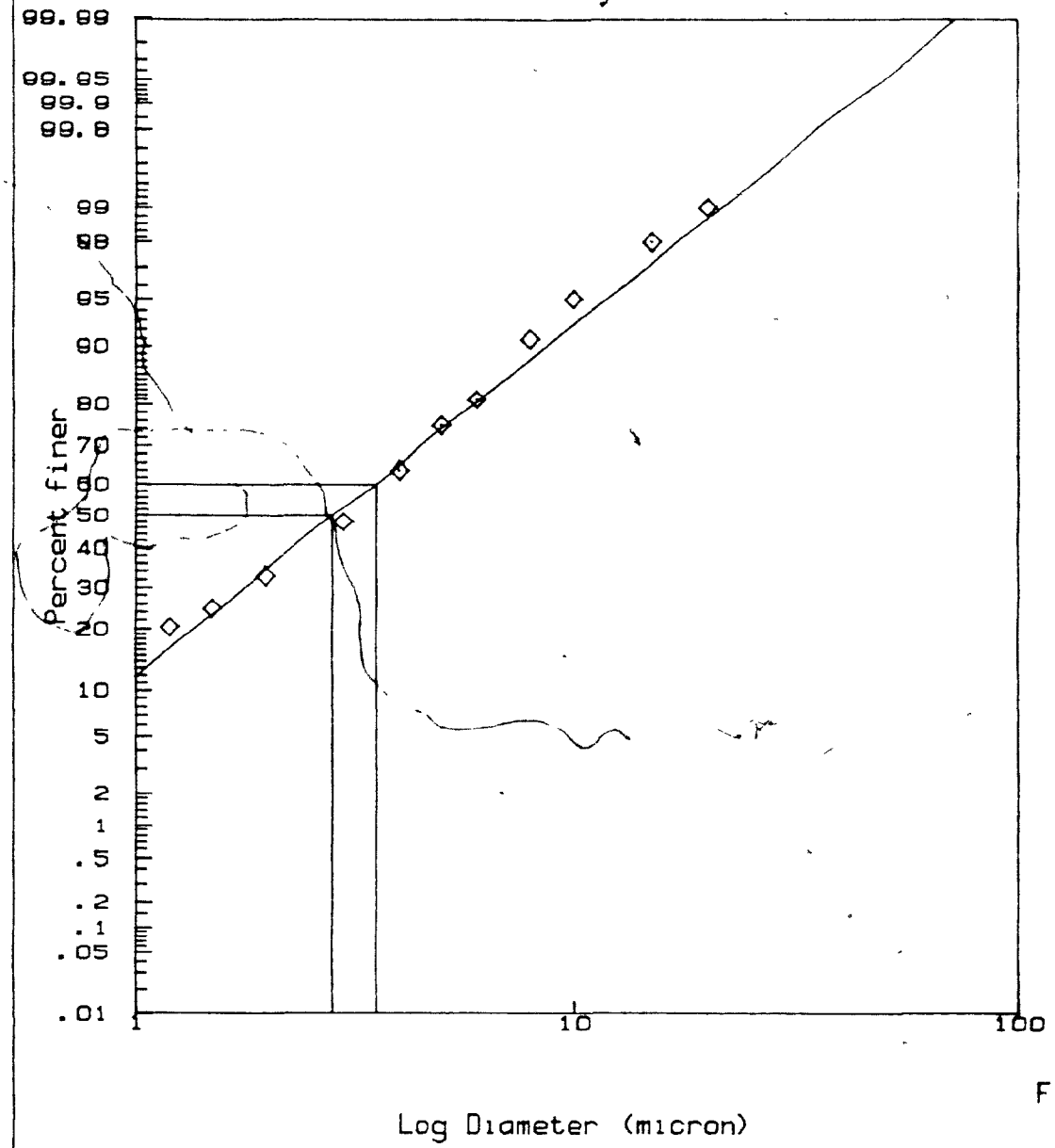

16% KAOLINITE FLAT D
CENTRIFUGE DATA
W=160 r.p.m.
SAMPLE FROM THE MIDDLE
OF THE SEDIMENT

PARTICLE SIZE ANLYSIS

D10	=	.93 micron	
D50	=	2.83 micron	
D60	=	3.54 micron	
Cu	=	3.82	(Cu = D60/D10)

%CLAY	(< 40micron)	= 99.87915
%CLAY	(< 4 micron)	= 65.39871
%CLAY	(< 1 micron)	=11.66702

FIGURE B.16 GRAIN SIZE DISTRIBUTION

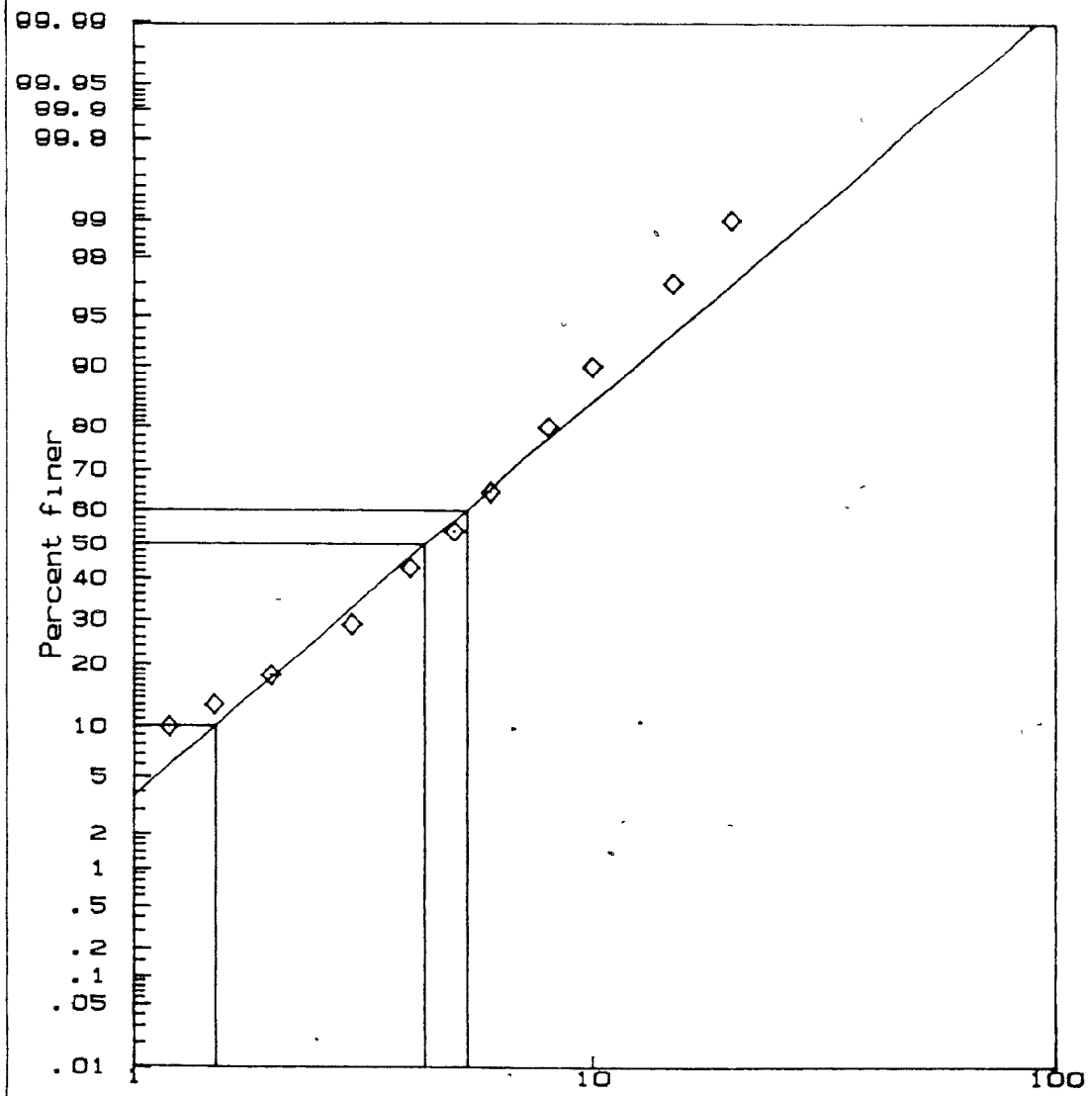

16% KAOLINITE FLAT D
CENTRIFUGE DATA
W=160 r.p.m
SAMPLE 1.0 cm. FROM THE
BOTTOM OF THE SEDIMENT

PARTICLE SIZE ANLYSIS

D10 = 1.51 micron
D50 = 4.31 micron
D60 = 5.32 micron
Cu = 3.52 (Cu = D60/D10)

%CLAY (< 40micron) = 99.66923
%CLAY (< 4 micron) = 46.34086
%CLAY (< 1 micron) = 3.73656

FIGURE B.17 GRAIN SIZE DISTRIBUTION

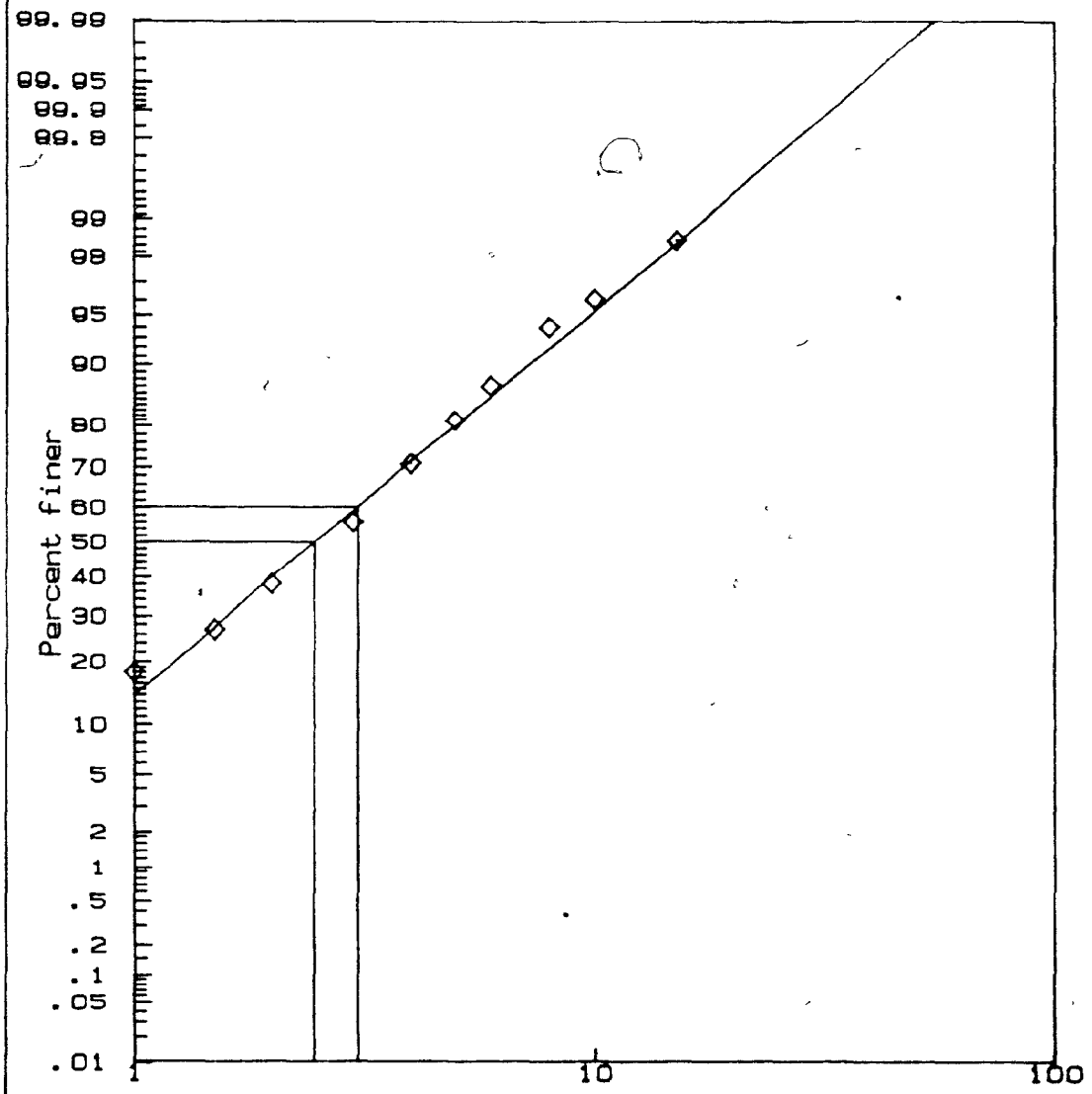

16% KAOLINITE FLAT D
CENTRIFUGE DATA
W=200 r.p.m.
SAMPLE FROM THE MIDDLE
OF THE SEDIMENT

PARTICLE SIZE ANLYSIS

D10	=	.85 micron
D50	=	2.48 micron
D60	=	3.07 micron
Cu	=	3.62 (Cu = D60/D10)

%CLAY (< 40micron) = 99.95475
%CLAY (< 4 micron) = 71.59518
%CLAY (< 1 micron) =13.93150

FIGURE B.18 GRAIN SIZE DISTRIBUTION

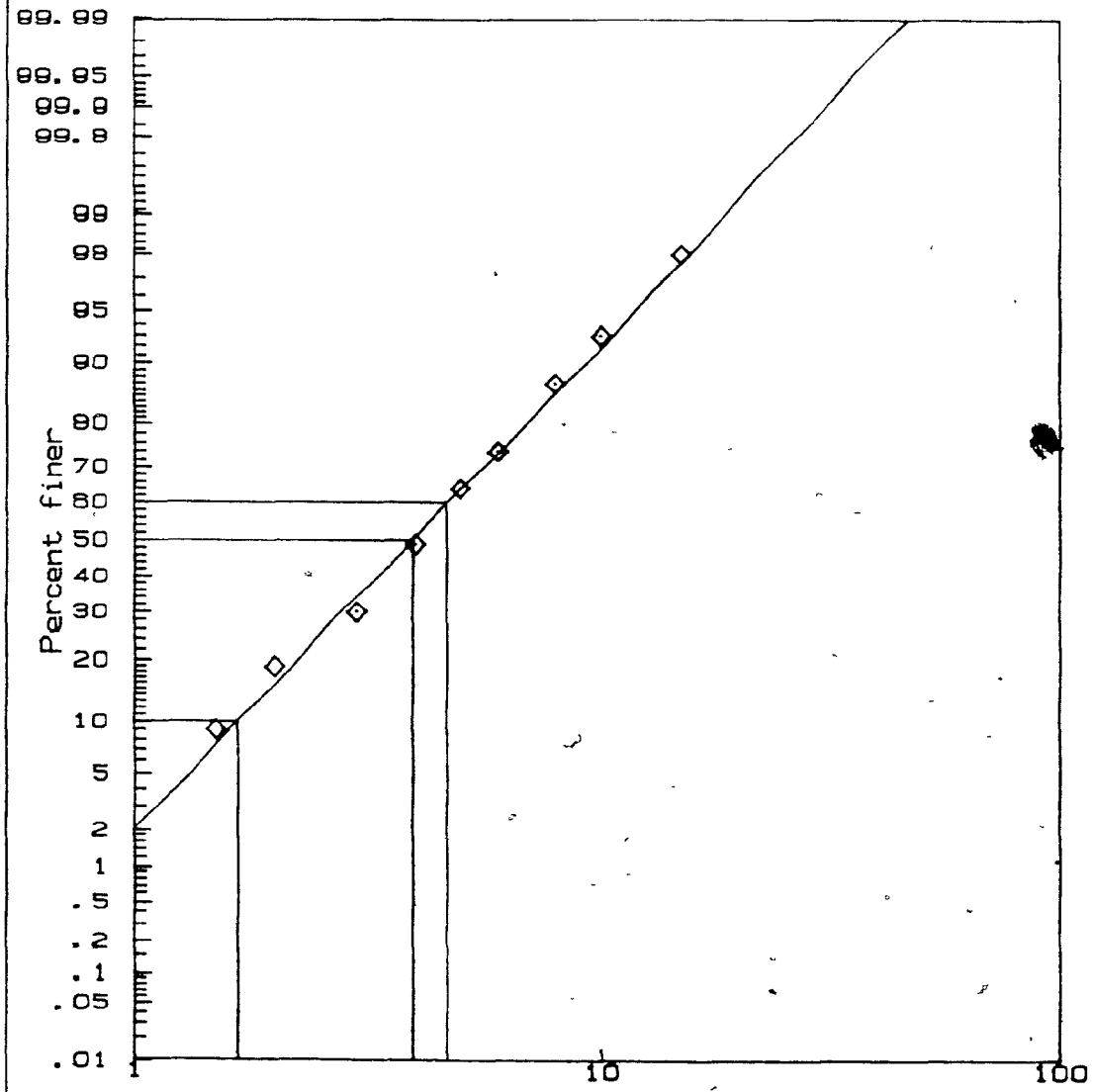

16% KAOLINITE FLAT D
CENTRIFUGE DATA
W=200 r.p.m.
SAMPLE 1.0 cm. FROM THE
BOTTOM OF THE SEDIMENT

PARTICLE SIZE ANLYSIS

D10	=	1.67 micron
D50	=	3.94 micron
D60	=	4.68 micron
Cu	=	2.80 (Cu = D60/D10)

%CLAY (< 40micron) = 99.97291
%CLAY (< 4 micron) = 50.86968
%CLAY (< 1 micron) = 2.02937

FIGURE B.19 GRAIN SIZE DISTRIBUTION

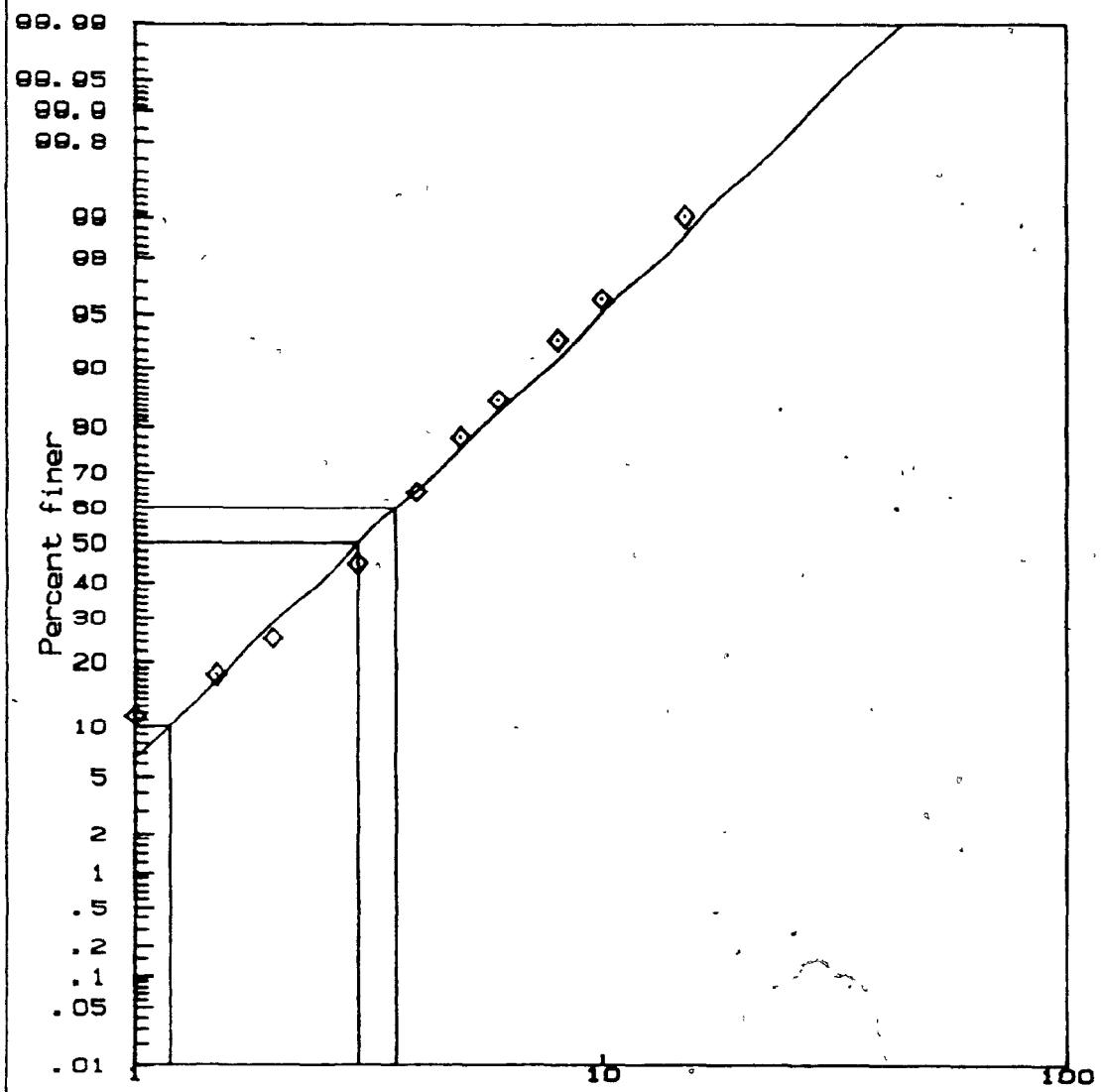

16% KAOLINITE FLAT D
CENTRIFUGE DATA
W=260 r.p.m.
SAMPLE FROM THE MIDDLE
OF THE SEDIMENT

PARTICLE SIZE ANLYSIS

D10	=	1.18 micron
D50	=	3.01 micron
D60	=	3.62 micron
Cu	=	3.05 (Cu = D60/D10)

%CLAY	(< 40micron)	= 99.98132
%CLAY	(< 4 micron)	= 65.27062
%CLAY	(< 1 micron)	= 6.51182

FIGURE B.20 GRAIN SIZE DISTRIBUTION

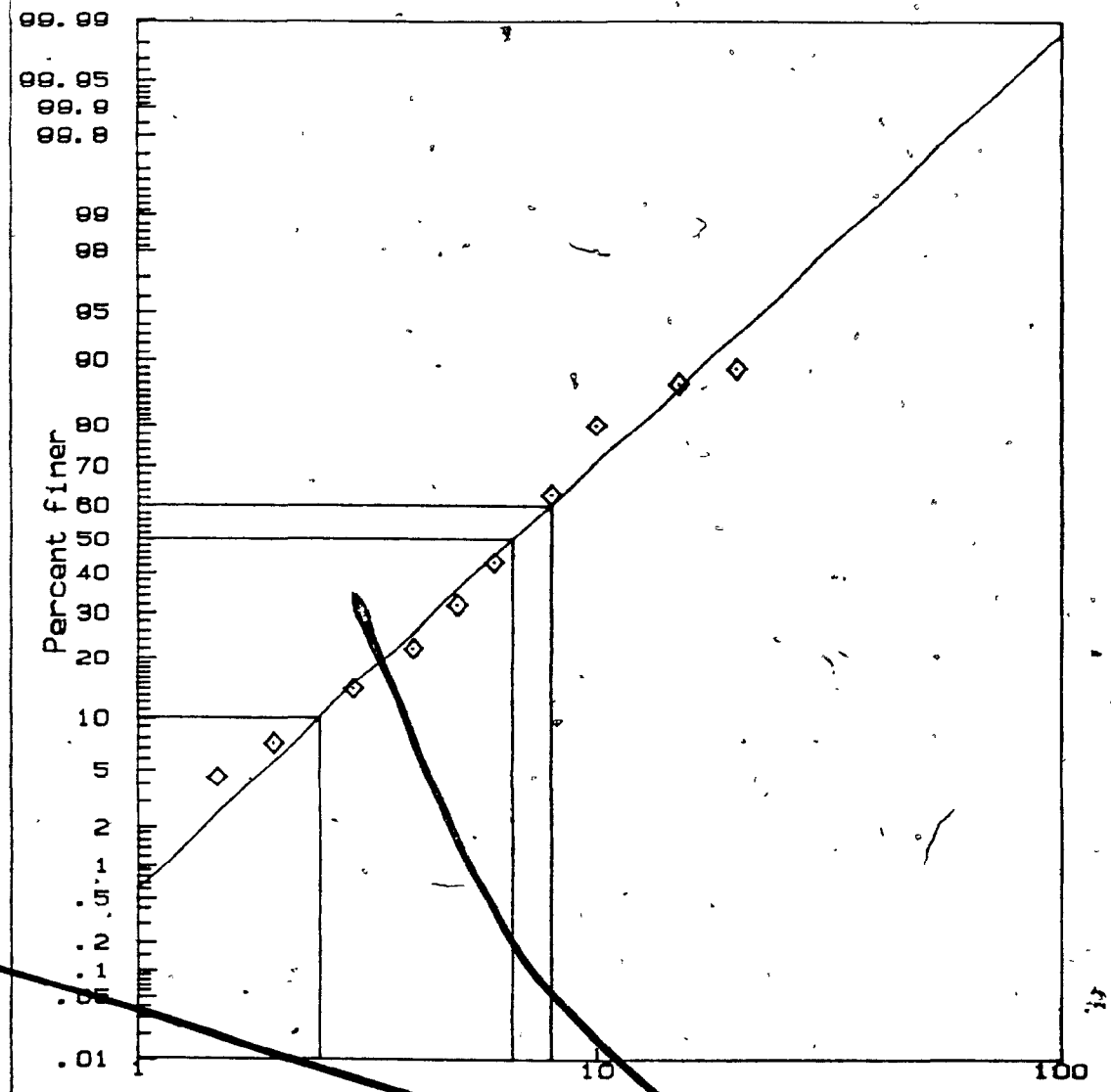

16% KAOLINITE FLAT D
CENTRIFUGE DATA
W=260 r.p.m.
SAMPLE 1.0 cm. FROM THE
BOTTOM OF THE SEDIMENT

PARTICLE SIZE ANLYSIS

D10 = 2.51 micron
D50 = 6.58 micron
D60 = 7.98 micron
Cu = 3.18 (Cu = D60/D10)

%CLAY (< 40micron) = 99.17181
%CLAY (< 4 micron) = 25.39966
%CLAY (< 1 micron) = .61539

FIGURE B.21 GRAIN SIZE DISTRIBUTION

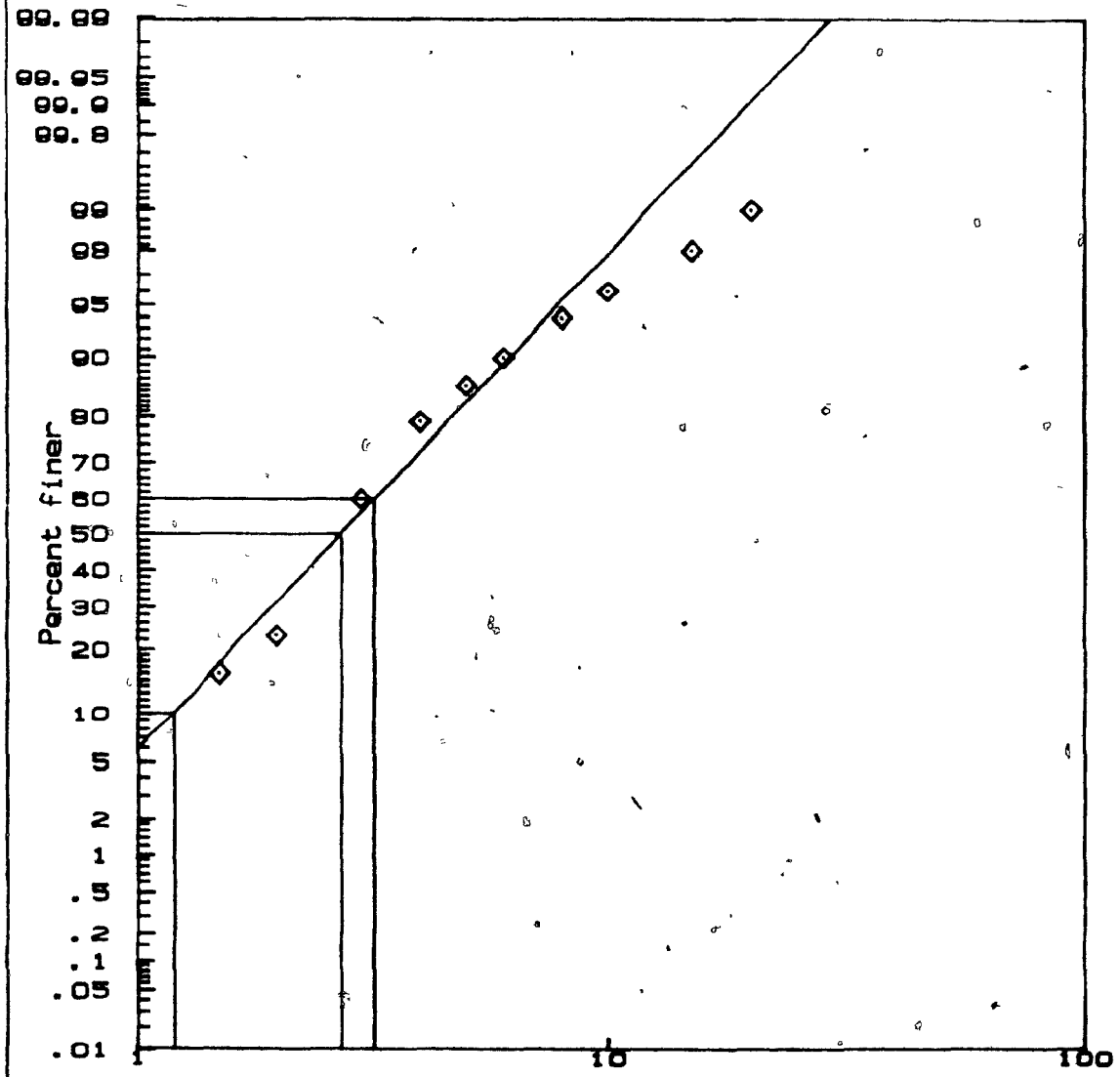

20% KAOLINITE FLAT D
CENTRIFUGE DATA
W=160 r.p.m.
SAMPLE FROM THE MIDDLE
OF THE SEDIMENT

PARTICLE SIZE ANLYSIS

D10	=	1.20 micron
D50	=	2.72 micron
D60	=	3.21 micron
Cu	=	2.67 (Cu = D60/D10)

%CLAY	(< 40micron)	= 99.99867
%CLAY	(< 4 micron)	= 72.60419
%CLAY	(< 1 micron)	= 5.85987

FIGURE B.22 GRAIN SIZE DISTRIBUTION

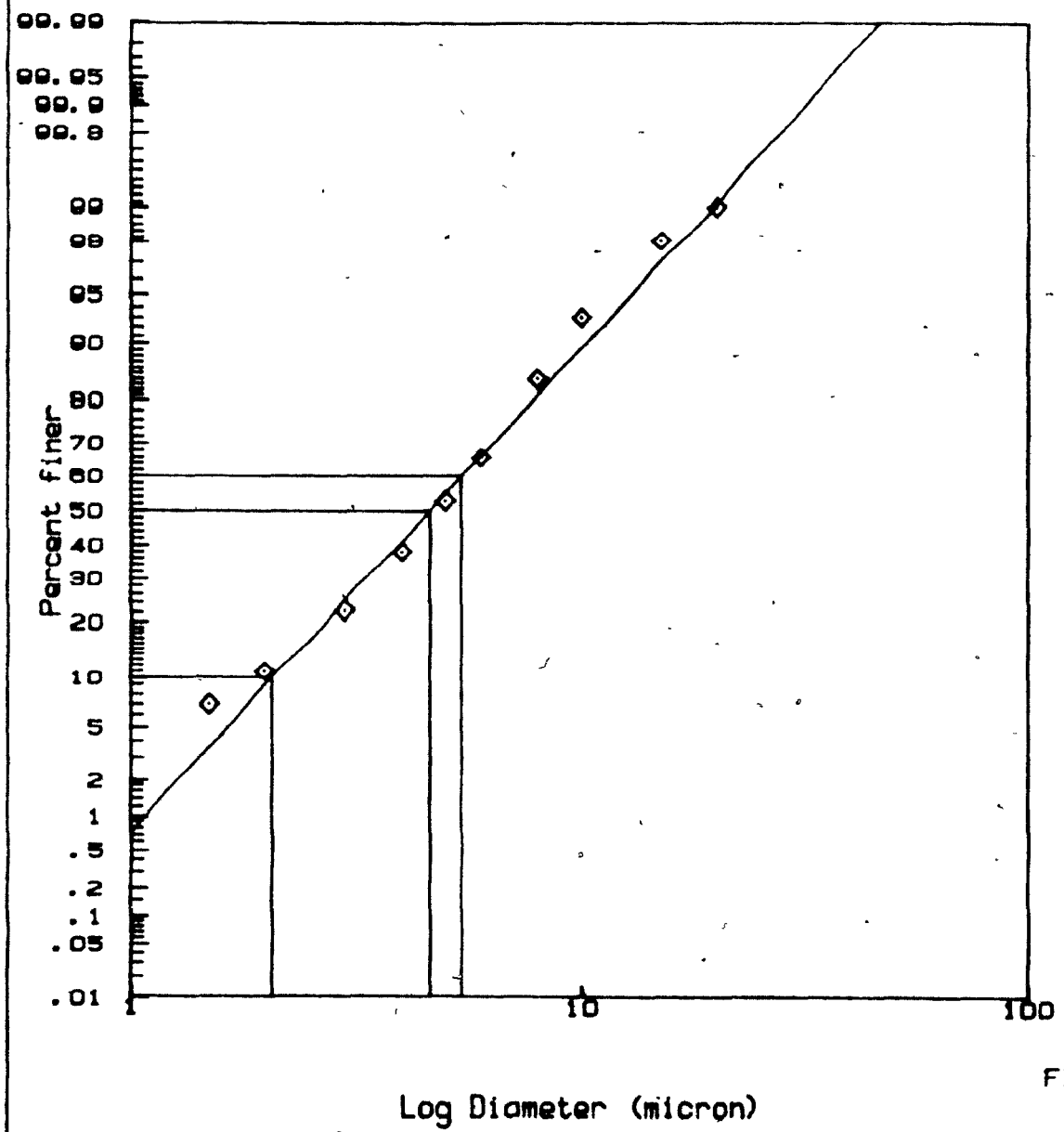

20% KAOLINITE FLAT D
CENTRIFUGE DATA
W=160 r.p.m.
SAMPLE 1.0 cm. FROM THE
BOTTOM OF THE SEDIMENT

PARTICLE SIZE ANLYSIS

D10 = 2.07 micron
D50 = 4.61 micron
D60 = 5.41 micron
Cu = 2.61 (Cu = D60/D10)

%CLAY (< 40micron) = 99.97238
%CLAY (< 4 micron) = 40.97445
%CLAY (< 1 micron) = .72404

FIGURE B.23 GRAIN SIZE DISTRIBUTION

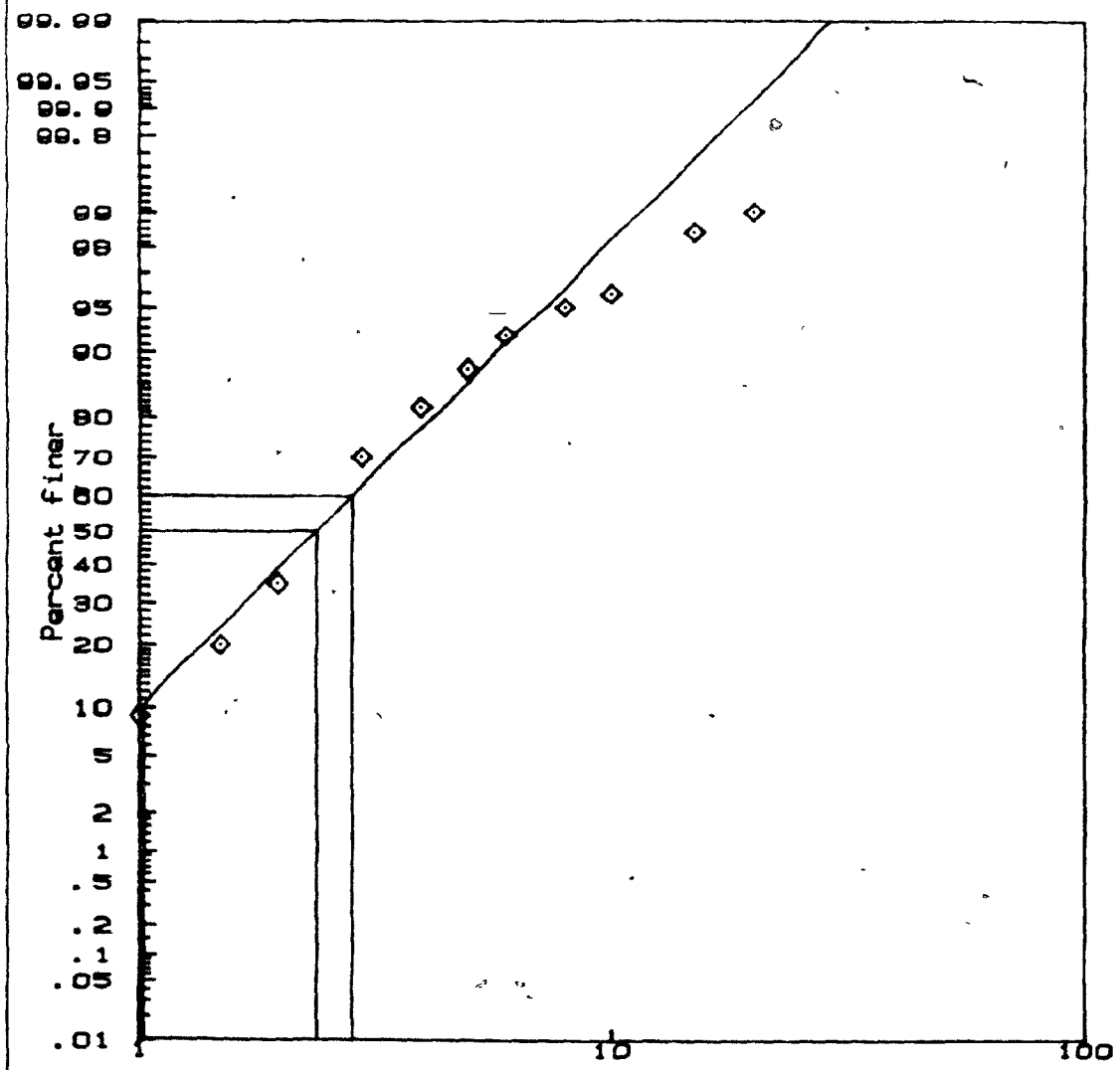

24% KAOLINITE FLAT D
CENTRIFUGE DATA
W=160 r.p.m.
SAMPLE FROM THE MIDDLE
OF THE SEDIMENT

PARTICLE SIZE ANLYSIS

D10	=	1.02 micron
D50	=	2.41 micron
D60	=	2.86 micron
Cu	=	2.80 (Cu = D60/D10)

%CLAY (< 40micron) = 99.99856
%CLAY (< 4 micron) = 77.44175
%CLAY (< 1 micron) = 9.49409

FIGURE B.24 GRAIN SIZE DISTRIBUTION

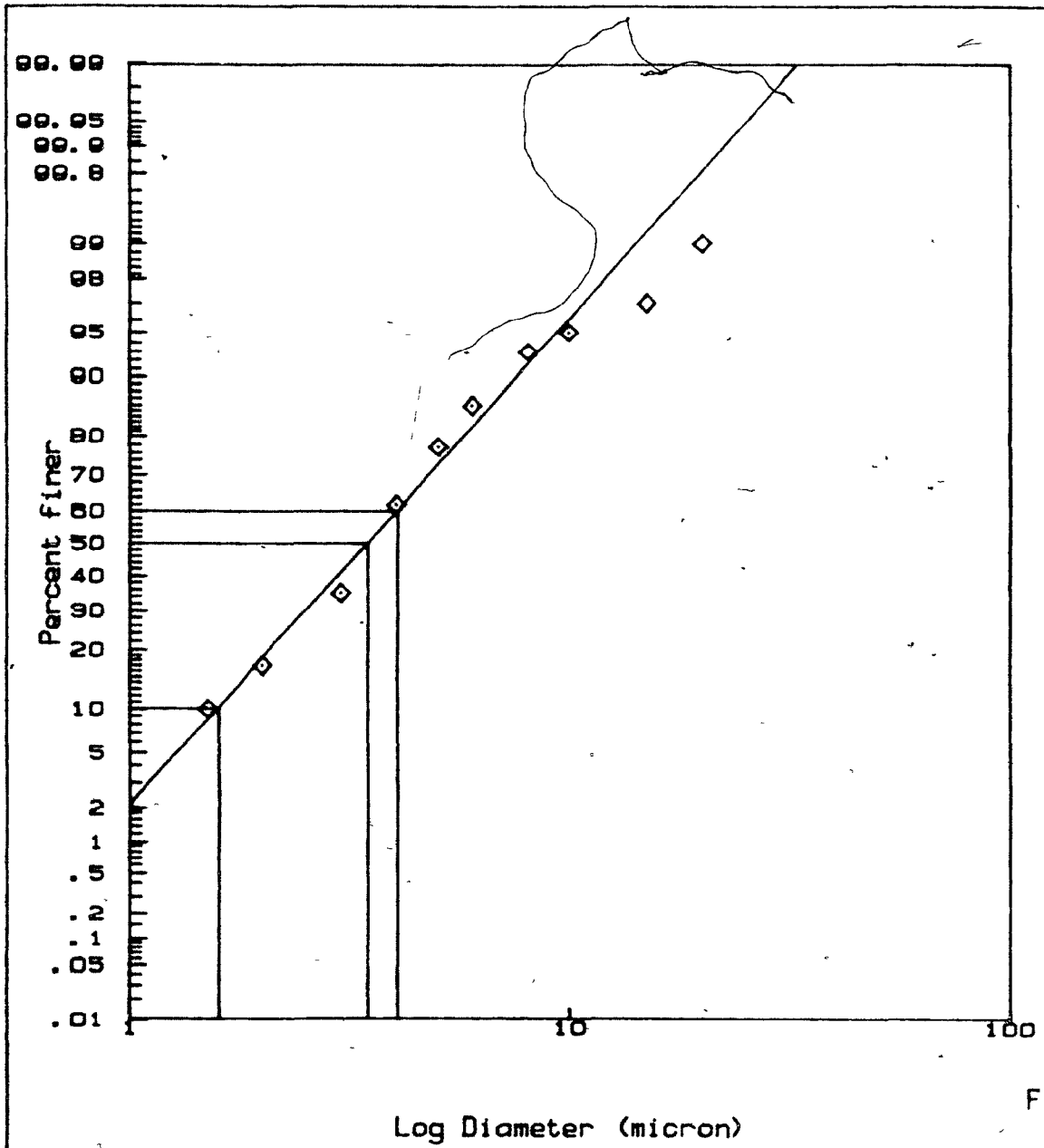

24% KAOLINITE FLAT D
CENTRIFUGE DATA
W=160 r.p.m.
SAMPLE 1.0 cm. FROM THE
BOTTOM OF THE SEDIMENT

PARTICLE SIZE ANLYSIS

D10	=	1.58 micron
D50	=	3.45 micron
D60	=	4.02 micron
Cu	=	2.54 (Cu = D60/D10)

%CLAY (< 40micron) = 99.99729
%CLAY (< 4 micron) = 59.70432
%CLAY (< 1 micron) = 2.08359

FIGURE B.25 GRAIN SIZE DISTRIBUTION

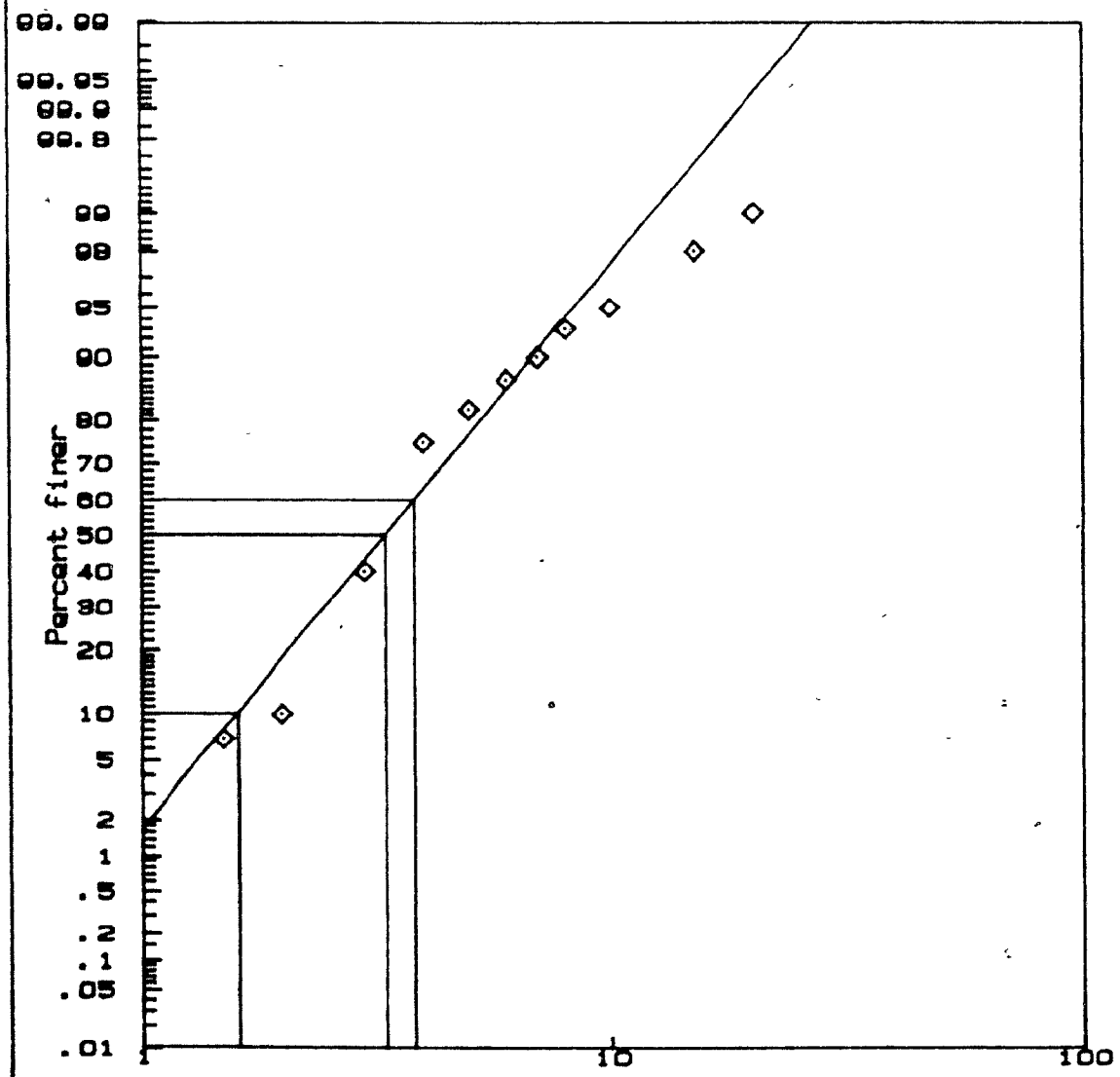

33% KAOLINITE FLAT D
CENTRIFUGE DATA
W=160 r.p.m.
SAMPLE FROM THE MIDDLE
OF THE SEDIMENT

PARTICLE SIZE ANLYSIS

D10 = 1.61 micron
D50 = 3.31 micron
D60 = 3.82 micron
Cu = 2.37 (Cu = D60/D10)

%CLAY (< 40micron) = 99.99953
%CLAY (< 4 micron) = 63.24792
%CLAY (< 1 micron) = 1.67215

FIGURE B.26 GRAIN SIZE DISTRIBUTION

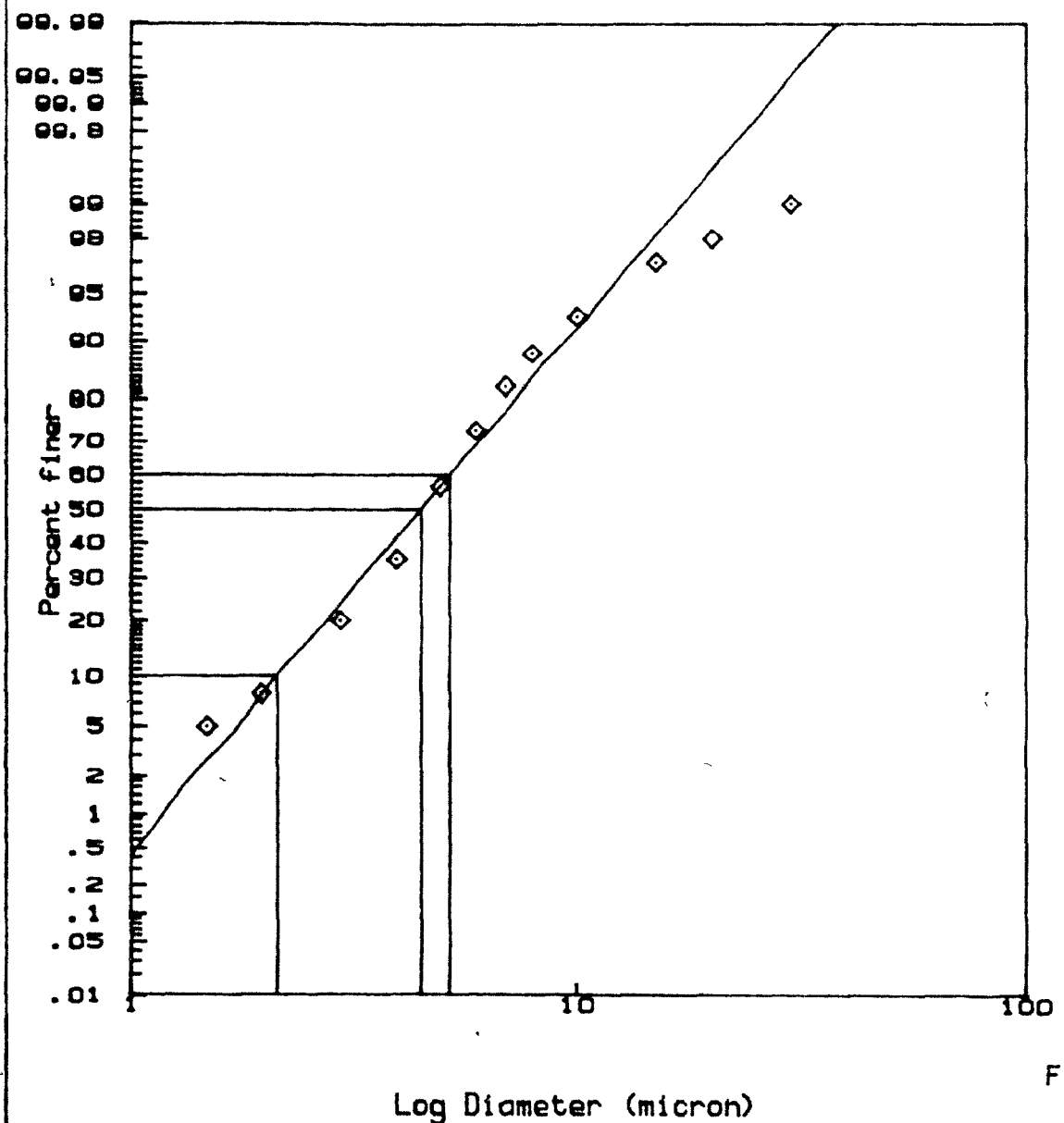

33% KAOLINITE FLAT D
CENTRIFUGE DATA
W=160 r.p.m.
SAMPLE 1.0 cm. FROM THE
BOTTON OF THE SEDIMENT

PARTICLE SIZE ANLYSIS

D10	=	2.17 micron
D50	=	4.53 micron
D60	=	5.24 micron
Cu	=	2.41 (Cu = D60/D10)

%CLAY (< 40micron) = 99.99277
%CLAY (< 4 micron) = 41.41356
%CLAY (< 1 micron) = .42001

FIGURE B.27 GRAIN SIZE DISTRIBUTION

FIGURE B.28 GRAIN SIZE DISTRIBUTION-HYDROMETER ANALYSIS

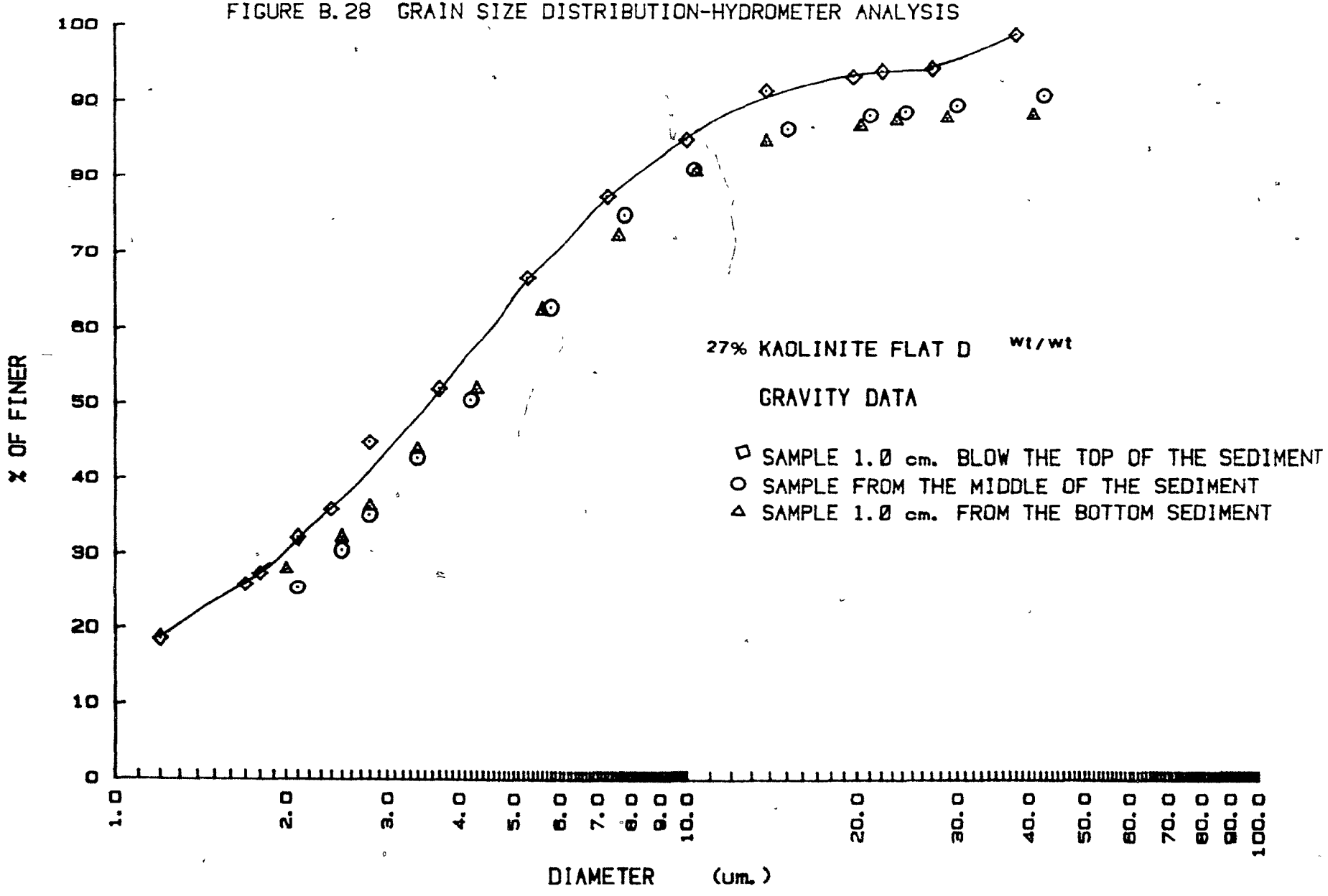

FIGURE B.29 - GRAIN SIZE DISTRIBUTION -HYDROMETER ANALYSIS

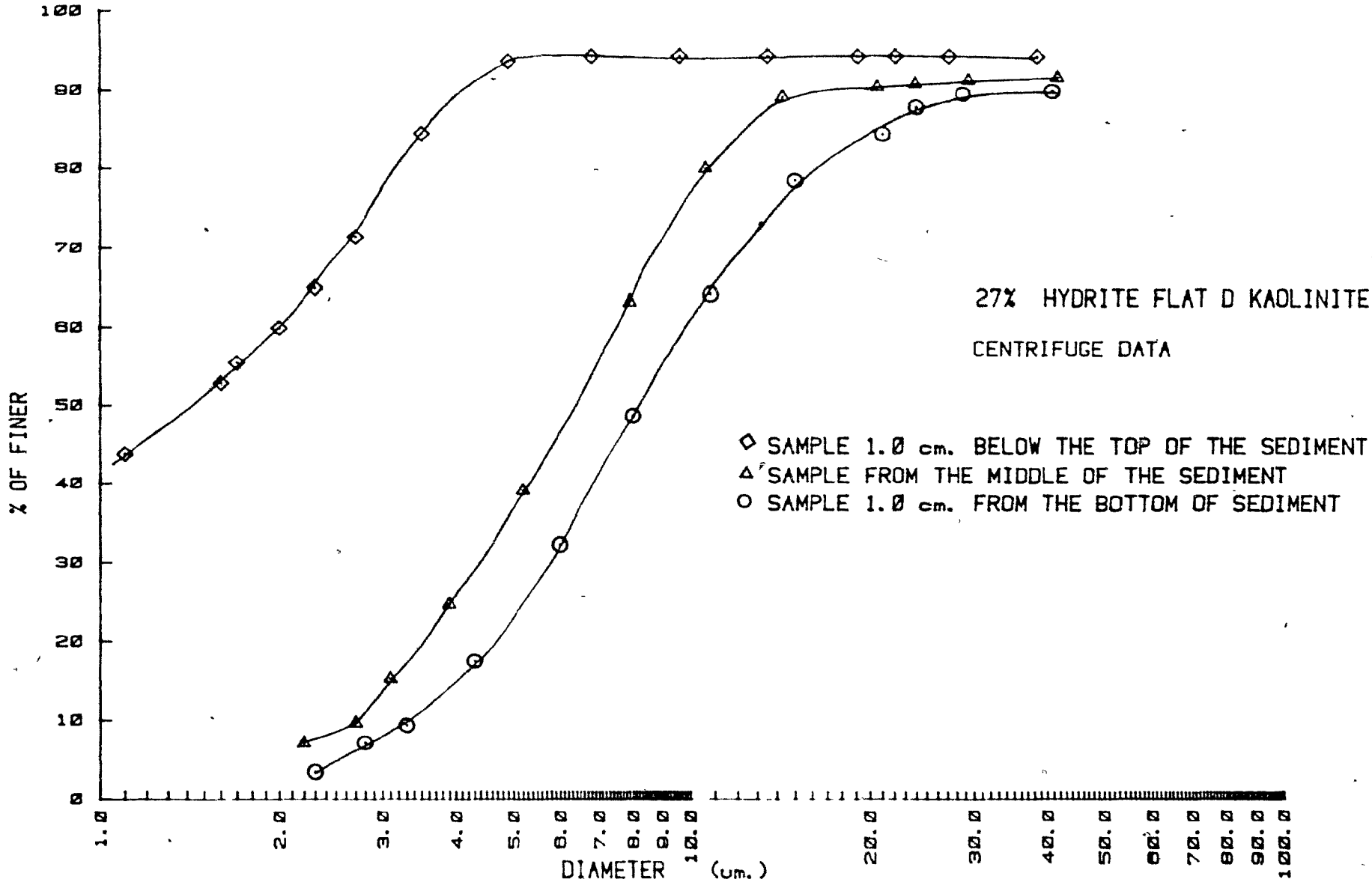

FIGURE B.32 Vg/Vc Vs. INITIAL CONCENTRATION AT DIFFERENT ROTATIONAL SPEEDS

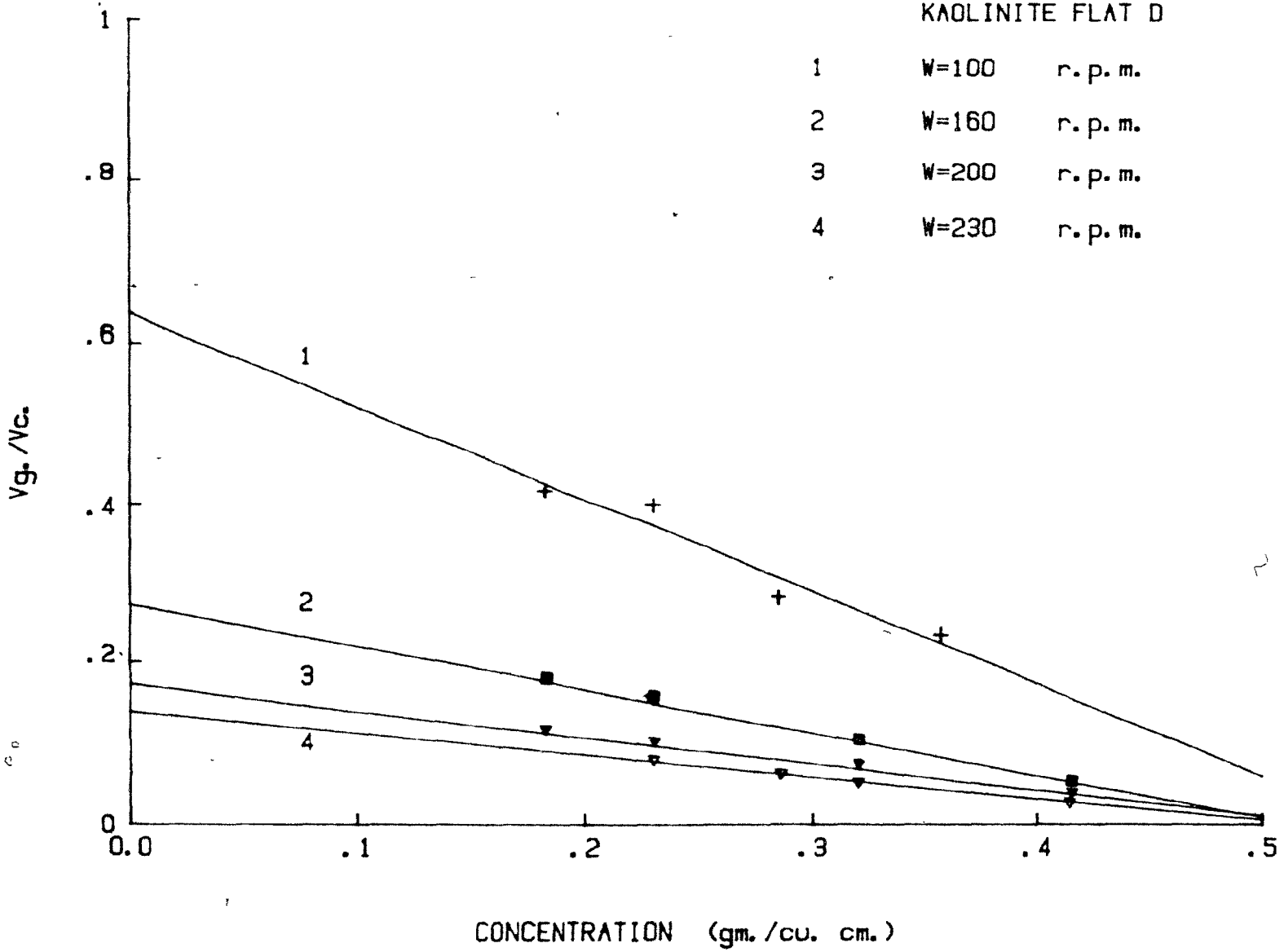

FIGURE B.31 LOG V Vs. LOG E (RICHARDSON AND ZAKI EQUATION)

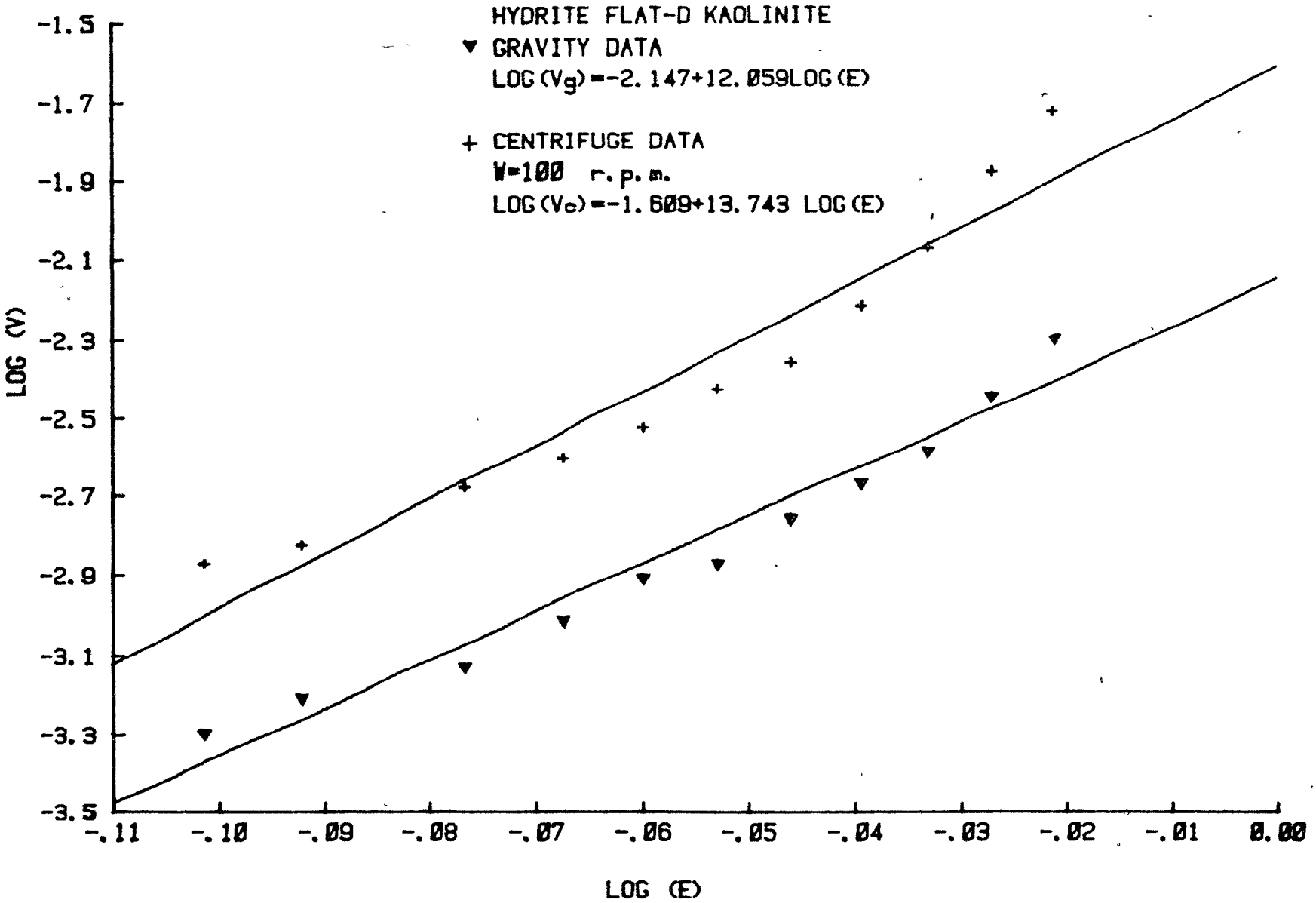

FIGURE B.32 LOG V Vs. LOG E (RICHARDSON AND ZAKI EQUATION)

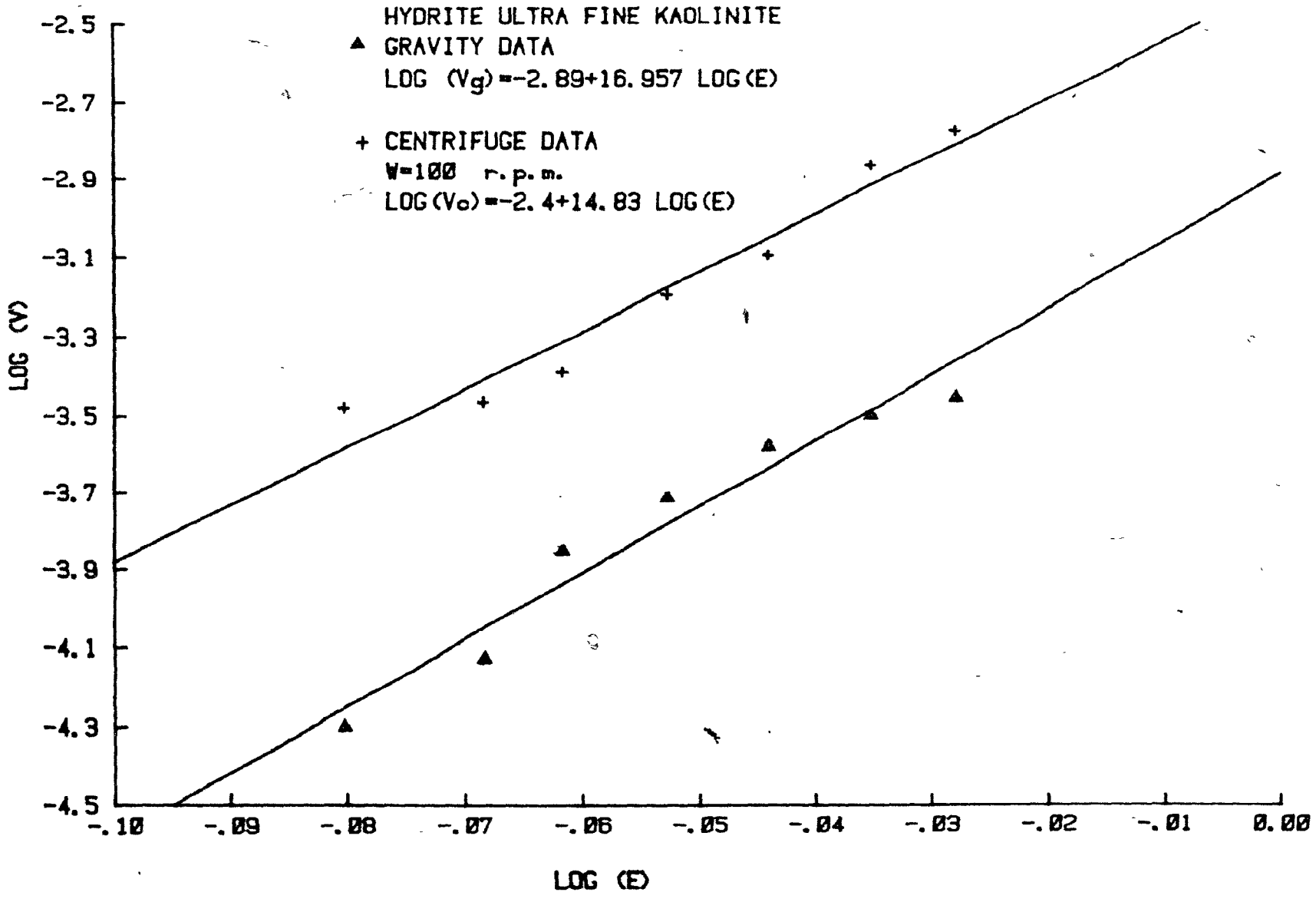

FIGURE B.33 LOG V/E Vs. (1-E) (STEINOUR EQUATIN)

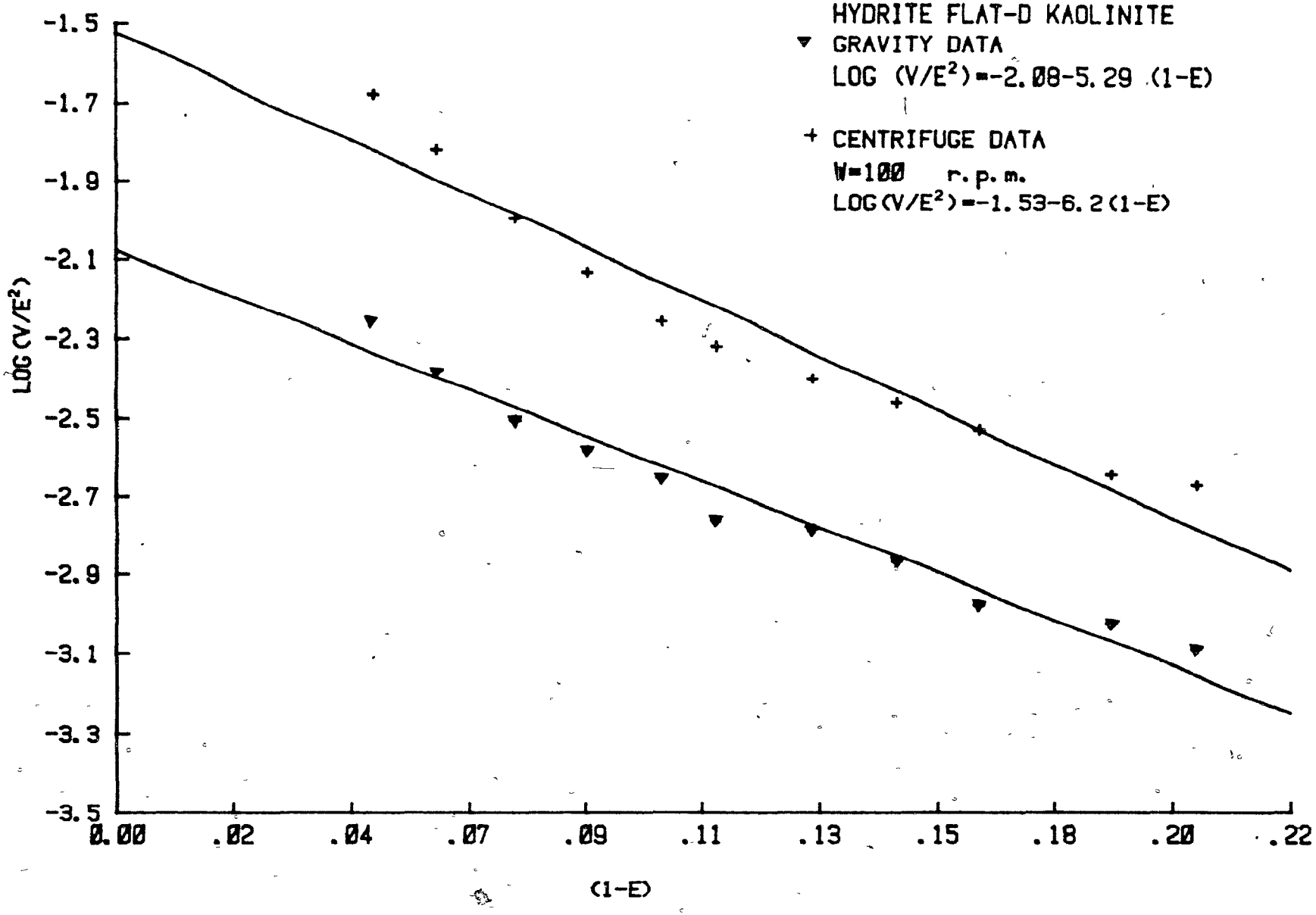

FIGURE B.34 LOG V/E Vs. (1-E) (STEINOUR EQUATIN)